THE STUDY OF COMPLIANT WALL EFFECTS ON PERISTALTIC TRANSPORT OF VISCOUS FLUID UNDER VARIOUS CONDITIONS

A THESIS

SUBMITTED TO THE

VISVESVARAYA TECHNOLOGICAL UNIVERSITY, BELAGAVI.

FOR THE AWARD OF THE DEGREE OF

DOCTOR OF PHILOSOPHY

IN

MATHEMATICS

BY

PRATIMA S. NAGATHAN

(USN 2BL11PGM01)

Research centre

(Affiliated to Visvesvaraya Technological University, Belagavi)

Department of Mathematics

BLDEA'S, V.P. Dr. P.G Halakatti College of Engineering and Technology,

Vijayapur – 586 103, Karnataka, India.

February – 2018

CERTIFICATE

This is to certify that the thesis entitled **THE STUDY OF COMPLIANT WALL EFFECTS ON PERISTALTIC TRANSPORT OF VISCOUS FLUID UNDER VARIOUS CONDITIONS** *submitted to Visvesvaraya Technological University, Belagavi, is the bonafide research work done by* **PRATIMA S. NAGATHAN** *under my supervision. The contents of the thesis have not been submitted elsewhere for the award of any degree.*

GURUNATH C. SANKAD

Supervisor

Department of Mathematics

(Affiliated to Visvesvaraya Technological University, Belagavi)

BLDEA'S, V.P. Dr. P.G Halakatti

College of Engineering and Technology,

Vijayapur – 586 103.

Karnataka, India.

Date: 16-05-2018

Place: Vijayapur.

Dedicated to

My Father

(Late. Dr. M. M. Kalburgi)

Acknowledgement

I would like to express my gratitude to those who made the writing of this thesis possible.

With great pleasure, I wish to record my deep sense of gratitude and indebtedness to Dr. G. C. Sankad, for his inspiring guidance, valuable advice and encouragement throughout the preparation of this thesis.

Also, I would wish to express my great thanks to Dr. M. B. Patil, President, BLDE Association, Vijayapur, for his valuable support. I also thank to our beloved Principal Dr. V. P. Huggi, for his support during my PhD work.

I welcome this opportunity to express my thanks to Dr. P. K. Gonnagar, Vice Principal and Head of the Department of Mathematics, BLDEA's V. P. Dr. P.G. Halakatti , Vijayapur, for his help, encouragement and support during the preparation process.

I would like to express my deepest gratitude and sincere thanks to my colleagues for guidance and encouragement throughout the development of this research.

Finally, I would like to extend my deepest thanks for my family members for their support and patience during this work.

Visvesvaraya Technological University

Jnana Sangama, Belagavi – 590 018.

Prof. Satish Annigeri Ph.D
Registrar (Evaluation)

Phone: (0831) 2498136
Fax: (0831) 2405461

Ref.No. VTU/BGM/Exam /2017-18/2652 *Date:* 23 FEB 2018

Acceptance Letter

Sir/Madam,

The soft copy of Ph.D./M.Sc. (Engineering by research) thesis of **Mr./Mrs. Nagathan Pratima Suresh.** bearing **USN 2BL11PGM01** has been submitted for Anti-plagiarism check at the office of the undersigned through "Turn-it-in" package. The scan has been carried out and the scanned output reveals a match percentage of **15% which is within the acceptable limit of 25%.**

To obtain the comprehensive report of the plagiarism test, research scholar can send a mail to **apc@vtu.ac.in**along with the USN, Name, Name of the Guide/Co-guide, Research centre and title of the thesis.

Registrar (Evaluation)

To, **Nagathan Pratima Suresh**

Research Scholar

Mathematics

BLDEA's College of Engineering & Tech., Bijapur.

Copy to: Dr. Gurunath C. Sankad., Asst.Prof.,Dept.of Mathematics.
BLDEA's V.P. Dr. P.G.H. College of Engineering & Tech., Bijapur.

Abstract

Peristaltic flow is a transport mechanism characterized by the contraction and relaxation of flexible tubes. Peristalsis is primarily used in the human body to transport fluids. Peristalsis is a fundamental process that moves food automatically through the digestive tract, urine from the kidneys to the bladder through the ureters, food mixing, chime movement in the intestine, movement of spermatozoa in the ducts efferent of the male reproductive organ, movement of egg in the female fallopian tube, and transport of bile in bile duct. It has been suggested that peristalsis may be associated with the vasomotion of small blood vessels. Also, in many practical mechanisms pertaining to biomechanical systems pumping occurs through peristalsis.

The peristaltic process has several applications as seen in the roller and finger pumps and in several bio-mechanical instruments (e.g., heart-lung machine, blood pump machine and dialysis machine). In nuclear industry the transportation of a toxic liquid uses peristalsis so that the valuable environment is not contaminated. The diameters of the tree trunks are found to change with time hence some investigators have studied peristalsis with reference to water transport in trees. The actual mechanism of motion of water to upper branches of tall trees from the ground is not well understood however it is speculated that free convection and peristalsis both contribute to this mechanism. Flow through porous matrix of the tree contributes to the translocation of water. Many researchers have contributed to explain peristaltic pumping in physiological systems through their experimental as well as theoretical research work. Thus, peristaltic flow has become the core interest of many recent studies of researchers/scientists owing to the wide applications.

Several attempts have been made to analyze the peristaltic transport of physiological fluids, which are non-Newtonian in behavior. In non-Newtonian fluids, the shear stress and the shear rate may be correlated where both shear stress and shear rate may be time dependent and the fluid exhibits viscous as well as elastic characteristics. Therefore it is difficult to describe the non-Newtonian fluids by a single constitutive relationship between stress and strain rate. Moreover these constitutive equations lead to complicated mathematical problems. The non-

Newtonian fluid study has gained interest due of its applications in several industrial and engineering processes. Many materials such as ketchup, blood, drilling mud, tooth-paste, certain polymer melts, oils and greases are treated as non-Newtonian fluids. It is known that blood, being a complex and electrically conducting fluid acts like a non-Newtonian fluid at low shear rates. Hence, numerous constitutive models have been projected to analyze the non-Newtonian characters of the fluid flow.

Flow through porous medium has captivated significant attention in recent years due to its prospective applications in nearly all fields of engineering, biomechanics and Geo-fluid dynamics. Analysis of flow past a porous medium is used immensely in biomedical problems to understand the transport process in lungs, gall bladder and kidneys, to investigate inter vertebral disc tissues, cartilage and bones etc. Some of the physiological systems such as blood vessel consist of porous layers. Since peristalsis is also important in blood vessels, it will be interesting to know the effects of permeability on the peristaltic pumping. Porous medium models are applied to identify the various medical conditions and treatments (as in tumor growth and injections).

As the fluid displays a loss of adhesion at the wetted wall, the fluid is made to slide along the wall resulting into slip flow, as seen in several applications: flow through pipes wherein chemical reactions occur at the walls, two-phase flows in porous slider bearings. Slippage is claimed to occur in non-Newtonian fluids, molten polymer and concentrated polymer solution as well.

The class of non-Newtonian fluids that considers the couple stress and Jeffrey fluids has distinct characters. The couple stress model displays a generalization of the classical viscous Newtonian model that permits the polar effects for instance the existence of couple stresses and body couples in the fluid medium. The vital feature of this fluid is that, the stress tensor is asymmetric. The equations managing the couple stress fluid transport are of higher order in consideration with the standard Navier-Stokes equations. The couple stress fluid flow analysis is very helpful to make out the insight of the diverse physical problems as it possesses the mechanism to explain the rheological complex fluids such as liquid crystals, lubricants that include small quantity of

polymer additive, human and animal blood and infected urine from a diseased kidney. Many authors have considered blood as a suspension of spherical rigid particles that give rise to couple stresses in a fluid.

The non-Newtonian Jeffrey fluid explains the effect of the ratio of relaxation to retardation time and has captured the interest of numerous researchers in fluid dynamics. The Jeffrey model is one of the simplest linear models that describe the non-Newtonian fluid properties. Study of peristaltic motion of a Jeffrey fluid is quite helpful in physiology and industry because of its large number of applications and in mathematics owing to its solutions of nonlinear equations and complicated geometries. In physiology, many systems in the living body make use of peristalsis to drive or to mix the contents of a tube. Applications of Jeffrey fluid can also be seen in science and engineering: food and slurry transportation, thermal oil recovery, food processing and polymer, etc.

In view of these, the study of peristaltic transport of a non-Newtonian fluid in porous medium is carried out in the thesis by considering characteristics such as wall effects, slip effects, Darcy effects, magnetic effects and heat transfer effects. The couple stress and Jeffrey fluid models are considered since these are considered to be better models for physiological fluids such as blood. The results are graphically illustrated with the help of MATHEMATICA software.

Contents

Chapter 1

INTRODUCTION

1.1 Fluid dynamics

Fluid is a substance that continuously deforms when applied by shearing stress, however small the stress may be. Fluid dynamics is the science that describes the flow of fluids and their interactions with solid bodies. The study of fluid dynamics of the elementary biological fluids like blood, air, etc is termed as 'bio-fluid dynamics'. It is employed for diagnosis, treatment and also for performing certain surgical procedures, associated with pulmonary, synovial and cardiovascular system disorders/diseases. The application of bio-fluid dynamics can be seen in the areas of physiology, where it explains how living things work. It also describes about their motions, development and understanding of the variety of diseases, connected with human body. In the field of mechanical and biological engineering, bio-fluid mechanics is the study of motion of biological fluids, such as, animal flight, blood flow in arteries etc. Many bio-fluid mechanical processes in the human body, are comparable to the flow modeled for the motion of a non-Newtonian fluid, through a deformable flexible tube subjected to the external and/or internal forces.

1.2 Peristaltic motion

Under many relevant conditions, the tube experiences very large deformations, and may approach complete collapse. There are two main approaches to describe such phenomena. The first approach is to solve the coupled fluid-structure problem, that is, both, the flow field and the tube deformation are simultaneously solved as a coupled system. The second approach, called peristalsis, describes a fluid system whose flow is driven by the deformation of the boundaries due to the outside forces. In a bio-fluid mechanical system, the peristaltic motion is the flow of fluids in a tube/channel by the means of muscular contraction and expansion, such as, in the esophagus, stomach, intestines, blood vessels etc.

Peristalsis (Figure 1.1) is defined as a continuous sinusoidal wave of relaxation and contraction moving on the walls of a flexible channel, thereby driving ahead the enclosed material. 'Peristaltikos' is a Greek word, from which peristalsis arises. It stands for the clasping and compressing. Peristaltic mechanism, occurs normally from a region of lower pressure to the higher pressure. Moreover, peristalsis is a well-known means of fluid motion in the biological system.

From the fluid mechanical point of view, peristaltic movement is considered as the dynamical interface of the fluid transport due to the progress of the flexible boundaries. The requirement for peristaltic pumping may arise in circumstances, whenever it is required to evade any internal moving part viz., blood that is pumped during the dialysis, must be prevented from being contaminated, piston, in the pumping procedure.

From the physiological point of view, peristalsis emerges to be the major mechanism for the transportation of urine through urethra, mixing of the food and movement of chyme in the intestines, movement of spermatozoa in the ducts efferent of the male and female reproductive organs, egg movement in the female fallopian tube and transport of bile in the bile duct. Even the vasomotion of the small blood vessels is supposed to be associated with peristalsis.

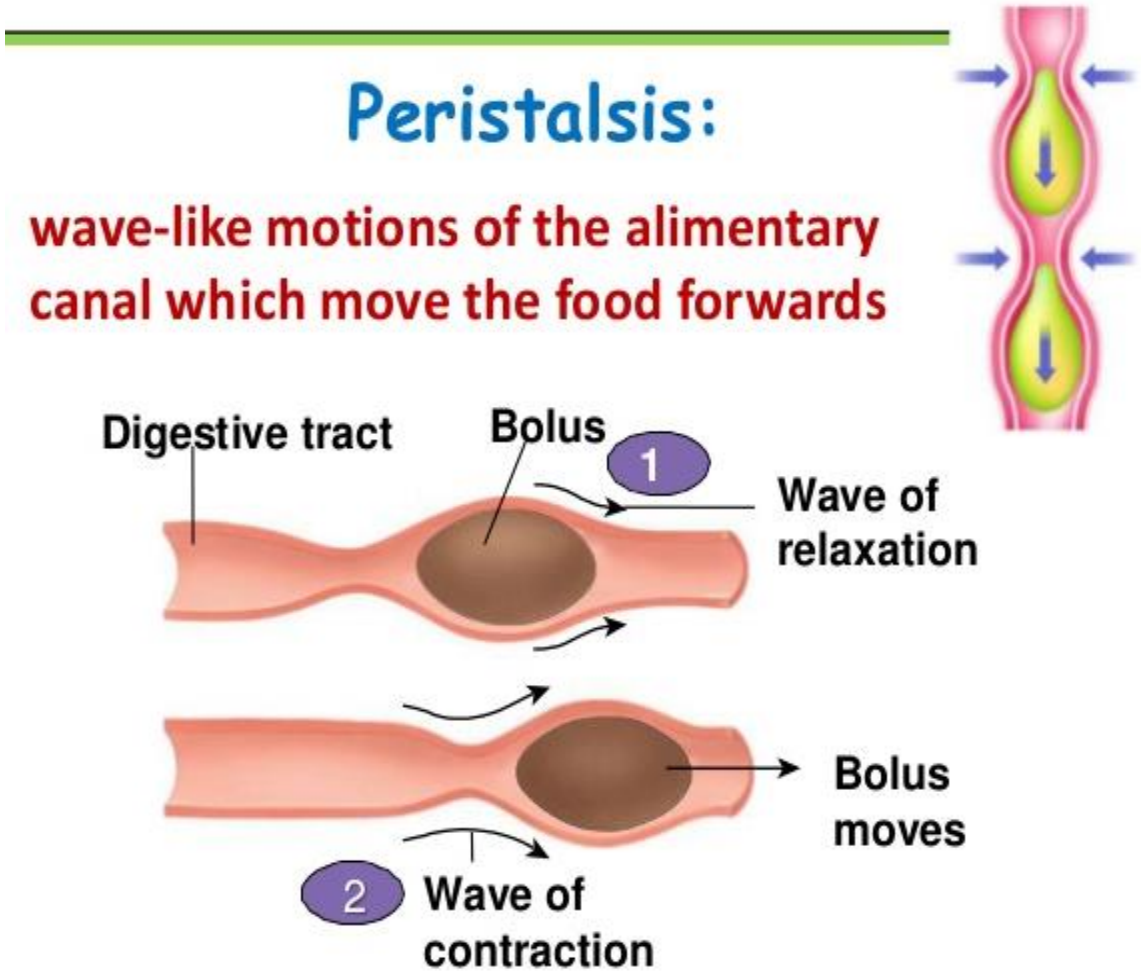

Figure 1.1: Peristaltic motion

1.2.1 Peristaltic pump

The bioengineering pumps can be broadly divided in two categories, one that are seen in the biological systems i.e. naturally occurring pumps; and then other ones are the artificial ones, made by man, and are used for biomedical appliances.

Oxygenator is an engineering device, used to oxygenate blood, known as the heart-lung machine (Figure 1.2(a)). It is used in the open-heart surgery, which serves the dual purpose of heart and lung. During this operation, the impure blood is taken out of the body and passed into the heart-lung machine for the purification and oxygenated blood will be sent back to the body. Finger and roller pumps use this mechanism of peristalsis to pump the blood. Thus, in view of mentioned applications, many scientists and researchers are showing core interest in peristaltic flow.

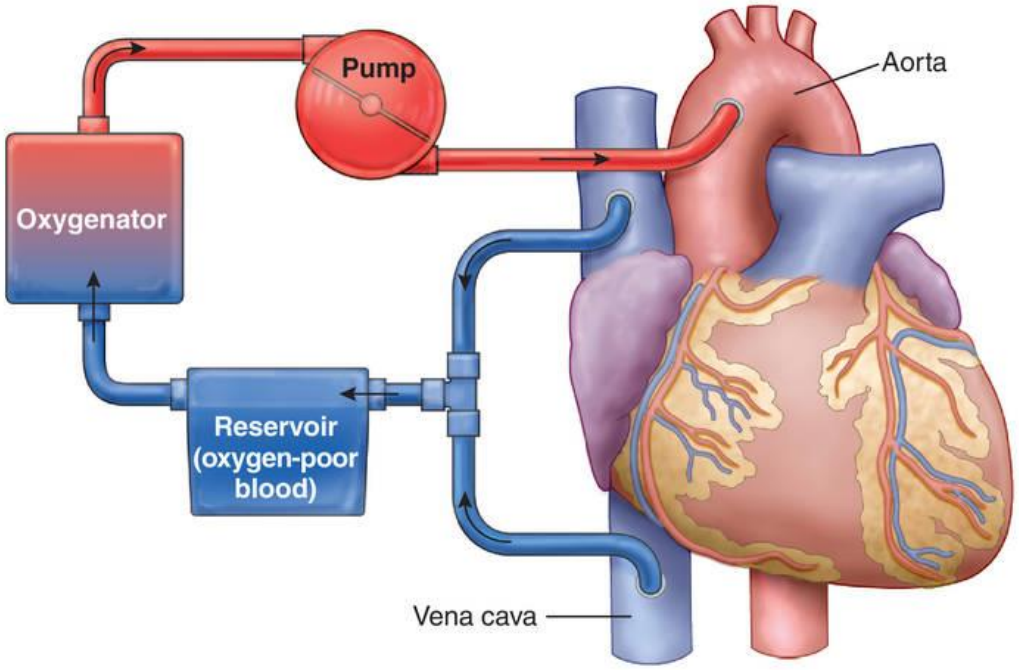

Figure 1.2(a): Heart lung machine

The peristaltic pump (1.2b) is based on alternative compression and relaxation action of the hose or tube taking the contents into the hose or tube, operating analogous to our throat and intestines. A rotating shoe or roller passes along the hose or tube compressing it totally and generating a seal between suction and discharge side of the pump, eliminating product slip.

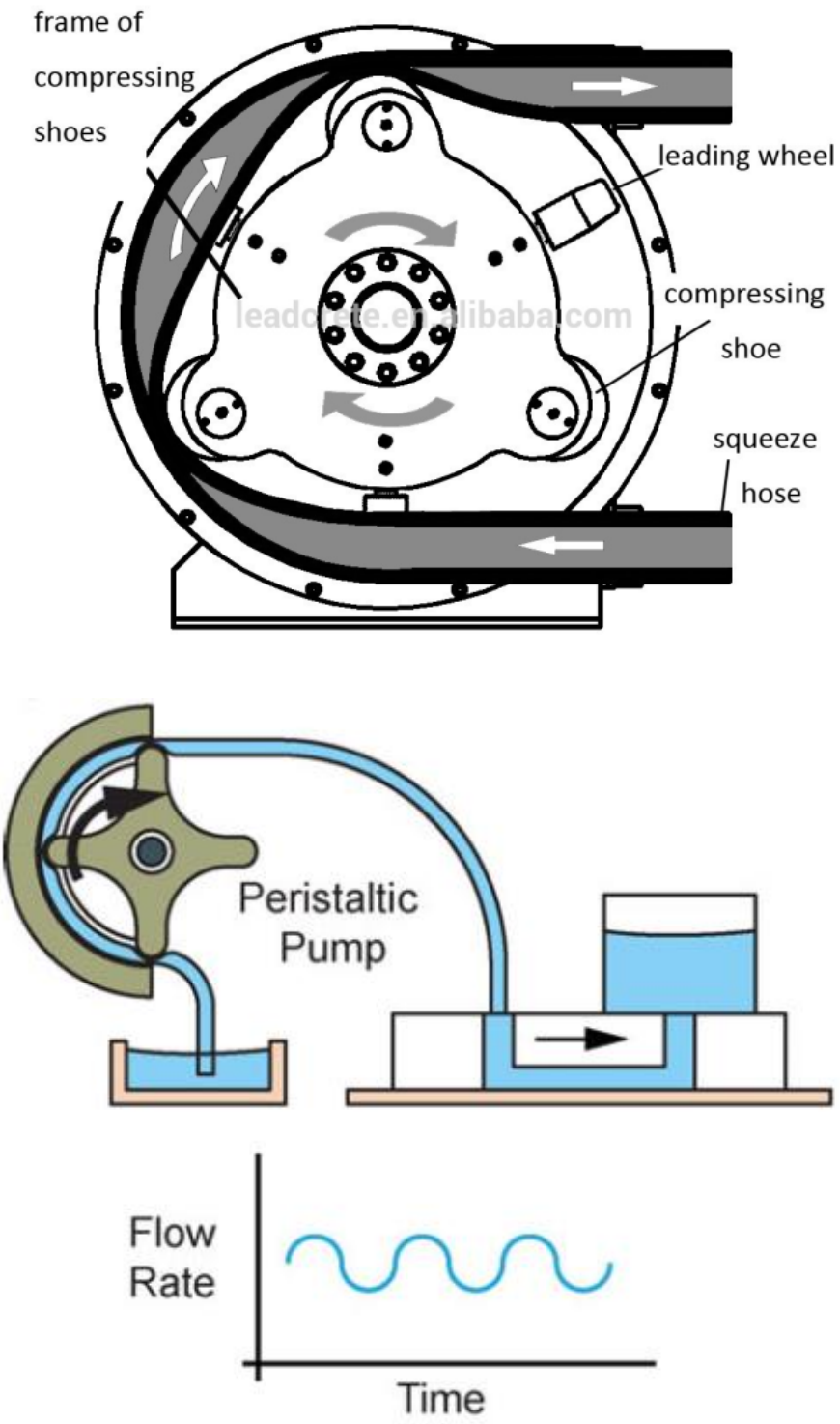

Figure 1.2(b): Bioengineering pumps

A non-biological application of peristalsis is the peristaltic pump, which is used to move clean/sterile or aggressive fluid through a tube without cross contamination between the exposed pump components and the fluid. As discussed by Jaffrin and Shapiro [1], the

presence of viscous forces can produce effective pumping. In nuclear industry peristalsis avoids polluting of the outside environment during the exclusion of toxic liquid. Observations reveal that transportation of water in tall trees is due to peristalsis. The porous matrix of the trees assists this water flow.

1.2.2 Peristalsis in Esophagus

In the esophagus (Figure 1.3) due to the periodic contraction of the esophageal wall, swallowing of the food bolus takes place. The bolus moves ahead due to pressure exerted by reflexive contraction of the posterior part of the bolus and relaxation experienced by anterior part. This way the peristaltic motion moves the food from esophagus to stomach and plays an important role.

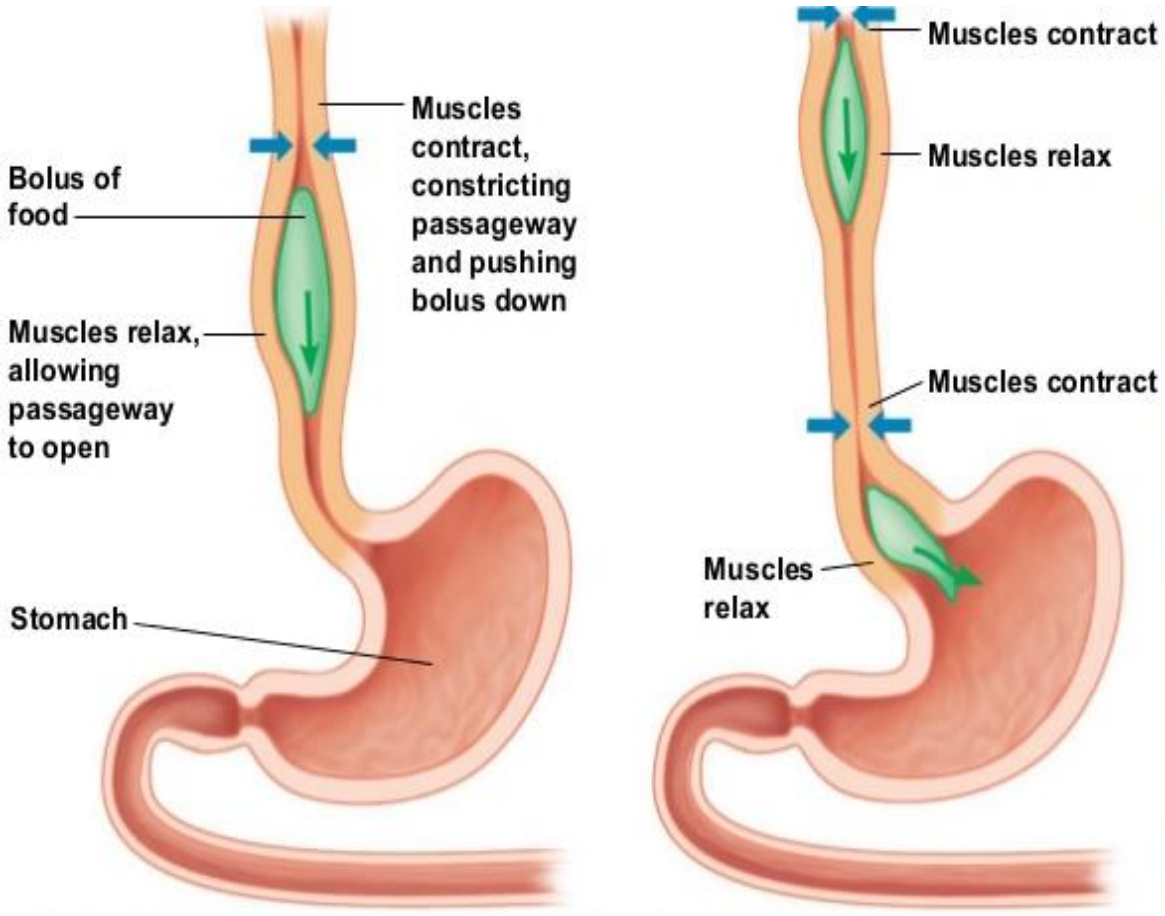

Figure 1.3: Peristalsis in Esophagus

1.2.3 Peristalsis in human digestive system

There are many organs in the human body, whose functioning involves the fluid motion. In the digestive tract, the wave like muscle contraction moves the food to various processing parts under peristalsis. The digestive system (Figure 1.4) is made up of two groups of organs. One group constitutes the gastrointestinal tract and the other group consists of the accessory organs that help in digestion. In the gastrointestinal tract, the mucous secreted by mucous wall lubricates the passage of food through the canal. The gastrointestinal tract includes the organs like mouth, pharynx, esophagus, stomach, small intestine, and large intestine. In some parts of the gastrointestinal tract, muscular contractions that may be described as peristaltic waves, not only churns and breaks down the food in the wall, but also propels the food along the tract and moves to anus. The accessory digestive organs are the tongue, teeth, salivary glands, liver, gallbladder, and pancreas.

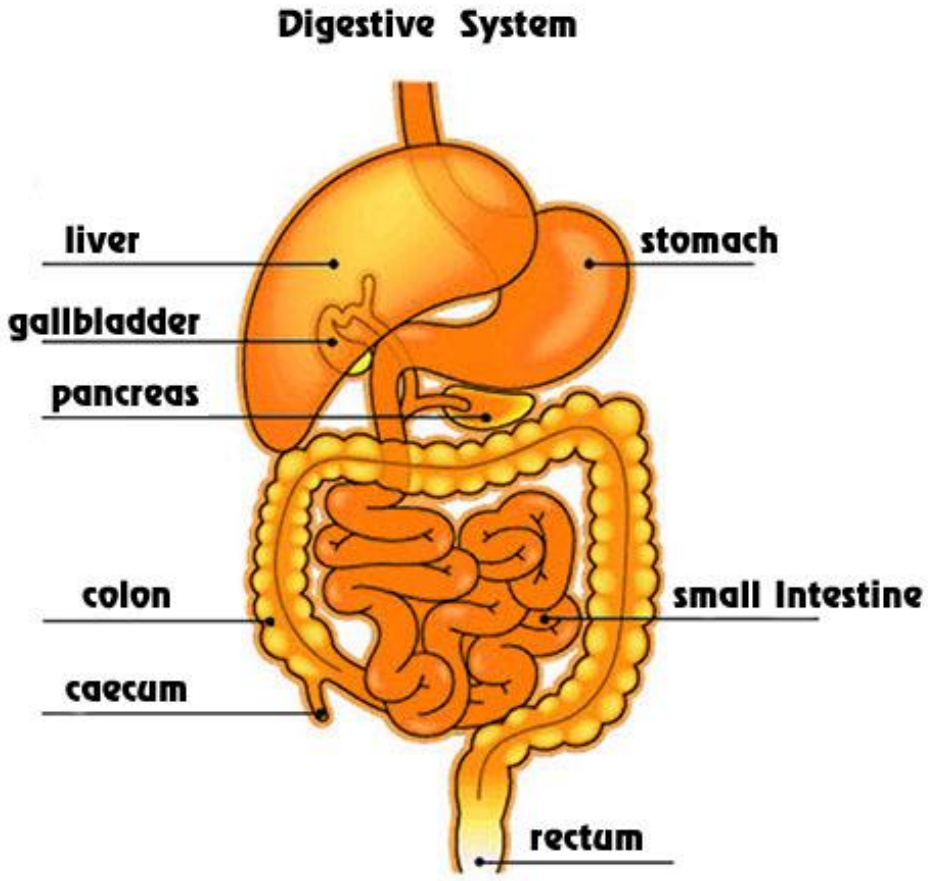

Figure 1.4: Human digestive system

1.2.4 Peristalsis in small intestine and large intestine

The main functions of digestion and waste elimination are carried out by the active peristaltic muscular contractions in the small and large intestines (Figure 1.5 and Figure 1.6). The law of peristalsis in small intestines is that the presence of the food serves as the normal stimulus causing relaxation below and compression above the food bolus. When the wave travels downwards the food is moved in a spiral manner and the direction of rotation is anticlockwise.

Large intestine points the lower end of the small intestine at the ileocolic sphincter, the last part in which the large intestine opens is the rectum together with anal canal. In large intestine peristaltic transport is weak.

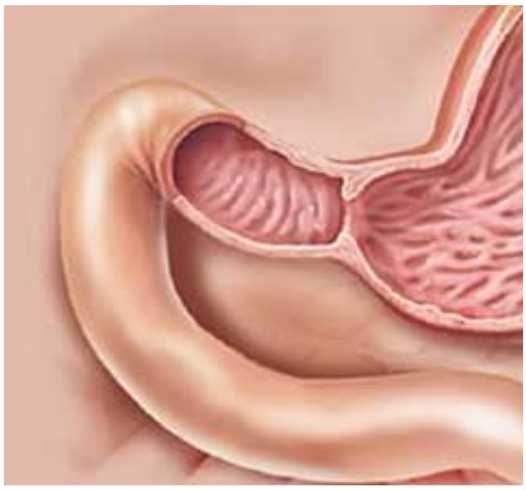

Figure 1.5: Small intestine

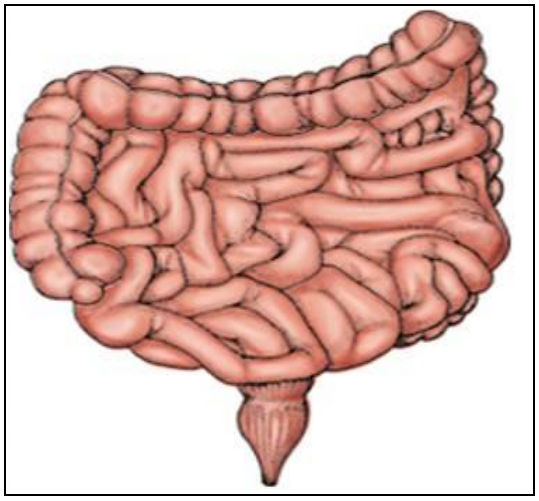

Figure 1.6: Large intestine

1.2.5 Ureteral peristalsis

The urinary system (Figure 1.7) is made up of the kidneys, ureters, bladder and urethra. Most of the metabolic wastes are eliminated from the body by the urinary system. A series of compressive zones that correspond to continuous waves due to active muscular contraction corresponds to the ureteral peristalsis. These move towards the bladder almost at a constant speed along the ureter.

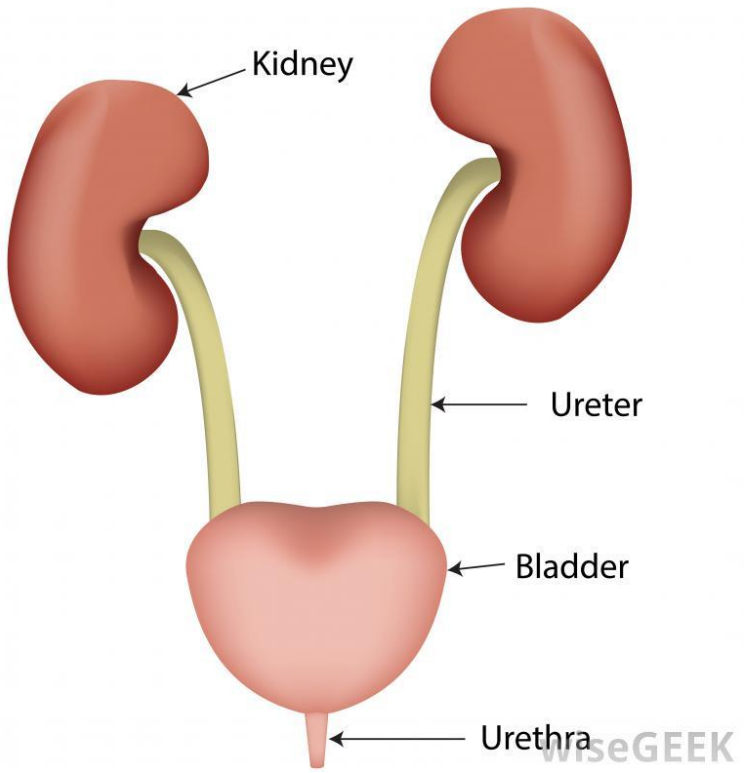

Figure 1.7:

Urine transport from kidney to bladder through urethra

There are two parts in urinary system. Kidneys to ureters are the upper part and bladder to urethra is a lower part. With the evolution of electrical action at pacemaker sites peristalsis gets initiated in the upper urinary tract. Peacemaker sites are located in the proximal part of the urine accumulatory system. Urine from the kidney to the bladder propagates due to renal pelvic and ureteral contractions when electrical activity transmits distally initiating the event of peristalsis. An effective contraction wave entirely covers the ureteral wall. The urine in between the two contracted waves turns up into bolus under normal flows. It is driven distally till it reaches the bladder passing through the uretero-

vesical junction. The uretero-vesical ducts in the ureters ensure that the waste fluid does not travel back in to the kidney.

1.3 Newtonian and non-Newtonian

Fluids can be classified as Newtonian and non-Newtonian (Figure 1.8). For a Newtonian fluid, the shear stress and the shear rate exhibit linear relationship passing through the origin, the coefficient of viscosity is considered as the constant of proportionality. For example, water, gasoline, alcohol, air and mineral oil.

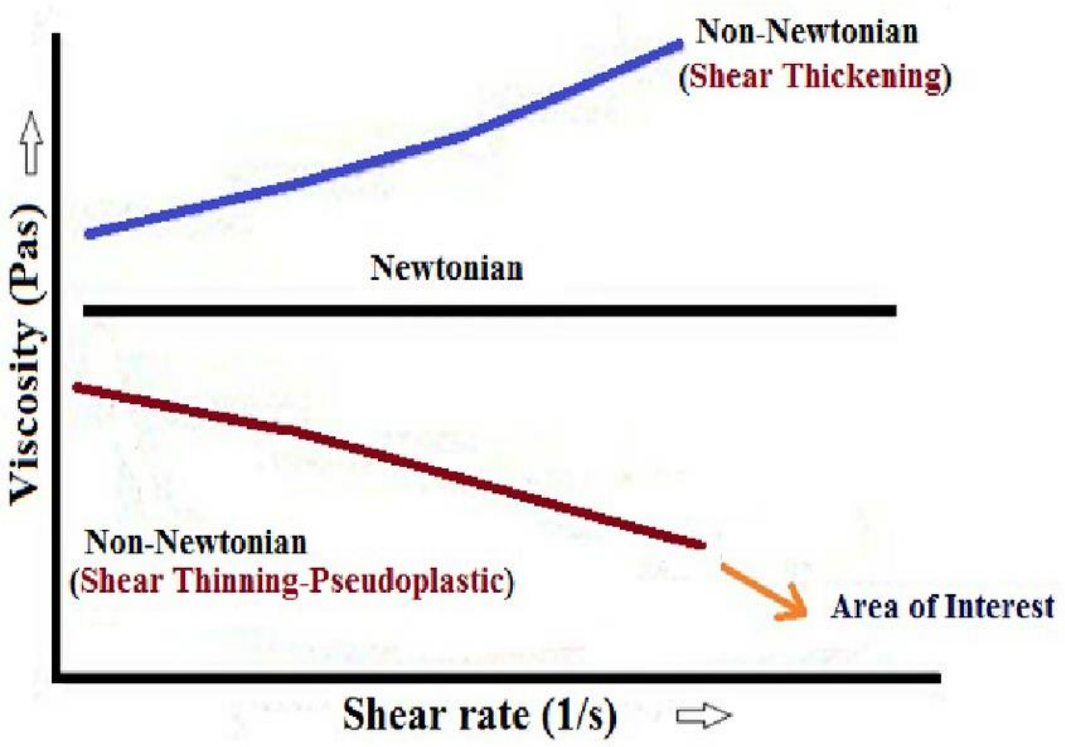

Figure 1.8: Newtonian and non-Newtonian rheology

In contrast, a non-Newtonian fluid exhibits non-linear relation between the shear stress and the shear rate. The fluid can even exhibit time dependent viscosity. The viscosity of non-Newtonian fluids depends on the shear rate and further a constant coefficient of viscosity cannot be defined. For example: custard, honey, ketchup, toothpaste and shampoo.

Earlier, blood was thought to be a Newtonian fluid. However later it was reported that viscoelasticity counts to be a basic rheological property of blood. The elastic behavior of red blood cells gives the viscoelastic property that makes human blood non-Newtonian.

Recently, due to the vast medical applications of non-Newtonian fluids, mathematical models have been developed considering the rheological behavior of blood by a number of researchers. However a single governing constitutive equation cannot describe all the properties of the non-Newtonian fluids.

1.4 Reflux and Trapping

Peristaltic flow is allied with two interesting phenomena: material reflux and fluid trapping. Reflux is defined as the presence of some fluid particles whose mean motion over one cycle is against the net pumping direction. Trapping describes the formation and downstream movement of free eddies named as fluid bolus. The net upstream convection of the fluid in opposition to the progressing boundary waves is referred as bolus. These two phenomena are of great physiological significance, as they may be accountable for formation of thrombus in blood, and pathological bacteria transport. From the fluid mechanics point of view, though these phenomena reveal the complexity they also motivate the primary study of peristaltic flows.

When the motion of the fluid is opposite to the peristaltic wave it is termed ‘reflux’. Due to the reflux motion the axial velocity might be negative. This occurs in certain abnormal conditions as in hydro ureters. The onset of reflux phenomenon is influenced by the non-Newtonian character.

Trapping is one of the chief characteristics of peristaltic transportation phenomenon. It takes place when the streamlines on the central line divide to encircle a bolus of fluid particles moving along the closed streamlines in the wave frame of reference. The trapped bolus then travel with the same speed as that of the wave propagation velocity. Trapping can be defined as the region of closed stream lines in the wave frame at high flow rates and large conclusions.

1.5 Porous media

Porous medium is a matter that consists of a solid matrix with inter-connected pores. Origin of the flow through porous media owes to Darcy's experimental law which states that the velocity is in proportion with the pressure gradient and do not contain the convective acceleration and viscous stress of the fluid.

Darcy's law gives an equation that explains the motion of a fluid through a porous medium. Henry Darcy's exploration into the hydrology of the water supply of Dijon and his experiments on steady-state unidirectional flow in a uniform medium exposed a proportionality involving flow rate and the applied pressure difference given by the relation $u = -\frac{k}{\mu}\frac{\partial p}{\partial x}$. Here $\frac{\partial p}{\partial x}$ denotes the pressure gradient in the direction of the flow and μ denotes the dynamic viscosity. The coefficient k denotes the specific permeability that depends on the geometry of the medium and is independent regarding the nature of the fluid.

Flow through porous media plays an important role in nearly all fields of engineering and biomechanics: material science, the petroleum industry, chemical engineering and in particular, in soil mechanics as well as in various areas of biomechanics. Most of the tissues in the body are deformable porous media (e.g. cartilage, bone, muscle, lungs (Figure 1.9), gall bladder (Figure 1.10)).

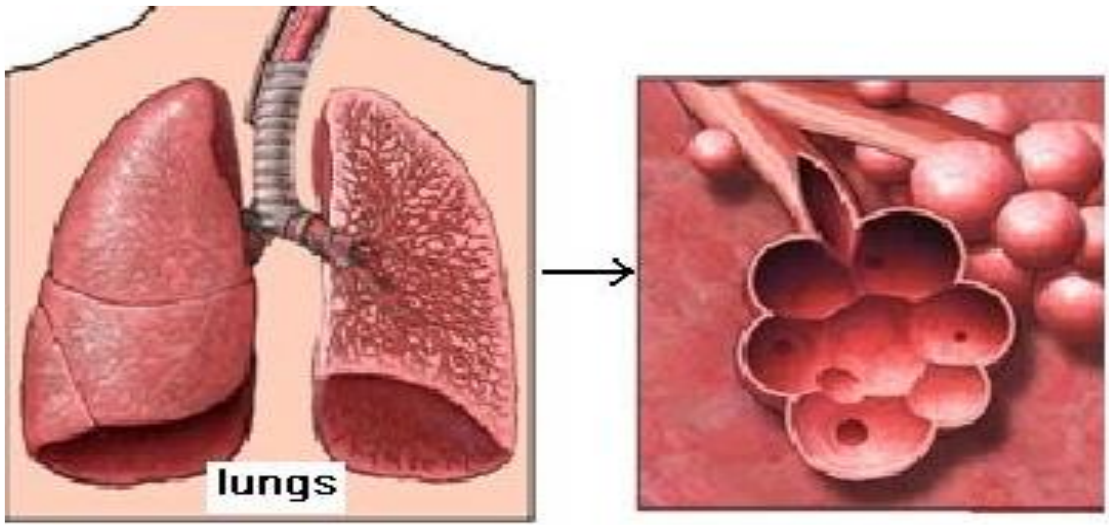

Figure 1.9: Human lungs

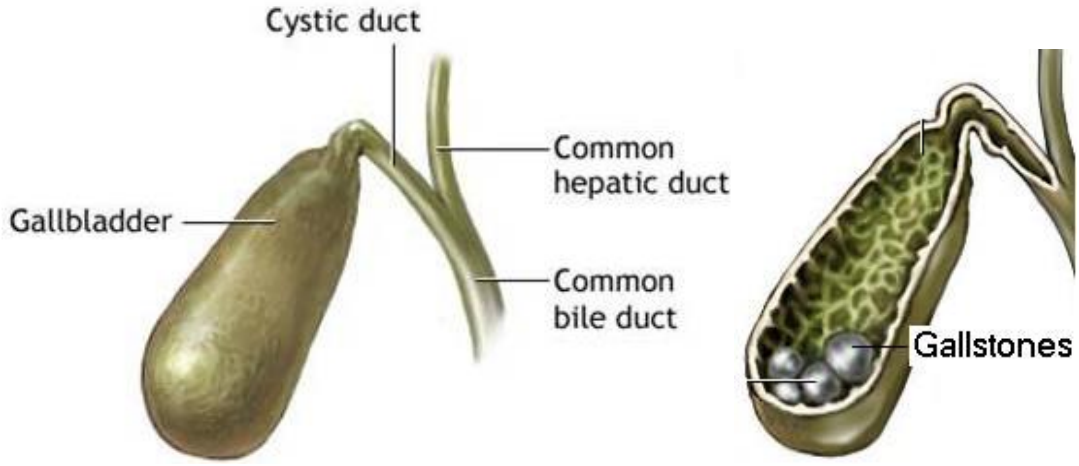

Figure 1.10: Gall bladder

Carbonate rock

Sand stone

Vesicular basalt

Beach sand

Figure 1.11: Examples of natural porous media

Many natural substances such as carbonate rock, sand stone, vesicular basalt, beach sand etc.(Figure1.11) can be considered as porous media. Physiological models of porous medium exploit the various medical conditions and treatments such as injections and tumor growth.

1.6 Slip condition

Usually, no slip condition is applicable when a Newtonian/non-Newtonian fluid move over an inflexible surface but when the fluid moves over a rough/porous lined surface, the no slip condition is inapplicable on that surface. The slip boundary condition was first initiated by Navier. It stated that at the boundary the velocity is in proportion to the shear stress.

Recent experiments show that slip displays an important part in the development of higher concentration variations in entangled polymeric solutions. Possibly two mechanisms for slip are noticed: desorption of absorbed molecules from the surface and sorting out of anchored chains from the bulk material. The effect of slip may be important on the flow behavior of gasses and liquids especially when the fluid film thickness is very small. The no slip condition states that velocity components vanish at the boundaries as the fluid flows over a rigid plate.

The existence of slip flow at the porous boundary has also been demonstrated by Beavers and Joseph [2] and it has further been supported by Saffman [3]. Saffman suggested the generalized Darcy law for the motion of a viscous fluid through non-homogeneous porous medium given by $u = \frac{\sqrt{Da}}{\beta}\frac{du}{dy} + o(k)$. This law is introduced to describe the flow within a boundary layer joining the Darcy flow region within the solid to a Stokes flow region outside. He observed that the particular form of the Beavers and Joseph slip condition is applicable for planar permeable boundaries. Further, he found that this condition is not valid to $o(k)$ using standard boundary layer techniques and shows that in the limit $k \to 0$.

1.7 Magnetohydrodynamics (MHD):

Magnetohydrodynamics (MHD) is the study of electrically conducting fluid influenced by electromagnetic field. The motion of conducting fluid generates electric currents across

the magnetic field that leads to the formation of mechanical forces and modify the motion of the fluid. The principle of magnetic field is applied in the medical field in the form of a device called Magnetic Resonance Imaging (MRI). The magneto hydrodynamic (MHD) peristaltic flow has gained importance in the study of conductive fluids such as blood and also in blood pump machines.

Flow of blood takes place in two layers. One in plasma layer which is near the wall and other one is the core layer which consists of suspension of cells in the plasma. The core is treated as magnetic field because red blood cells have iron which is magnetic in nature. Magnetism affects the human body through the nervous system, circulatory system and the endocrine system.

The basic equations that govern the flow influenced by MHD (after neglecting displacement currents) are

1. Generalized Ohm's law is: $\bar{J} = \sigma(\bar{E} \times + \bar{q} \times \bar{B})$ and
2. Maxwell's equations are: $\nabla \cdot \bar{B} = 0,\ \nabla \times \bar{E} = -\frac{\partial \bar{B}}{\partial t},\ \nabla \times \bar{B} = \mu_m \bar{J}$.

where $\bar{E}$ is the electric field, $\bar{J}$ is the Joule current, μ_m is the magnetic permeability, $\bar{B}$ is the external magnetic field, $\bar{q}$ is the velocity vector and σ is the electrical conductivity of the fluid.

The assumptions made are

- The magnetic Reynolds number is low because, compared to the applied magnetic field the induced magnetic field is minute.
- The electric field is presumed as zero.
- Through the flow field μ_m is constant.

1.8 Heat transfer

The study of peristaltic transport along with heat transfer has attracted many researchers due to various applications in biomedical science. Heat transfer in human body is currently considered as one of the significant areas of research because of its involvement in many complicated practices as in: dilution technique in examining blood flow, destruction of undesirable cancer tissues, evaluating skin burns, vasodilation and radiation

between surface and its environment, paper making and food processing. The blood flow rate under thermal conditions is computed using the concept of heat transfer. In regard of the human thermoregulation structure and thermotherapy, bio-heat transfer in tissues has been attracted by the biomedical engineers.

The basic equation that govern the flow under heat transfer is the first law of thermodynamics (i.e. conservation of energy), written in the following form (assuming no mass transfer).

$\rho C_p \frac{\partial T}{\partial t} = K\nabla^2 T + \bar{q}v$, where $\bar{q}v$ is the volumetric heat source, ρ is the density of the fluid, T is the temperature of the fluid, K is the thermal conductivity, C_p is the specific heat at constant pressure.

1.9 Literature survey

The relevance of peristaltic flow in physiology was brought out mainly through the works of Kill [4]. The study on the mechanics of peristaltic motion was first experimentally examined by Latham [5]. These experimental results were in accordance with the theoretical results examined by Shapiro [6]. Burns and Parkes [7] considered the above experimental work and sinusoidal variations on the walls to investigate the flow of a viscous fluid through a pipe and a channel. A theoretical establishment of peristaltic flow developed by sinusoidal transverse waves of small amplitude for inertia-free Newtonian fluids was suggested by Fung and Yih [8]. They found that a backward motion in the mid region of the stream is generated when pumping in opposition to a positive pressure gradient is higher than a critical value. Shapiro et al. [9] obtained the solution in the closed form considering a continuous train of peristaltic waves for low Reynolds number flow, under large wavelength and arbitrarily chosen wave amplitude. They found that there were two major phenomena: trapping and reflux in physiology. A long wavelength approach to peristaltic motion was also carried by Zien and Ostrach [10]. Jaffrin and Shapiro [1] explained the basic principles of peristaltic pumping. They studied consequence of the different parameters governing the flow. Comparison of experiment and theory in peristaltic flow was analyzed by Yin and Fung [11]. Bohme and Friedrich [12] observed peristaltic transport mechanism of an incompressible visco-elastic fluid.

Pozrikidis [13] investigated the flow in two-dimensional channel with sinusoidal waves under the assumption of creeping motion.

Theoretical study of viscous effects in peristaltic pumping was investigated by Provost and Schwarz [14]. Toklu [15] developed a new mathematical model for peristaltic motion in the esophagus. Obtaining the manometric dimensions of luminal pressure in the esophagus he studied with both mechanical as well as biological point of analysis.

A huge work covering on mathematical and experimental models in a Newtonian or non-Newtonian fluid in a conduit has been carried out. Most of the researchers examined the fluid to behave like a Newtonian fluid (with constant viscosity) for psychological peristalsis including the flow of blood in arterioles. Gupta and Seshadri [16] investigated the transportation of a viscous Newtonian fluid under peristalsis. Misery et al. [17] investigated an incompressible generalized Newtonian fluid flow in a planar conduit under peristaltic movement. Abd El Naby and Misery [18] examined the impacts of an endoscope on the peristaltic flow of generalized Newtonian fluid. A Newtonian fluid in an asymmetric channel was considered by Mishra and Rao [19] for peristaltic transport analysis. Mekheimer [20] observed peristalsis in an annulus considering Newtonian fluids. The effect of variable viscosity of Newtonian fluid moving in an asymmetric channel under peristalsis was explored by Hayat and Ali [21].

It is known that many of the physiological fluids act as non-Newtonian fluids. Lew et al. [22] stated that chyme is a non-Newtonian substance which has plastic-like property. Taking a non-Newtonian power-law fluid into consideration theoretical analysis of blood motion was given by Raju and Devanathan [23]. Gold Smith and Skalak's [24] study revealed that in the body organs, the viscosity of the fluid shows a discrepancy across the thickness of the duct. Considering the casson model-II, the peristaltic flow in blood was studied by Srivastava and Srivastava [25]. Rath and Reese [26] examined peristaltic flow of non-Newtonian fluids containing small spherical particles. Srivastava and Srivastava [27] looked into the peristaltic flow of a non-Newtonian fluid to know its applications in small intestine and vas deferens. Regarding blood as a non-Newtonian fluid Maiti and Misra [28] examined the features of peristaltic transport in micro-vessels.

In many of the investigations the walls of the duct are assumed to be rigid, but in most of the physiological situations, the walls are elastic in nature, i.e., walls get excited by the smooth muscle contractions whose tension controls its deformation.

Mittra and Prasad [29] analyzed the transport of Newtonian fluid under peristalsis to know the effects of the viscoelastic behavior of walls. The dynamic mechanism is presumed to be due to the imposition of moderate amplitude sinusoidal wave on the flexible walls of the channel. Muthu et al. [30] observed the impact of compliant wall properties on the transport of a micropolar fluid under peristalsis. The wall property effects on the peristaltic transport of a dusty fluid have been analyzed by Srinivasacharya et al. [31]. They found the expressions for mean velocity of the fluid and solid particles, and mean flow rate. Mokhtar et al. [32] developed a model to analyze the effect of wall characteristics of a viscous fluid flowing under peristalsis. Impact of compliant wall properties on the transport of a Herschel-Bulkley fluid under peristalsis is observed by Sankad and Radhakrishnamacharya [33]. Ali et al. [34] illustrated the importance of wall impacts on the transport of Maxwell fluid under peristalsis. Sankad and Radhakrishnamacharya [35] examined the effect of compliant wall properties on the motion of micropolar fluid considering long wavelength approximation.

It is observed that several physiological fluids flow in porous medium. The study of flows through porous media has become prominent due to the vast applications in physiological and geophysical fluid dynamics.

Several researchers have applied the generalized Darcy's law in their research on porosity. Flow in porous medium studied by using Darcy's law is given by Scheidegger [36]. A generalized Newtonian fluid flowing inside a channel with porosity, under peristalsis was analyzed by Elshehawey et al. [37]. They investigated the flow assuming long wavelength, in a moving frame of reference moving with the velocity same as that of the wave. Flow through porous medium channel under peristalsis was observed by Maiti and Misra [38]. Tripathi et al. [39] studied creeping sinusoidal motion through a highly permeable two dimensional channel considering a bio-rheological fluid for observation.

It has been noticed that slippage can take place in non-Newtonian fluids also. The study of peristalsis with slip effects has expected significant interest in the last few decades due to its applications in industry and physiological processes.

Kwang and Fang [40] analyzed the peristaltic flow inside a 2D micro channel containing a Newtonian fluid, influenced by slip. Experimental analysis of Tretheway et al. [41] reveals that fluid displays slip flow whenever the mean free path of the molecules is in comparison with the space between the plates as observed in the micro channels or the nano channels. Analytical solutions have been obtained by Hron et al. [42] for motions

comprising of a generalized fluid having double complexity, assuming that at the boundary, the flow satisfies Navier slip conditions. Ellahi [43] examined the effects of slip on the non-Newtonian transport in a channel. Motion of a nano fluid through a channel moving under peristalsis having compliant walls and slip effect was studied by Mustafa et al. [44]. They discussed the analytic expressions regarding temperature and nono particle concentration through Homotopy analysis method. Sreenadh et al. [45] examined analytical derivations for peristaltic transport of conducting nano fluids in an asymmetric channel with slip effects of velocity, temperature and concentration.

MHD deals with the dynamics of electrically conducting fluids. The study of magnetohydrodynamic (MHD) flow problems has been a subject of concern due of its vast engineering and medical relevance. MHD flows have various applications in medical devices and bioengineering, especially for reduction of bleeding during surgeries, cancer treatment causing hyperthermia and transport of drugs to the targets by means of magnetic particles.

Srivastava and Agrawal [46] have observed that blood constitutes of plasma where in red cells occur in suspension. They considered blood as an electrically conducting fluid. Agarawal and Anwaruddin [47] inspected the consequences of magnetic field being applied on the peristaltic transport of blood with the assumption of long wavelength. They clarified that for flow of blood within the arteries by way of arteriosclerosis or arterial stenosis, magnetic field influence may be employed for controlling the pumping action of blood while doing the cardiac operations. The influence of slip on the sinusoidal motion of MHD fluid wherein the viscosity is variable is examined by Ali et al. [48]. Hayat et al. [49] carried out the research on the flow of a Johnson-Segalman fluid in a channel, considering compliant wall under peristalsis, to analyze the effects of magnetic field. Sankad and Radhakrishnamacharya [50] studied micropolar fluid influenced by MHD peristaltic motion under wall effects. Jain et al. [51] observed the consequences of MHD flow of blood in narrow capillaries. The influence of magnetic and wall properties on the transport of micropolar fluid under peristalsis was put forth by Afifia et al. [52]. Gupta [53] studied the magnetic effect on the flow of blood through small vessels. The flow of dusty fluid under MHD effect through a porous uniform channel having elastic wall properties has been studied by Parthasarathy et al. [54].

Heat transfer plays a significant role in the cooling processes of industrial and medical applications. Many of the physiological fluids as well as fluids in engineering system have thermodynamic properties.

Radhakrishnamacharya and Radhakrishna Murthy [55] examined the interaction of heat flow and peristalsis of an incompressible viscous fluid moving inside a two dimensional non uniform channel. Using the long wave approximation Vajravelu et al. [56] looked into the effects of heat transmission in a vertical porous annulus underneath peristaltic motion. Radhakrishnamacharya and Srinivasulu [57] studied effect of wall properties and heat transfer on peristaltic transport. The peristaltic transport inside a porous space having MHD and compliant walls was studied for heat and mass transfer analysis by Srinivas and Kothandapani [58]. Ramana Kumari and Radhakrishnamacharya [59] examined the peristaltic motion underneath the influence of magnetic effect and examined the slip and wall effects due to heat transfer. Considering the movement of food bolus inside the esophagus, Sreenadh et al. [60] explored the effects of heat transfer and wall properties under peristalsis. The wall property effects and heat transfer influence on the flow of power-law fluid under the peristaltic motion has been analyzed by Hayat et al. [61]. The consequences of wall effects on the motion of a dusty fluid through porous peristaltic conduit under heat and mass transfer is worked out by Eldabe et al. [62]. The resulting equations were solved analytically by perturbation technique. Eldabe et al. [63] studied the peristaltic motion of non-Newtonian MHD fluid through a permeable channel. Hina [64] examined peristaltic transport of Eyring-Powell MHD fluid with slip and wall effects under heat/mass transfer. The transport of Williamson fluid in an asymmetric peristaltic inclined channel with porosity was examined by Ramesh and Devakar [65] to analyze the heat and magnetic effects. The peristaltic transport of a Third grade fluid with hall current and heat transfer was investigated by Vafai et al. [66]. Sinha et al. [67] took into consideration the heat transfer effect on unsteady magnetohydrodynamic flow of blood in a permeable vessel under the existence of non uniform heat resource.

1.10 Problem statement

The exploration of couple stress fluid is of importance to understand various physiological problems as it holds the mechanism that describes rheologically complex fluids viz. liquid crystals , polymeric suspensions, animal and human blood.

It is considered that the blood and other physiological fluids exhibit Newtonian as well as non-Newtonian behaviors. Among the wide range of non-Newtonian fluids Jeffrey fluid model is preferred as the Newtonian fluid model can also be obtained by Jeffrey model.

Thus, in view of studying couple stress fluid and Jeffery fluid the following research issues have been considered.

What effects do the wall and slip properties have on the peristaltic transport of a couple stress fluid in a permeable medium? What effect may this flow have if influenced by MHD effect and further by MHD as well as heat effects? Further what might be the consequences of the flow on trapping phenomenon?

In addition what might be the effects of the above studies when a Jeffery fluid is taken into consideration instead of the couple stress fluid.

1.11 Objective of the research

The objective of the thesis is to examine peristalsis by analytical method, and assess appropriate conclusions when applied to the peristaltic problems. The mathematical formulation is based on some suppositions leading to tractable analytical solutions of the problem to examine the relation between parameters.

The main objective is to study the flow of couple stress fluid and Jeffrey fluid models to examine the slip effect, MHD and heat transfer effects in a uniform peristaltic porous channel having compliant walls. The flow is modeled taking into consideration long wave length and small Reynolds number approximations.

The significant concepts and the governing equations of the two non-Newtonian fluid models, namely, couple stress fluid and Jeffrey fluid used in this thesis are described below.

1.12 Methodology

The regular perturbation method is applied for solving the various problems. Here long wave length approximation and low Reynolds number assumptions are made.

The long wave length approximation assumes that the half width of the peristaltic channel is small in comparison with the wave length. Further low Reynolds number ensures the flow to be inertia free. These considerations are significant for the case of physiological flows wherein half width of the arterioles, veins and intestine are considered to be small in comparison to the wavelength of the peristaltic wave.

1.13 Couple stress fluid

The discrepancy of the real fluids compared with that of the behavior of Newtonian fluids is well explained by the couple stress fluid theory. The equations that govern the couple stress fluid motion are none other than the Navier Stokes equations, except for the order of this differential equation is greater by two. Since the introduction of this theory in 1966 by Stokes [68] many researchers in the field of fluid dynamics have concentrated on the study of couple stress fluid flow.

The equations of motion characterizing the incompressible couple stress fluid motion, (after neglecting body couples and body forces) as given by Stokes are

$$\nabla \cdot \vec{q} = 0, \tag{1.1}$$

$$\rho\left[\frac{\partial \vec{q}}{\partial t} + \vec{q} \cdot \nabla \vec{q}\right] = -\nabla p - \mu \nabla^2 \vec{q} - \eta \nabla^4 \vec{q}, \tag{1.2}$$

where $\bar{q}$ denotes velocity vector, p denotes pressure, t denotes time, ρ denotes density, η denotes the couple stress viscosity and μ denotes the coefficient of viscosity.

The equations (1.1) and (1.2) respectively represent the principles of mass conservation and linear momentum.

The constitutive equation containing the deformation rate tensor d_{ij} and stress tensor t_{ij} is written as

$$t_{ij} = -P\delta_{ij} + \lambda(\nabla \cdot \vec{q})\delta_{ij} + 2\mu d_{ij} - \frac{1}{2}\epsilon_{ijk}\left(m_{,k} + 4\eta_1 \omega_{k,rr}\right). \tag{1.3}$$

For the couple stress tensor, m_{ij} in the theory, a linear constitutive relation is observed as

$$m_{ij} = \frac{1}{3} m\delta_{ij} + 4\eta_1 \omega_{j,i} + 4\eta' \omega_{i,j}\,, \tag{1.4}$$

where $\omega_{i,j}$ denotes the spin tensor, d_{ij} denotes the tensor of deformation rate derived from the velocity vector and m denotes the trace of the couple stress tensor. The viscosity coefficients are denoted by λ and μ the couple stress viscosity coefficients are denoted by η_1, η'.

These constants are bounded by the following inequalities:

$$\mu \geq 0; \qquad 3\lambda + 2\mu \geq 0; \qquad |\eta'| \leq \eta_1. \tag{1.5}$$

Here $l = \sqrt{\frac{\eta_1}{\mu}}$ is the length parameter that measures the polarity of the fluid model characteristically and for non polar fluids this parameter is identically zero.

The velocity vector $\vec{q}$ and the effect of couple stresses on the tangential component of the spin vector $\varpi = \frac{1}{2}\nabla \times \vec{q}$ can be prescribed so as to synchronize with their respective values on the boundary.

As the couple stress fluid possess the mechanism that explains complex rheological fluids as seen in blood and liquid crystals, the study of couple stress fluid has gained importance in the recent years. Couple stress fluid takes the particle size into account wherein it represents a Newtonian fluid as a special case. Numerous research works pertaining to couple stress fluid is brought out by Srivastava [69]. The research carried on the couple stress fluid is much helpful in many physical problems as it can explain the rheologically complex fluids like liquid crystals.

The transport of couple stress fluid under peristalsis has been analyzed by El Shehawey and Mekheimer [70]. Kothandapani and Srinivas [71] examined the MHD peristaltic flow influenced by heat to examine the compliant wall impact on the motion of couple stress fluid. Pulsatile flow in a permeable medium flexible channel under peristalsis was studied by Ravi Kumar and Siva Prasad [72], for a couple stress fluid. Pandey and Chaube [73] gave a report on the motion of couple stress fluid under peristalsis, within a conduit having wall properties. They showed that the boundary velocity of the fluid reduces with gain in couple stress parameter. The couple stress fluid was analyzed for peristaltic flow to know the relevance in hemodynamics by Maiti and Misra [74]. Raghunath Rao and Prasad Rao [75] examined the flow of a couple stress fluid under peristalsis moving through a two dimensional flexible permeable medium and they observed that pressure rise has reverse actions compared to frictional force. Ravi Kumar

[76] studied the couple stress fluid flowing through a magnetohydrodynamic permeable medium channel leaning to the horizontal to analyze the blood flow under peristalsis with slip condition.

1.14 Jeffrey fluid

The Jeffrey fluid model is used to model the particular physiological flow of fluids as it is a simple linear model that makes use of the time derivative in place of convective derivative and represents a rheology away from the Newtonian fluid. But, consequently the model for Newtonian fluid can also be figured out with the help of Jeffrey model as a particular case. Researchers have analyzed the Jeffrey fluid under various conditions.

Though the study of Jeffrey fluid leads to complicated geometries and solutions of nonlinear equations, flow of Jeffrey fluid under peristalsis has gained importance because of its extensive applications in industry and physiology. Numerous systems in the body use this technique to propel and to mix the contents.

The equations that govern the flow of a Jeffrey fluid are

$$\bar{T} = -\bar{P}\bar{I} + \bar{S},$$

$$\bar{S} = \frac{\mu}{1+\lambda_1}\left(\frac{\partial \bar{\gamma}}{\partial t} + \lambda_2 \frac{\partial^2 \bar{\gamma}}{\partial t^2}\right),$$

where λ_1 denotes the ratio of the relaxation to retardation times, λ_2 denotes the retardation (delay) time, $\bar{I}$ denotes the identity tensor, $\bar{P}$ denotes the pressure, $\bar{S}$ denotes the extra stress tensor, $\bar{T}$ denotes the Cauchy stress tensor and $\bar{\gamma}$ denotes the shear rate.

Many non-Newtonian fluids such as viscoelastic fluids including Maxwell fluid models, Casson models and Oldroyd-B models needs modification of the momentum conservation equation. Inspite of numerous rheological models being developed the Jeffrey model is identified to be simple, yet elegant rheological model. This model was primarily established for simulation of flow problems in concern with the earth's crust.

The Jeffrey model includes a viscoelastic model that shows the characteristics of yield stress, shear thinning and high shear viscosity. As and when the wall stress becomes very much higher compared to the yield stress, the wall shear stress becomes very high and the Jeffrey's model disintegrates to a Newtonian model.

Kothandapani and Srinivas [77] considered the Jeffrey fluid and explored the motion through an asymmetric channel influenced by magnetic field and peristalsis. Hayat et al. [78] examined the consequences of magnetic effect and endoscope on the peristaltic flow involving Jeffrey fluid. Pandey and Tripathi [79] modeled Jeffrey fluid flow under the unsteady peristaltic motion. Suryanarayana Reddy et al. [80] did their advanced research work on the peristaltic transport in a porous conduit inclined to the horizontal and influenced by magnetic field. They considered Jeffrey fluid for their analysis.

Considering the peristaltic motion in a vertical porous stratum, the effects of heat transfer over the flow of Jeffrey fluid is examined by Vajravelu et al. [81]. Peristaltic transport of a Jeffrey fluid with partial slip in a MHD asymmetric conduit is inspected by Rajanikanth et al. [82]. Considering the Jeffrey fluid flowing in a rectangular duct Nadeem et al. [83] studied peristalsis with compliant wall effects. Abd- Alla et al. [84] investigated gravity and magnetic effects on the Jeffrey fluid through a non-symmetric peristaltic channel. Ellahi and Hussain [85] examined the flow in a rectangular duct to analyze the simultaneous effects of MHD and partial slip considering the Jeffery fluid under peristaltic motion. Analysis of pumping when a power-law fluid comes in contact with a Jeffrey fluid was carried out by Sreenadh et al. [86]. The sinusoidal flow was considered in an inclined channel having porous walls.

1.15 Outline of the Thesis

This thesis deals with some results on time average velocity, heat transfer coefficient and temperature distribution with respect to various parameters. Analyzing some of the research papers concerned with peristalsis, study has been carried out to give details of the results that have not yet been provided.

Chapter 1 presents the introduction and provides motivation to the research work carried out in the thesis. A survey of pertinent literature is given to show the significance of the problems considered. The basic equations governing the flow of couple stress and Jeffrey fluids are given.

Chapters 2 to 4 considers peristaltic motion of couple stress fluid wherein chapters 5 to 7 deal with peristaltic motion of Jeffrey fluid under different conditions. For the analysis long wavelength approximation and low Reynolds number assumptions are considered.

Chapter 2 reports the peristaltic transport of an incompressible couple stress fluid in a uniform channel having compliant wall and slip effects in porous medium. The elastic wall properties in peristalsis are studied through the dynamic boundary conditions. Obtaining solutions for the time average velocity and stream function, the effects of various parameters like elastic parameters, Darcy number and slip effects have been examined through the graphs. In case of presence of elasticity parameters, we observe that the time average velocity decreases as the couple stress parameter increases. It is observed that with the increase of slip parameter, the time average velocity increases. The physiological benefit of this analysis may be owed to the study of microcirculatory flow of blood under the slip condition. The trapped bolus is observed to increase in size with increase in couple stress parameter and Darcy number while it decreases with the slip parameter.

The effectiveness of the analytical solution of time average velocity for magnetohydrodynamic (MHD) peristaltic flow of an electrically conducting incompressible and viscous couple stress fluid in a uniform porous channel with elastic walls is analyzed and assessed in chapter 3. Using dynamic boundary conditions, analytic expressions have been expressed for time average velocity and stream function. The effects of slip condition are studied. Various aspects like Hartmann number, Darcy number, slip parameter, couple stress parameter are discussed through graphs under the presence and absence of both stiffness and viscous damping force. It is noticed that the magnitudinal value of time average velocity decreases with increase in the Hartmann number in presence of elastic parameters. As the Darcy number *Da* increases, the time average velocity decreases. Further, it is observed that trapping occurs and size of the bolus increases with Hartmann number.

In chapter 4, the magnetohydrodynamic (MHD) couple stress fluid is considered to flow under porous peristaltic movement to study the wall, slip and heat transfer effects. Obtaining the solutions for coefficient of heat transfer, time average velocity and temperature distribution the impacts of various parameters are explored through graphs. It is observed that enhancing the values of slip parameter, Brinkman number, Darcy number and the elastic parameters the temperature profile increases. Also, as the value of Darcy number is raised the absolute value of heat transfer coefficient rises.

Chapter 5 deals with the peristaltic flow of an incompressible Jeffrey fluid in a permeable channel having wall properties to analyze the slip effects. Velocity per one wave length

and stream functions, are obtained mathematically. The flow is examined to study the results of various parameters. The influence of Jeffrey parameter, permeability parameter, slip parameter and elastic parameters are discussed and shown graphically. It is found that the time average velocity reduces as the Darcy number and slip parameter increase and increases as the Jeffrey parameter rises. It is found that the size of the trapped bolus increases with Darcy number.

Chapter 6 presents new analytic results for magnetohydrodynamic (MHD) motion of a Jeffrey fluid. The Jeffrey fluid is assumed to flow through the porous space under slip effects. The magnetic field is applied uniformly along the y-axis. The flow under investigation is considered to be moving along with the velocity of the wave. The solutions for time average velocity and stream function are obtained using lubrication approach. Also, graphs are drawn for the relevant parameters to explore the characteristics of velocity field and stream lines. It is found that the value of average velocity increases due to an increase in Jeffrey parameter and Hartmann number. Further, it is observed that the trapped bolus diminishes with increase in the values of Jeffrey parameter and Hartmann number. Studies through MHD flows give an insight into the therapeutic use of imposing external magnetic field in the clinical treatment of hemodynamic diseases, like hypertension.

Chapter 7 deals with incompressible Jeffrey fluid under peristalsis moving in a permeable conduit. Magnetic effect and slip effect are studied for this channel under the existence of wall slip and heat transfer. Time average velocity, heat transfer coefficient and temperature distributions are obtained analytically. Effects of Hartmann number (magnetic number), slip parameter, elasticity parameters and Brinkman number on the coefficient of heat transfer and temperature distribution field are graphically discussed. It is observed that in the case of temperature distribution the flow intensity enhances with rise in the Darcy number, while it reduces with enhancement in the Brinkman number and slip parameter. Graphs reveal that the heat transfer coefficient increases magnitudinally with increase in Jeffrey parameter and Hartmann number.

Chapter 8 gives the main conclusions and scope for future study.

Chapter 2

Influence of the Wall Properties on the Peristaltic Transport of a couple Stress Fluid with Slip Effects in Porous Medium

2.1 Introduction

Peristaltic motion is a well-known natural phenomenon of fluid mixing and transport that takes place in biological tracts. The mechanism behind this is the progressive wave moving along the boundaries of the tract from the region of low pressure to high pressure through pumping action studied by Yin and Fung [87]. In particular, it occurs in many physiological situations like transport of mixture of food grains and liquids in the esophagus, transport of urine through the ureter, in small blood vessels to transport blood, etc. This system appears in many industrial and physiological processes to pump sanitary and corrosive fluids.

Kill's [4] research work has given relevance about the physiological applications of peristalsis. Latham [5] initiated the concept of peristaltic mechanism. Since then, this mechanism has turned into a major area of research in the direction of the numerous applications in field of biomedical engineering and technology. Shapiro et al. [9] talked more about peristaltic flow under long wavelength and small Reynolds number assumptions. Weinberg et al. [88] observed pumping through peristalsis experimentally. Misra and Pandey [89] studied the blood flow in small vessels by modeling the peristaltic flow mathematically.

The couple stress fluid is treated as a specialized class of non-Newtonian fluids that takes the effect of particle size into account. Stokes [68] did the first attempt to study couple stress. Taking into account the proportion of erythrocytes (particles), Stokes observed flow of blood in micro vessels. Due to the non-Newtonian behavior of blood, many researchers have examined the peristaltic motion of non-Newtonian fluids by considering different kind of fluid model under different conditions, wherein they found distinguishable effects of wall motion on velocity and other flow characteristics. Some researchers have carried out the flow of non-Newtonian fluids considering blood as the couple stress fluid moving under peristalsis. Although a certain amount of slip exists in real systems, researchers have considered the no slip condition. There are two distinctive groups of fluid that come into view to slip. One group has rarefied gases examined by Kwang and Fung [90], the other group has a large amount of flexible character. In these fluids, few slippage takes place under tangential traction which is large. Sobh [91] studied the impact of slip velocity for a couple stress fluid within non uniform and uniform channels under peristalsis. Alsaedi et al. [92] examined peristalsis of a couple stress fluid

with in a uniform porous medium. Hina et al. [93] observed peristaltic flow of couple stress fluid with wall properties.

The study of couple stress fluids has applications in lubrication theory, squeeze film and in the bearing system. Also, it has several industrial applications such as thickened oils, synthetic fluid, colloidal solutions, freezing of metallic plate in a bath, etc.

In this chapter, a uniform channel is considered for the analysis of peristaltic motion. The flow is modeled for couple stress fluid along with slip conditions at the boundary. The channel medium is assumed to be porous having compliant wall properties. Assuming low Reynolds number and long wavelength approximations the analytic solutions for time average velocity and stream function are obtained. The consequences of various parameters on peristaltic flow are examined.

2.2 Physical assumptions of the problem

The peristaltic motion in a porous uniform two dimensional channel of width $2d$ is considered with an incompressible couple stress fluid inside. A sinusoidal wave is assumed to travel down the elastic membranes of the channel with constant speed c. Cartesian coordinate system with x -axis and y -axis along and normal to the direction of the mean position of the elastic walls are taken into consideration as shown in Figure 2.1.

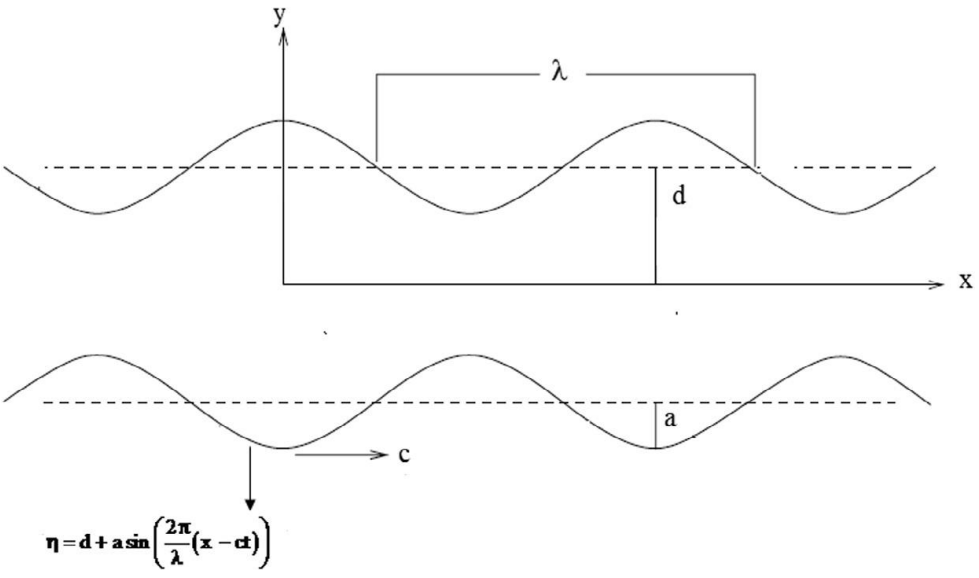

Figure 2.1: Motion of the fluid through a channel

The equation of vertical displacement of wave shape of the channel membrane is represented as

$$y = \pm\eta(x,t) = \pm(d + a\,sin\frac{2\pi}{\lambda}(x - ct)), \tag{2.1}$$

where a is the wave amplitude, t is the time and λ is length of the wave.

The flexible wall motion is governed by the following equation

$$L(\eta) = p - p_0. \tag{2.2}$$

Here, L represents the elastic wall motion with viscous damping force given by

$$L = -T\frac{\partial^2}{\partial x^2} + m\frac{\partial^2}{\partial t^2} + C\frac{\partial}{\partial t}. \tag{2.3}$$

Here T, m and C respectively represent elastic wall tension, mass of a substance applied to a given area and damping force of the viscous material. Interaction pressure is denoted by p. Due to the tension in the muscles pressure is exerted on the outer surface of the wall and is denoted by p_0. Only the lateral movements normal to the direction of the undeformed position takes place as the channel walls are inextensible and $p_0 = 0$ (assumption). Hence it can be assumed that there is no horizontal displacement.

The basic equations governing the peristaltic transport of the couple stress fluid flow through the permeable medium for negligible body couples and body forces are

The equation of mass conservation is

$$\frac{\partial u}{\partial x} + \frac{\partial u}{\partial y} = 0. \tag{2.4}$$

The equations of momentum conservation are

$$\rho\left(\frac{\partial u}{\partial t} + u\frac{\partial u}{\partial x} + v\frac{\partial u}{\partial y}\right) = -\frac{\partial p}{\partial x} + \mu\nabla^2 u - h\nabla^4 u - \mu\frac{u}{k}, \tag{2.5}$$

$$\rho\left(\frac{\partial v}{\partial t} + u\frac{\partial v}{\partial x} + v\frac{\partial v}{\partial y}\right) = -\frac{\partial p}{\partial y} + \mu\nabla^2 v - h\nabla^4 v - \mu\frac{v}{k}. \tag{2.6}$$

Velocity component along the horizontal (x-axis) path is $u(x,y,t)$ and along the vertical(y-axis) path is $v(x,y,t)$, k denotes the porous permeability, ρ denotes the

density of the fluid, μ denotes the coefficient of viscosity and h the constant related with couple stress, also $\nabla^2 = \frac{\partial^2}{\partial x^2} + \frac{\partial^2}{\partial y^2}$, $\nabla^4 = \nabla^2\nabla^2$.

The conditions at the boundary are

$$\frac{\partial u}{\partial y} = 0, \quad \frac{\partial^3 u}{\partial y^3} = 0, \qquad at \quad y = 0, \tag{2.7}$$

$$u = -d\frac{\sqrt{Da}}{\beta}\frac{\partial u}{\partial y}, \quad at \ y = \pm\eta(x,t), \tag{2.8}$$

represents the slip condition where Da is the Darcy number and β is the slip parameter.

$$-\left(\frac{\partial^2 v}{\partial x^2} - \frac{\partial^2 u}{\partial x \partial y}\right)\frac{\partial \eta}{\partial x} + \frac{\partial^2 v}{\partial x \partial y} - \frac{\partial^2 u}{\partial y^2} = 0, \qquad at\ y = \pm\eta(x,t)\,. \tag{2.9}$$

The boundary condition with reference to Mittra and Prasad [29] is

$$\frac{\partial}{\partial x}L(\eta) = -\rho\left(\frac{\partial u}{\partial t} + u\frac{\partial u}{\partial x} + v\frac{\partial u}{\partial y}\right) + \mu\nabla^2 u - h\nabla^4 u - \mu\frac{u}{k}, \quad at \ y = \pm\eta(x,t), \tag{2.10}$$

where

$$\frac{\partial}{\partial x}L(\eta) = \frac{\partial p}{\partial x} = -T\frac{\partial^3 \eta}{\partial x^3} + m\frac{\partial^3 \eta}{\partial x \partial t^2} + C\frac{\partial^2 \eta}{\partial x \partial t}. \tag{2.11}$$

Substituting the subsequent dimensionless parameters

$$x' = \frac{x}{\lambda}, y' = \frac{y}{d}, t' = \frac{ct}{\lambda}, u' = \frac{u}{c}, v' = \frac{\lambda v}{cd}, p' = \frac{d^2 p}{\mu\lambda c}, \beta' = \frac{\beta}{d}, \eta' = \frac{\eta}{d}, \tag{2.12}$$

in the equations (2.4) – (2.10), gives

$$\frac{\partial u}{\partial x} + \frac{\partial u}{\partial y} = 0, \tag{2.13}$$

$$R_e\delta\left(\frac{\partial u}{\partial t} + u\frac{\partial u}{\partial x} + v\frac{\partial u}{\partial y}\right) = -\frac{\partial p}{\partial x} + \left(\delta^2\frac{\partial^2 u}{\partial x^2} + \frac{\partial^2 u}{\partial y^2}\right) - \frac{1}{\alpha^2}\left(\delta^2\frac{\partial^2}{\partial x^2} + \frac{\partial^2}{\partial y^2}\right)\left(\delta^2\frac{\partial^2 u}{\partial x^2} + \frac{\partial^2 u}{\partial y^2}\right) - \frac{u}{Da}, \tag{2.14}$$

$$R_e\delta^3\left(\frac{\partial v}{\partial t}+u\frac{\partial v}{\partial x}+\ v\frac{\partial v}{\partial y}\right)=-\frac{\partial p}{\partial y}+\delta^2\left(\delta^2\frac{\partial^2 v}{\partial x^2}+\frac{\partial^2 v}{\partial y^2}\right)-\frac{\delta^2}{\propto^2}\left(\delta^2\frac{\partial^2}{\partial x^2}+\frac{\partial^2}{\partial y^2}\right)\left(\delta^2\frac{\partial^2 v}{\partial x^2}+\right.$$

$$\left.\frac{\partial^2 v}{\partial y^2}\right)-\delta^2\frac{v}{Da}\,, \tag{2.15}$$

$$\frac{\partial u}{\partial y}=0,\quad \frac{\partial^3 u}{\partial y^3}=0,\qquad at\quad y=0, \tag{2.16}$$

$$u=-\frac{\sqrt{Da}}{\beta}\frac{\partial u}{\partial y}\,,\quad at\quad y=\pm\eta(x,t)=\pm\left(1+\varepsilon sin2\pi(x-t)\right), \tag{2.17}$$

$$-\left(\delta^4\frac{\partial^2 v}{\partial x^2}-\delta^2\frac{\partial^2 u}{\partial x\partial y}\right)\frac{\partial \eta}{\partial x}+\delta^2\frac{\partial^2 v}{\partial x\partial y}-\frac{\partial^2 u}{\partial y^2}=0,$$

$$at\ y=\pm\eta(x,t)=\pm\left(1+\varepsilon sin2\pi(x-t)\right) \tag{2.18}$$

and

$$-R_e\delta\left(\frac{\partial u}{\partial t}+u\frac{\partial u}{\partial x}+\ v\frac{\partial u}{\partial y}\right)+\left(\delta^2\frac{\partial^2 u}{\partial x^2}+\frac{\partial^2 u}{\partial y^2}\right)-\frac{1}{\alpha^2}\left(\delta^2\frac{\partial^2}{\partial x^2}+\frac{\partial^2}{\partial y^2}\right)\left(\delta^2\frac{\partial^2 u}{\partial x^2}+\frac{\partial^2 u}{\partial y^2}\right)-\frac{u}{Da}=$$

$$E_1\ \frac{\partial^3 \eta}{\partial x^3}+\ E_2\ \frac{\partial^3 \eta}{\partial x\partial t^2}+\ E_3\ \frac{\partial^2 \eta}{\partial x\partial t}\,,\ \ at\ y=\pm\eta(x,t). \tag{2.19}$$

Here $R_e=\frac{\rho cd}{\mu}$ is the Reynolds number, $Da=\frac{k}{d^2}$ is the Darcy number (porous parameter), $\alpha\ =\sqrt{\frac{\mu}{h}}d$ is the couple stress parameter, $\delta=\frac{d}{\lambda}$ is wall slope parameter and $\varepsilon=\frac{a}{d}$ is the amplitude ratio are the geometric parameters. Further $E_1=\frac{-Td^3}{c\mu\lambda^3}$, $E_2=\frac{mcd^3}{\mu\lambda^3}$, $E_3=\frac{Cd^3}{\mu\lambda^2}$ are the elasticity parameters. The parameter E_1 represents the inflexibility (rigidity), E_2 stiffness (mass characterizing parameter) and E_3 viscous damping force (damping nature of the membrane).

2.3. Method of Solution

Assuming the wavelength to be large and the flow to be inertia free, the equations (2.13) – (2.19) become

$$\frac{\partial u}{\partial x}+\frac{\partial u}{\partial y}=\ 0\,, \tag{2.20}$$

$$0 = -\frac{\partial p}{\partial x} + \frac{\partial^2 u}{\partial y^2} - \frac{1}{\alpha^2}\frac{\partial^4 u}{\partial y^4} - \frac{u}{Da}\ , \tag{2.21}$$

$$0 = -\frac{\partial p}{\partial y}, \tag{2.22}$$

$$\frac{\partial u}{\partial y} = 0, \quad \frac{\partial^3 u}{\partial y^3} = 0, \qquad at \quad y = 0, \tag{2.23}$$

$$u = -\frac{\sqrt{Da}}{\beta}\frac{\partial u}{\partial y}, \quad at \quad y = \pm\eta(x,t) = \pm\big(1 + \varepsilon sin2\pi(x-t)\big), \tag{2.24}$$

$$\frac{\partial^2 u}{\partial y^2} = 0, \qquad at \quad y = \pm\eta(x,t) = \pm\big(1 + \varepsilon sin2\pi(x-t)\big) \tag{2.25}$$

and

$$\frac{\partial^2 u}{\partial y^2} - \frac{1}{\alpha^2}\frac{\partial^4 u}{\partial y^4} - \frac{u}{Da} = E_1\frac{\partial^3 \eta}{\partial x^3} + E_2\frac{\partial^3 \eta}{\partial x \partial t^2} + E_3\frac{\partial^2 \eta}{\partial x \partial t}\ , at\ y = \pm\eta(x,t). \tag{2.26}$$

The solution of equations 2.21 and 2.22 with the boundary conditions 2.23 to 2.26, gives

$$u(x,y,t) = \frac{\alpha^2 E}{m_1 - m_2}\left[\frac{\sqrt{Da}}{\beta}\frac{1}{\sqrt{m_1}}\{tanh\sqrt{m_1}\,\eta\} - \frac{\sqrt{Da}}{\beta}\frac{1}{\sqrt{m_2}}\{tanh\sqrt{m_2}\,\eta\} + \frac{1}{m_1} - \frac{1}{m_2} - \right.$$

$$\left.\frac{1}{m_1}\left\{\frac{cosh\sqrt{m_1}y}{cosh\sqrt{m_1}\eta}\right\} + \frac{1}{m_2}\left\{\frac{cosh\sqrt{m_2}y}{cosh\sqrt{m_2}\eta}\right\}\right]. \tag{2.27}$$

Here $m_1 = \frac{\alpha^2 + \alpha\sqrt{\alpha^2 - 4N}}{2}$, $m_2 = \frac{\alpha^2 - \alpha\sqrt{\alpha^2 - 4N}}{2}$, $N = \frac{1}{Da}$,

$E = -8\varepsilon\pi^3 cos2\pi(x-t)(E_1 + E_2) + 4\varepsilon\pi^2 E_3 sin2\pi(x-t)$.

Using equation 2.27, the expression for time average velocity $\bar{u}(y)$, over a period time is

$$\bar{u}(y) = \int_0^1 u\, dt. \tag{2.28}$$

Introducing ψ, the stream function, such that

$$u = \frac{\partial \psi}{\partial y}, \ and \quad v = -\frac{\partial \psi}{\partial x}. \tag{2.29}$$

Using equation 2.27 in $u = \frac{\partial \psi}{\partial y}$ and integrating along with the condition $\psi = 0 \ at \ \ y = 0$, we obtain the stream function as

$$\psi(x,y,t) = \frac{\alpha^2 E}{m_1 - m_2}\left[\frac{\sqrt{Da}}{\beta}\frac{1}{\sqrt{m_1}}\{tanh\sqrt{m_1}\eta\}y - \frac{\sqrt{Da}}{\beta}\frac{1}{\sqrt{m_2}}\{tanh\sqrt{m_2}\eta\}y + \frac{y}{m_1} - \frac{y}{m_2} - \frac{1}{m_1}\left\{\frac{sinh\sqrt{m_1}y}{(\sqrt{m_1})cosh\sqrt{m_1}\eta}\right\} + \frac{1}{m_2}\left\{\frac{sinh\sqrt{m_2}y}{(\sqrt{m_2})cosh\sqrt{m_2}\eta}\right\}\right]. \quad (2.30)$$

The solution in equation 2.27 under the absence of slip and porosity match with the result of chapter 6 in the thesis of Sankad [94].

2.4 Results and Discussion

The results are graphically illustrated with the help of MATHEMATICA software. All the results for time average velocity $\bar{u}(y)$ (equation 2.28) have been obtained in the form of two arbitrary functions, $m_1 = \frac{\alpha^2 + \alpha\sqrt{\alpha^2 - 4N}}{2}$ and $m_2 = \frac{\alpha^2 - \alpha\sqrt{\alpha^2 - 4N}}{2}$, which depend on couple stress parameter α and Darcy number Da. So the computations have been performed for the real values of m_1 and m_2 i.e. $\alpha^2 > \frac{4}{Da}$.

In order to see the effects of rigidity E_1, stiffness E_2, viscous damping force E_3, couple stress parameter α, slip parameter β and Darcy number Da.

The variations of rigidity parameter E_1 of the elastic wall in presence of stiffness $E_2 \neq 0$ in the compliant wall and absence of damping force $E_3 = 0$ on the time average velocity $\bar{u}(y)$ is plotted in Figure 2.2. One can conclude that the time average velocity $\bar{u}(y)$ diminishes as the wall rigidity E_1 enhances. Further, from Figure 2.3 the time average velocity $\bar{u}(y)$ reduces with increasing E_1 under the absence of stiffness $E_2 = 0$ and damping force $E_3 = 0$ in the wall.

Figure 2.4 shows that with increase in the wall stiffness E_2, with $E_1 \neq 0$ and $E_3 = 0$, the time average velocity $\bar{u}(y)$ decreases. The impact of E_3 of the elastic wall in presence of E_1 and E_2 over the average velocity $\bar{u}(y)$ is depicted in Figure 2.5. The time average velocity $\bar{u}(y)$ decrease as E_3 increases interpreting physically that dampness gives an adverse effect on the wall. Figure 2.6 depict that with enhance in the viscous damping force E_3, with $E_1 \neq 0$ and $E_2 = 0$, the time average velocity $\bar{u}(y)$ increases.

In presence of E_1, E_2 and E_3, the time average velocity $\bar{u}(y)$ reduces as the couple stress parameter α increases as revealed in Figure 2.7. This result is in agreement with that Pandey and Chaube [73]. Further, the time mean velocity $\bar{u}(y)$ rises with increase in α in case of $E_1 \neq 0$ and $E_2 = E_3 = 0$ as shown in Figure 2.8. For $E_1 \neq 0$ it is observed that the time average velocity $\bar{u}(y)$ increases with increasing slip parameter β as in Figure 2.9 and Figure 2.10 when $E_2 \neq 0$, $E_3 \neq 0$ and $E_2 = E_3 = 0$ respectively. That is, more the fluid slips at the boundary, less is its viscosity causing increase in the velocity. From Figure 2.11 decrease in the time average velocity $\bar{u}(y)$ is noticed with increase in Da in presence of E_1, E_2 and E_3. Further $\bar{u}(y)$ increases with increase in Da when $E_1 \neq 0$, $E_2 = E_3 = 0$, as shown in Figure 2.12.

Using the equation 2.30 trapping phenomenon is observed for various parameters and plotted in Figures 2.13 to 2.18. It can be seen that the trapped bolus increases for increasing E_1, E_2 and E_3 as shown in Figures 2.13(a & b), 2.14(a & b) and 2.15(a & b) respectively. The consequence of couple stress parameter α on stream line pattern is shown Figures 2.16 (a & b). It can be examined that trapping phenomena takes place and the trapped bolus enhances along with rise in the couple stress parameter. This result is an agreement with that of Hina et al. [93]. The trapped bolus decreases for increasing values of slip parameter β as shown in Figures 2.17(a & b).The influence of Darcy number Da on trapping is analyzed in Figures 2.18(a & b). It reveals that the volume of the trapped bolus increases with increasing permeability.

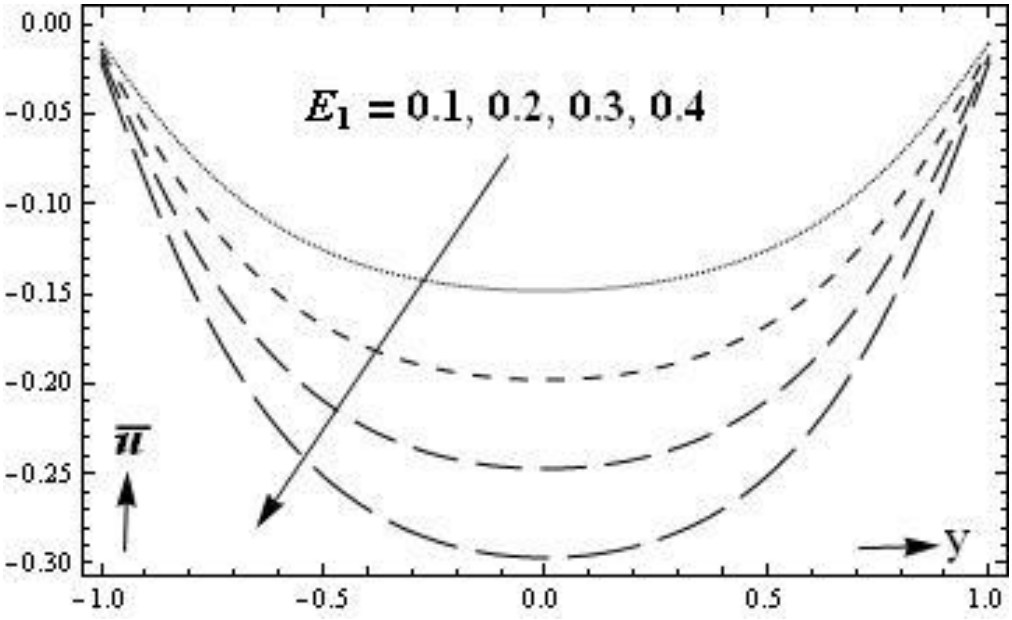

Figure 2.2: Consequence of E_1 on average velocity $\bar{u}(y)$.
$(\epsilon = 0.2; E_2 = 0.2; E_3 = 0.0; \alpha = 7; Da = 0.1; \beta = 0.01)$

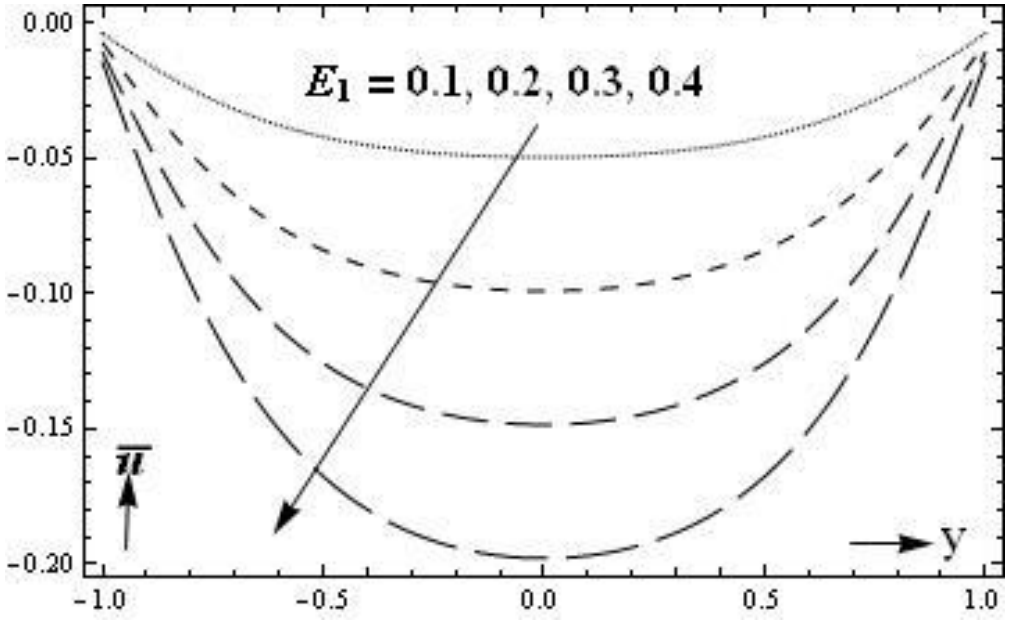

Figure 2.3: Consequence of E_1 on average velocity $\bar{u}(y)$.
$(\epsilon = 0.2;\ E_2 = 0.0; E_3 = 0.0; \alpha = 7; Da = 0.1; \beta = 0.01)$

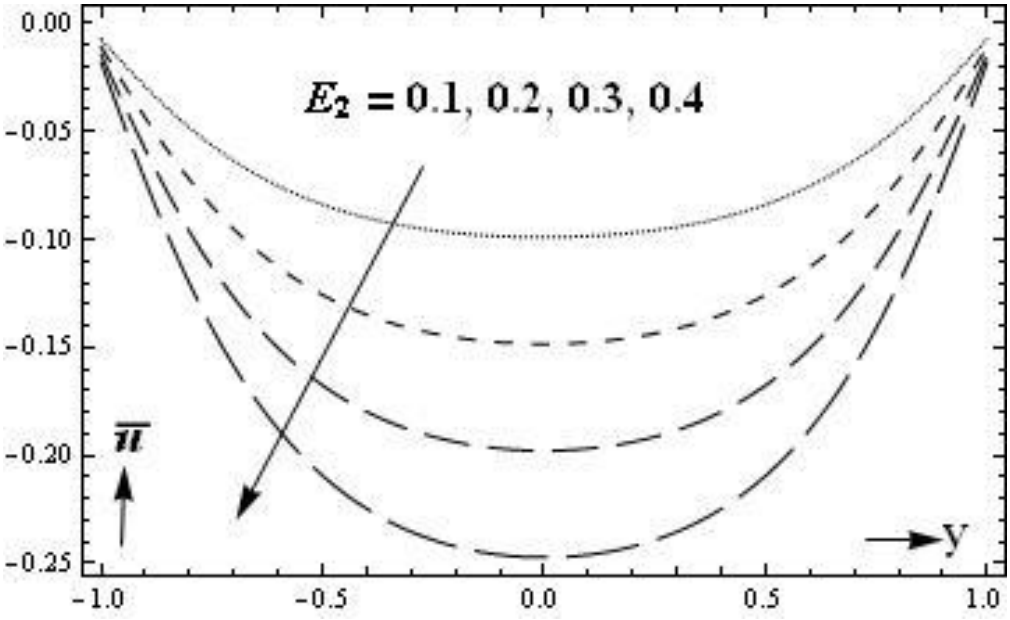

Figure 2.4: Consequence of E_2 on average velocity $\overline{u}(y)$.

$(\epsilon = 0.2; E_1 = 0.1; E_3 = 0.0; \alpha = 7; Da = 0.1; \beta = 0.01)$

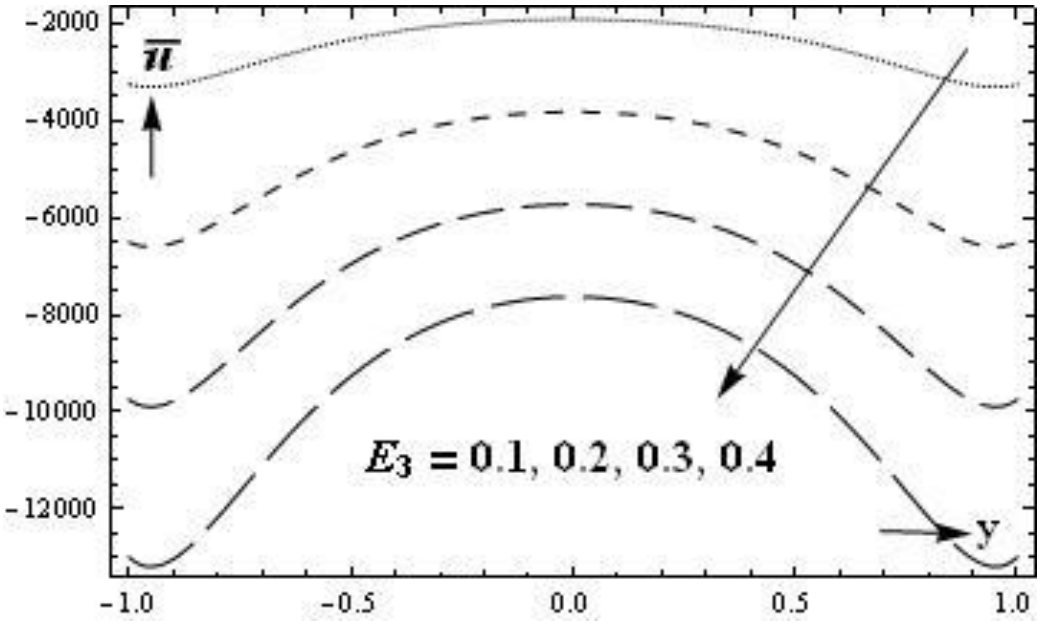

Figure 2.5 : Consequences of E_3on average velocity $\overline{u}(y)$.

$(\epsilon = 0.2; E_1 = 0.1; E_3 = 0.2; \alpha = 7; Da = 0.1; \beta = 0.01)$

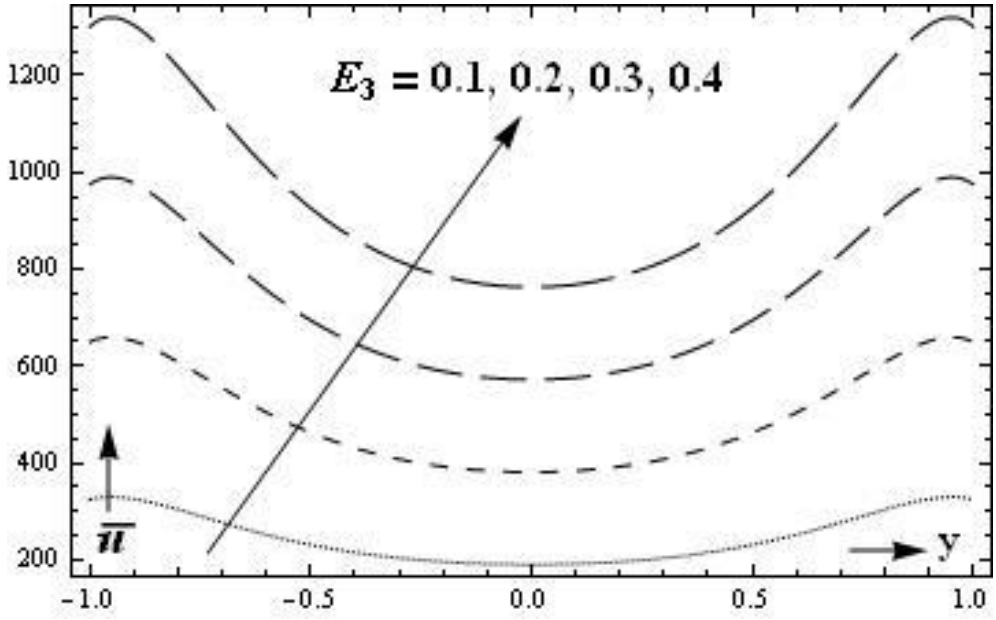

Figure 2.6 : Consequences of E_3on average velocity $\bar{u}(y)$.

$(\epsilon = 0.2; E_1 = 0.1; E_3 = 0.0; \alpha = 7; Da = 0.1; \beta = 0.01)$

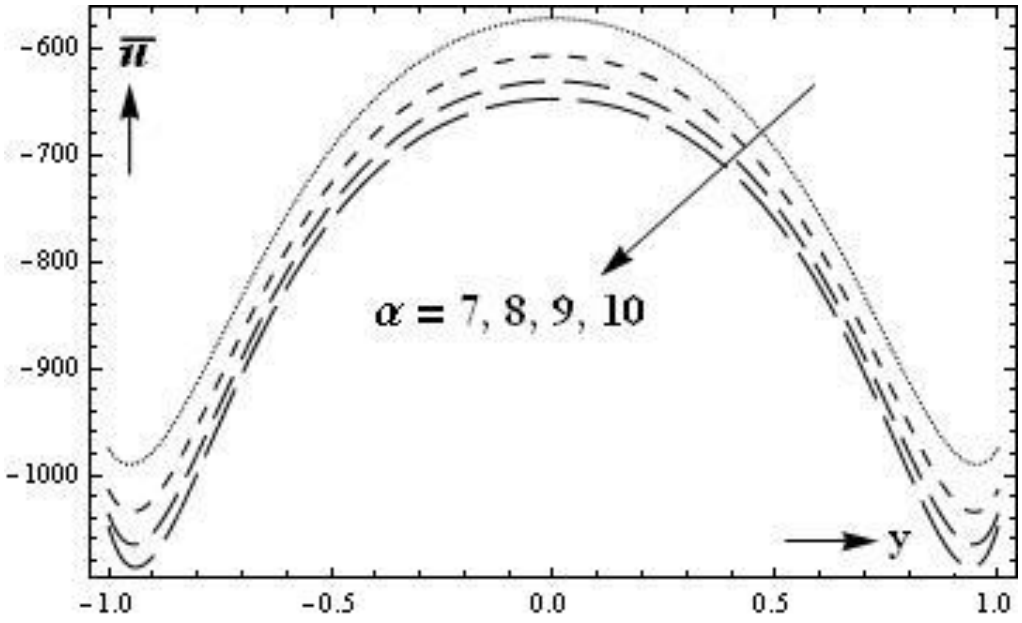

Figure 2.7 : Consequences of α on average velocity $\bar{u}(y)$.

$(\epsilon = 0.2; E_1 = 0.1; E_2 = 0.0; E_3 = 0.3; Da = 0.1; \beta = 0.01)$

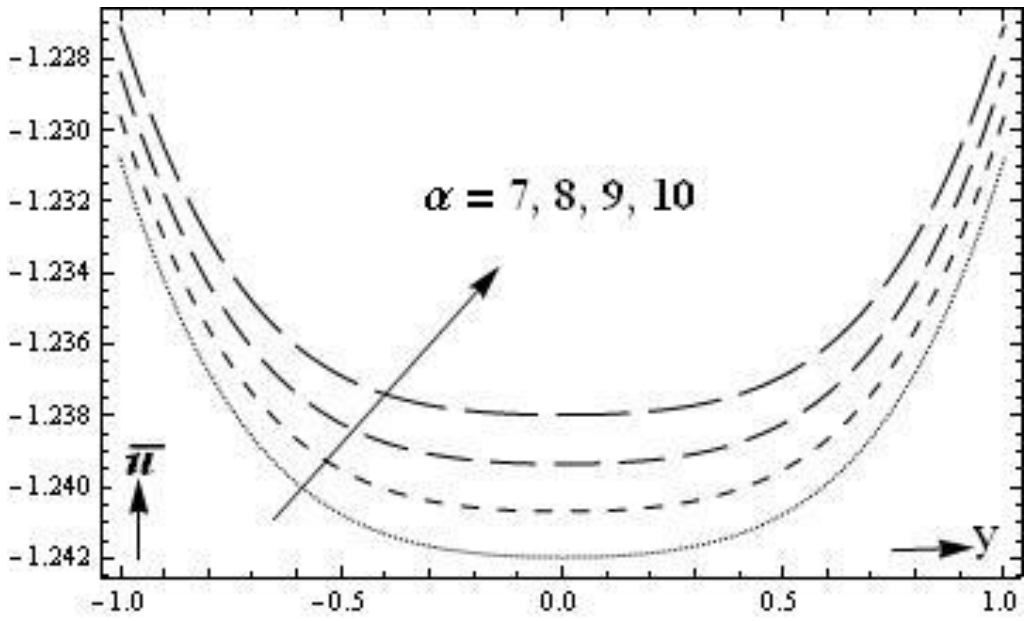

Figure 2.8 : Consequences of α on average velocity $\bar{u}(y)$.

$(\epsilon = 0.2; E_1 = 0.1; E_2 = 0.0; E_3 = 0.0; Da = 0.1; \beta = 0.01)$

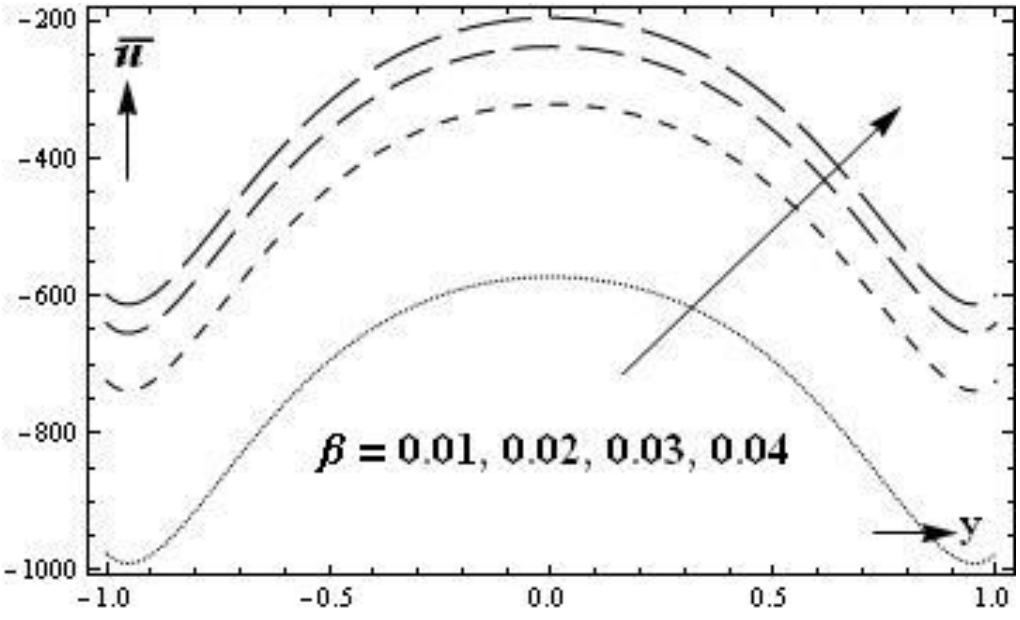

Figure 2.9: Consequence of β on average velocity $\bar{u}(y)$.

$(\epsilon = 0.2; E_1 = 0.1; E_2 = 0.2; E_3 = 0.3; Da = 0.1; \alpha = 7)$

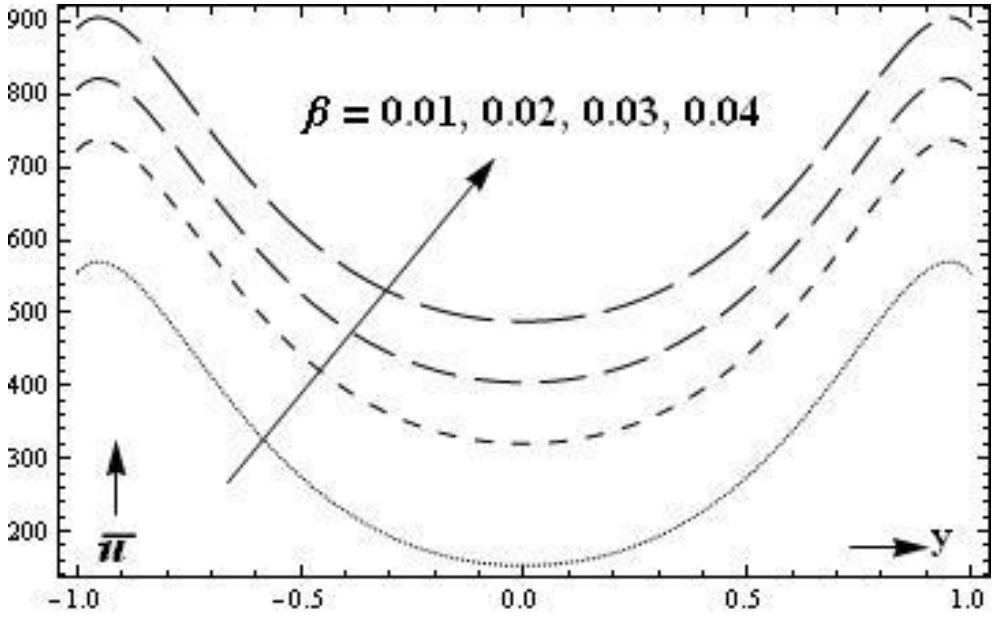

Figure 2.10: Consequence of β on average velocity $\bar{u}(y)$.

$(\epsilon = 0.2; E_1 = 0.1; E_2 = 0.0; E_3 = 0.0; Da = 0.1; \alpha = 7)$

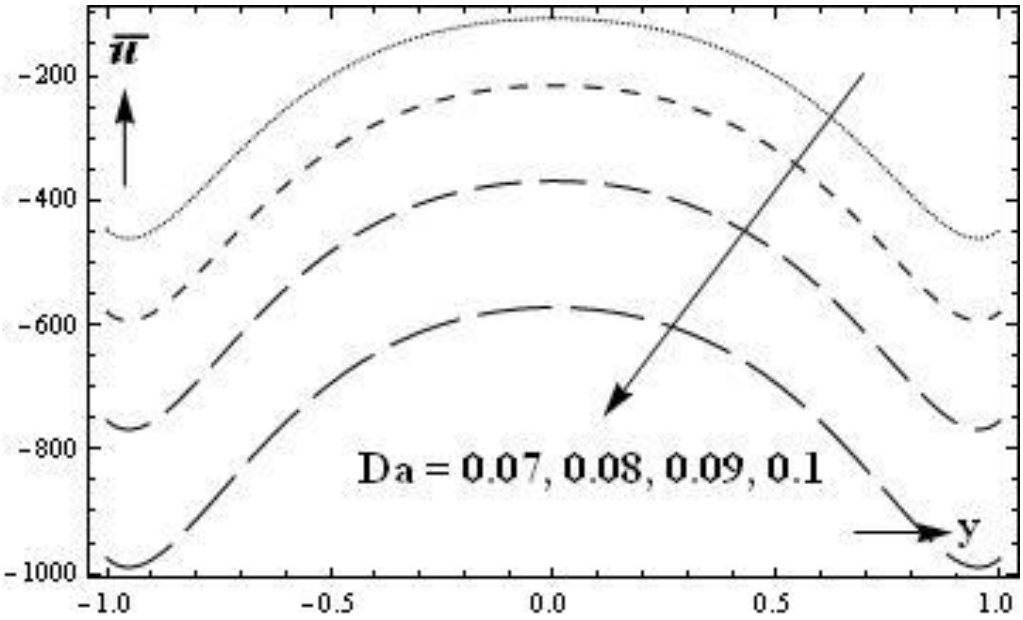

Figure 2.11 : Consequences of Da on average velocity $\bar{u}(y)$.

$(\epsilon = 0.2; E_1 = 0.1; E_2 = 0.2; E_3 = 0.3; \alpha = 7; \beta = 0.01)$

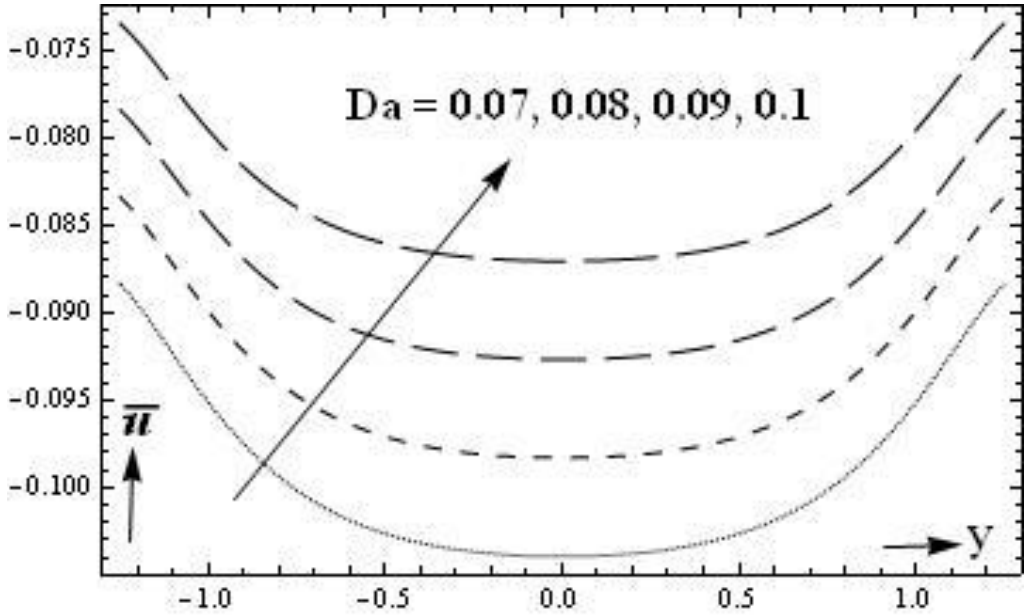

Figure 2.12 : Consequences of Da on average velocity $\bar{u}(y)$.

$(\epsilon = 0.2; E_1 = 0.1; E_2 = 0.0; E_3 = 0.0; \alpha = 7; \beta = 0.01)$

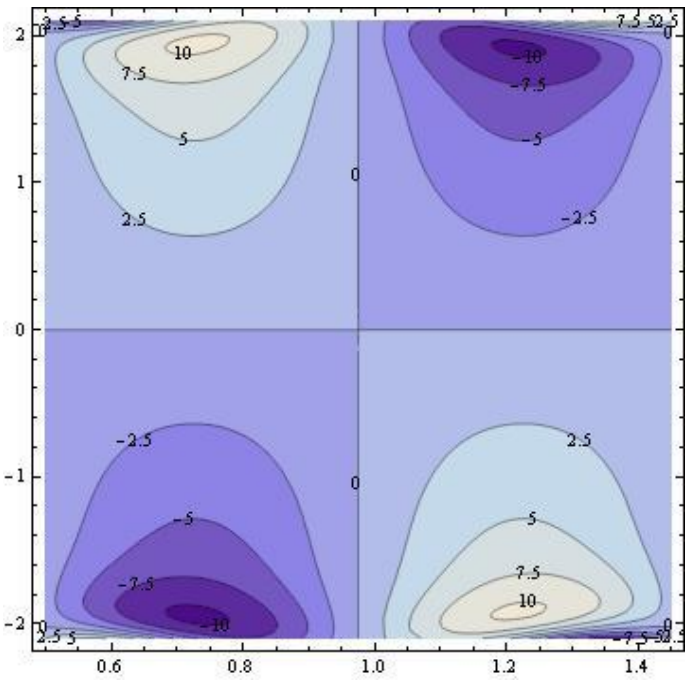

Figure 2.13(a): Stream lines for E_1= 0.1.

($\epsilon = 0.1; E_2 = 0.2; E_3 = 0.3; \alpha = 7; \beta = 0.01;$ Da $= 0.01$)

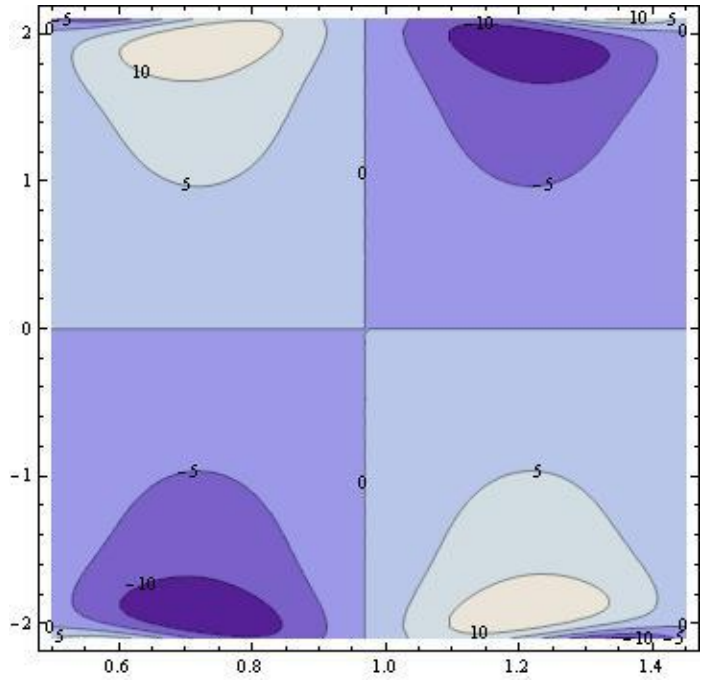

Figure 2.13(b): Stream lines for E_1= 0.2.

($\epsilon = 0.1; E_2 = 0.2; E_3 = 0.3; \alpha = 7; \beta = 0.01;$ Da $= 0.01$)

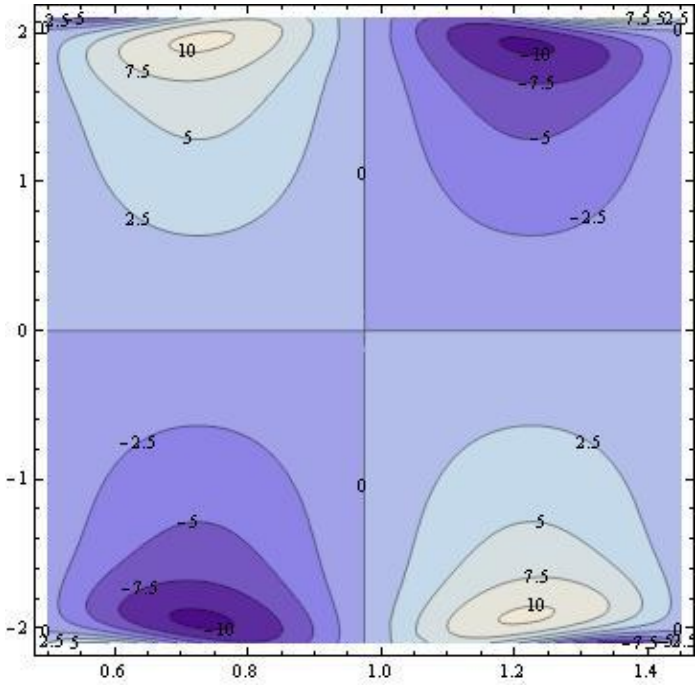

Figure 2.14(a): Stream lines for E_2 = 0.2.

($\epsilon = 0.1; E_1 = 0.1; E_3 = 0.3; \alpha = 7; \beta = 0.01;$ Da $= 0.01$)

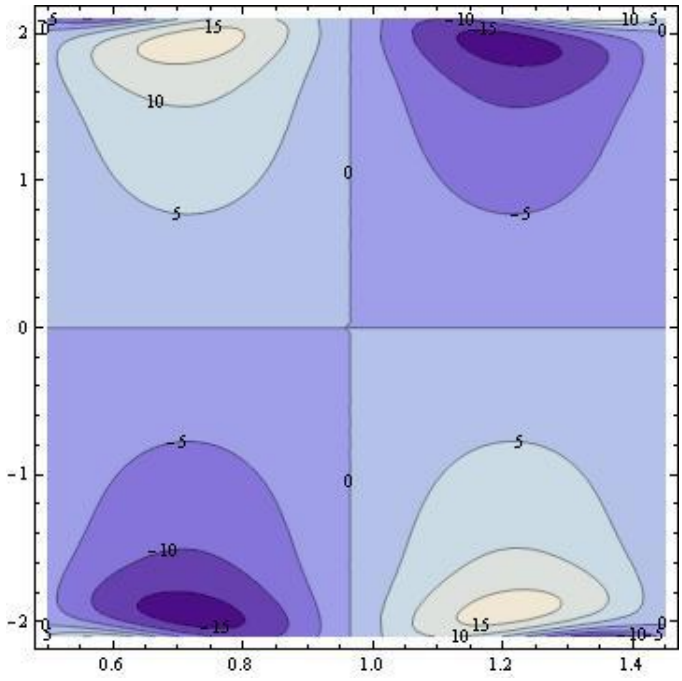

Figure 2.14(b): Stream lines for E_2 = 0.4.

($\epsilon = 0.1; E_1 = 0.1; E_3 = 0.3; \alpha = 7; \beta = 0.01;$ Da $= 0.01$)

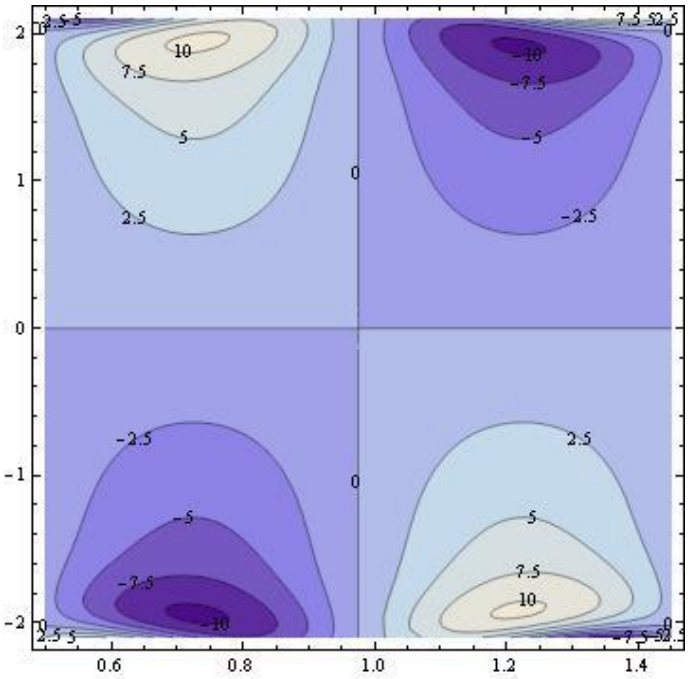

Figure 2.15(a): Stream lines for E_3 = 0.3.

($\epsilon = 0.1; E_1 = 0.1; E_2 = 0.2; \alpha = 7; \beta = 0.01;$ Da $= 0.01$)

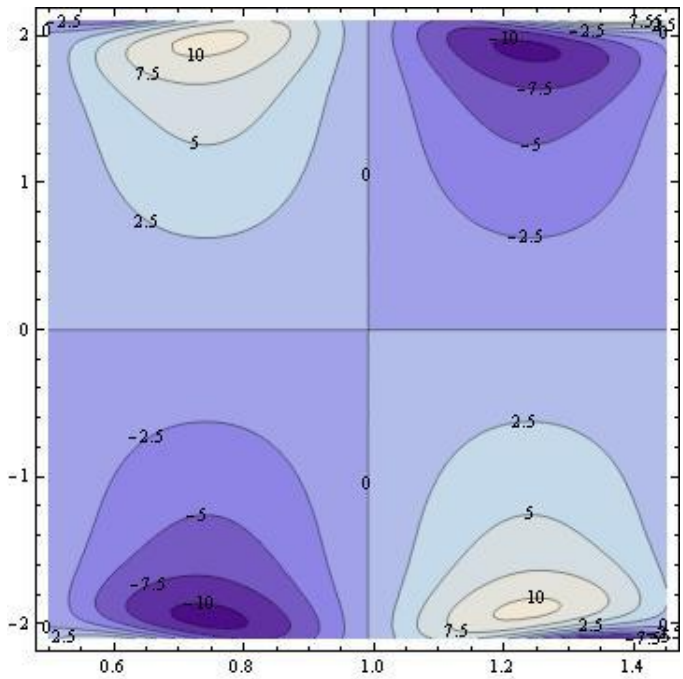

Figure 2.15(b): Stream lines for E_3 = 0.5.

($\epsilon = 0.1; E_1 = 0.1; E_2 = 0.2; \alpha = 7; \beta = 0.01;$ Da $= 0.01$)

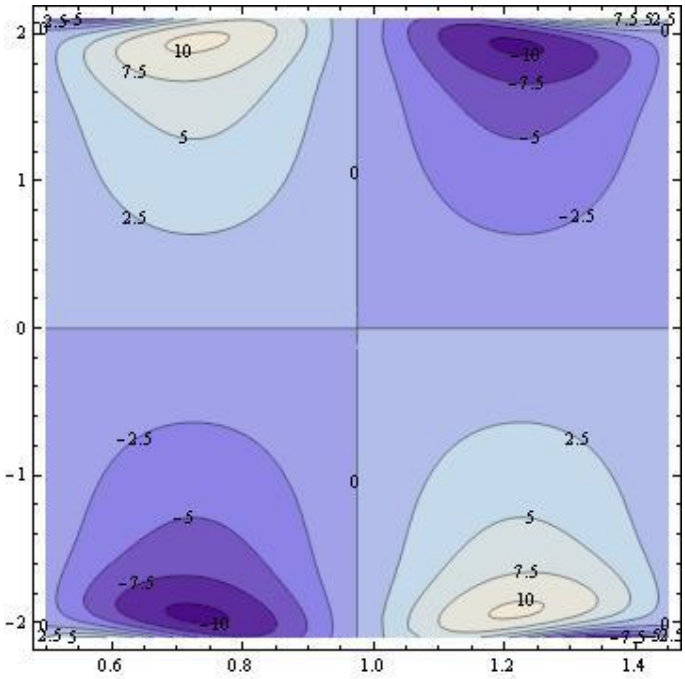

Figure 2.16(a): Stream lines for α = 7.

($\epsilon = 0.1; E_1 = 0.1; E_2 = 0.2; E_3 = 0.3; \beta = 0.01;$ Da $= 0.01$)

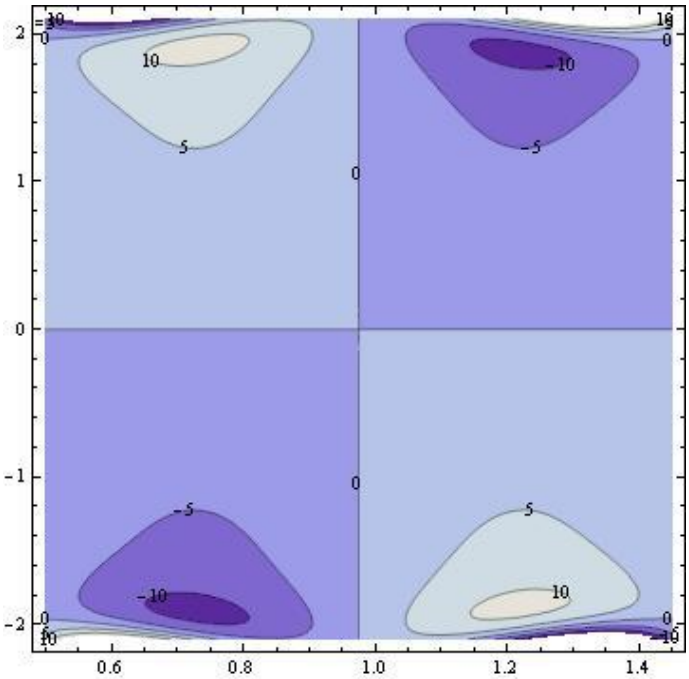

Figure 2.16(b): Stream lines for $\alpha = 8$.

($\epsilon = 0.1; E_1 = 0.1; E_2 = 0.2; E_3 = 0.3; \beta = 0.01;$ Da $= 0.01$)

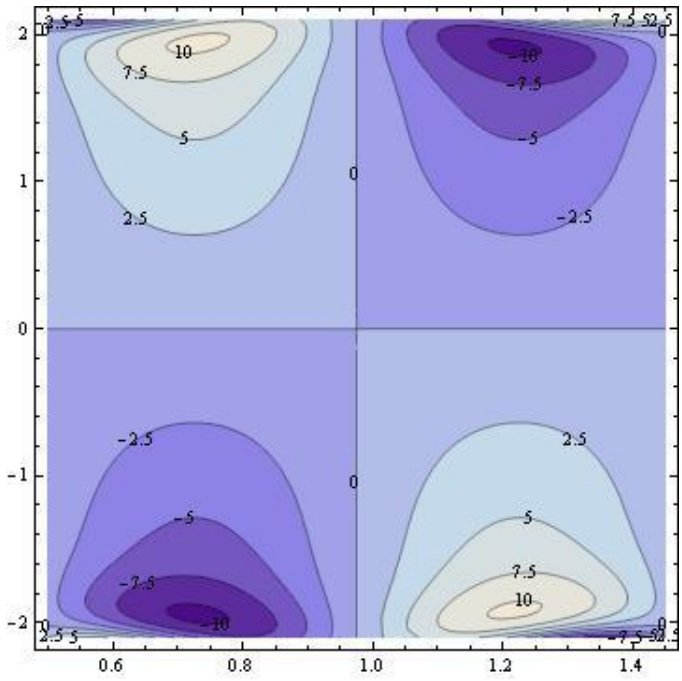

Figure 2.17(a): Stream lines for β = 0.01.

($\epsilon = 0.1; E_1 = 0.1; E_2 = 0.2; E_3 = 0.3; \alpha = 7;$ Da $= 0.01$)

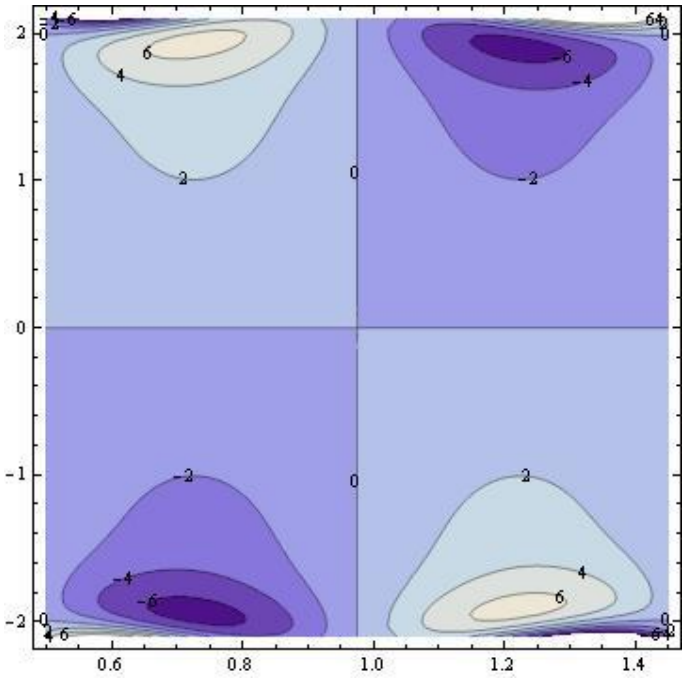

Figure 2.17(b): Stream lines for β = 0.02.

($\epsilon = 0.1; E_1 = 0.1; E_2 = 0.2; E_3 = 0.3; \alpha = 7;$ Da $= 0.01$)

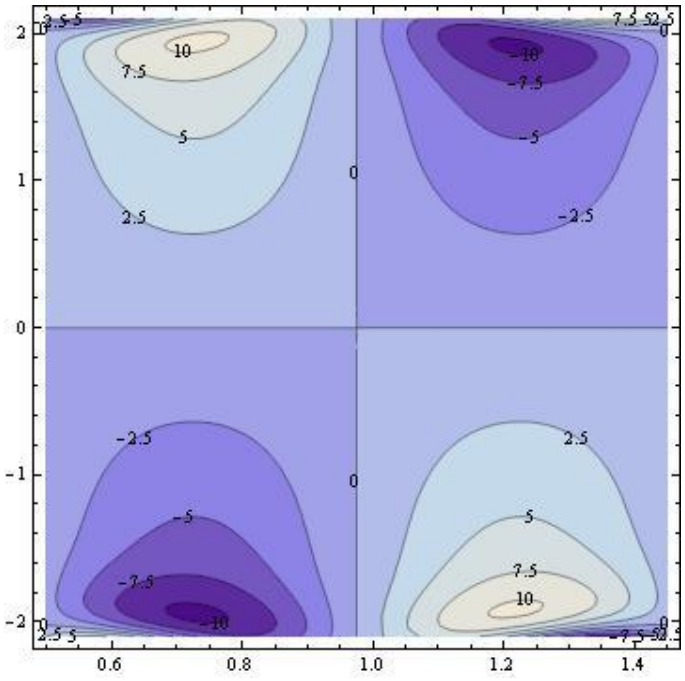

Figure 2.18(a): Stream lines for Da $= 0.01$.

($\epsilon = 0.1; E_1 = 0.1; E_2 = 0.2; E_3 = 0.3; \alpha = 7; \beta = 0.01$)

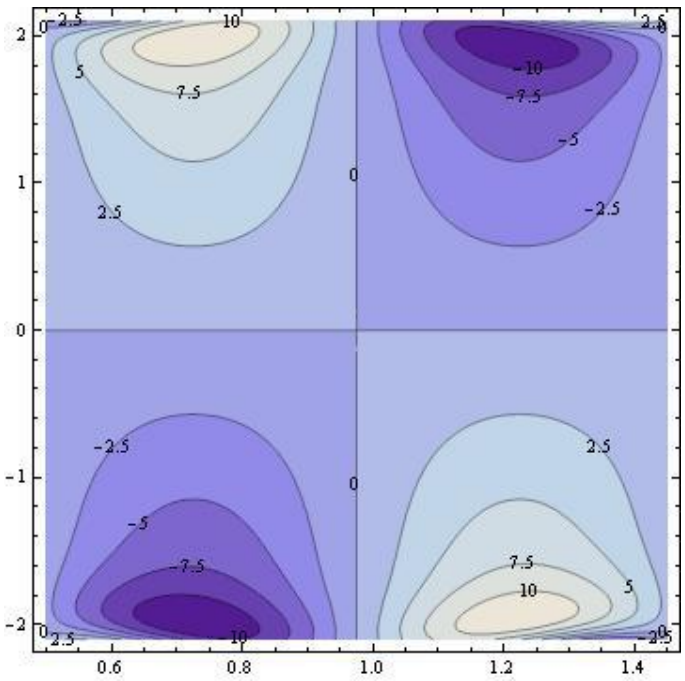

Figure 2.18(b): Stream lines for Da $= 0.011$.

($\epsilon = 0.1; E_1 = 0.1; E_2 = 0.2; E_3 = 0.3; \alpha = 7; \beta = 0.01$)

Chapter 3

Unsteady MHD Peristaltic Flow of a Couple Stress Fluid Through Porous Medium with Wall and Slip Effects

3.1 Introduction

In the last chapter, the couple stress fluid flow is investigated under the peristaltic motion in a two dimensional uniform porous channel having elastic wall and slip effects. This study is further analyzed for magnetic effect in this chapter.

The study of magnetic field with porous medium is very important both from theoretical as well as practical point of view; because most of the natural phenomena of the fluid flow are connected with porous medium, for instance, filtration of fluids, underground water and oil, reservoir and fluid through pipes. In some pathological situations, the distribution of fatty cholesterol and artery-clogging blood clots in the lumen of the coronary artery can be considered as equivalent to a fictitious porous medium.

Magnetohydrodynamics (MHD) deals with the study of electrically conducting fluids under the influence of electromagnetic field. Research has revealed that several physiological fluids have electrically conducting properties in engineering systems. MHD peristaltic flow is being studied due to its significance in blood pump machines, behavioral modification in cells and tissues, problems about urinary tract and treatment of gastrointestinal mobility related disorders.

Sud et al. [95] examined blood flow under magnetic field effect. They found that a suitable magnetic field helps in accelerating the velocity of blood. Srinivasacharya and Radhakrishnamacharya [96] investigated wall effects on MHD under peristalsis. The effect of couple stress fluid motion under peristalsis induced by a magnetic field is analyzed by Mekheimer [97]. Sankad and Radhakrishnamacharya [98] studied compliant wall effect on peristaltic transport of couple stress fluid in a magnetic field conduit. The effect of inclination of the channel to the horizontal, on the flow of a couple stress fluid applied by a magnetic field, under peristaltic motion is investigated by Shit and Roy [99]. Peristaltic motion of couple stress fluid through porous medium under MHD is examined by Hummady and Abdulhadi [100]. Dheia and Abdulhadi [101] examined MHD and wall properties through porous medium under peristalsis. Tajoddin and Khan [102] investigated slip effect on MHD non-Newtonian fluid through compliant walls of the peristaltic channel.

Keeping this in view, in this chapter, the influence of magnetic field on the peristaltic motion of a couple stress fluid with wall and slip effects is examined. The channel is considered to be porous.

3.2 Physical assumptions of the problem

An incompressible viscous flow through a porous medium is modeled for a couple stress fluid under magnetic field as shown in Figure 3.1. The flow geometry is considered same as in previous chapter.

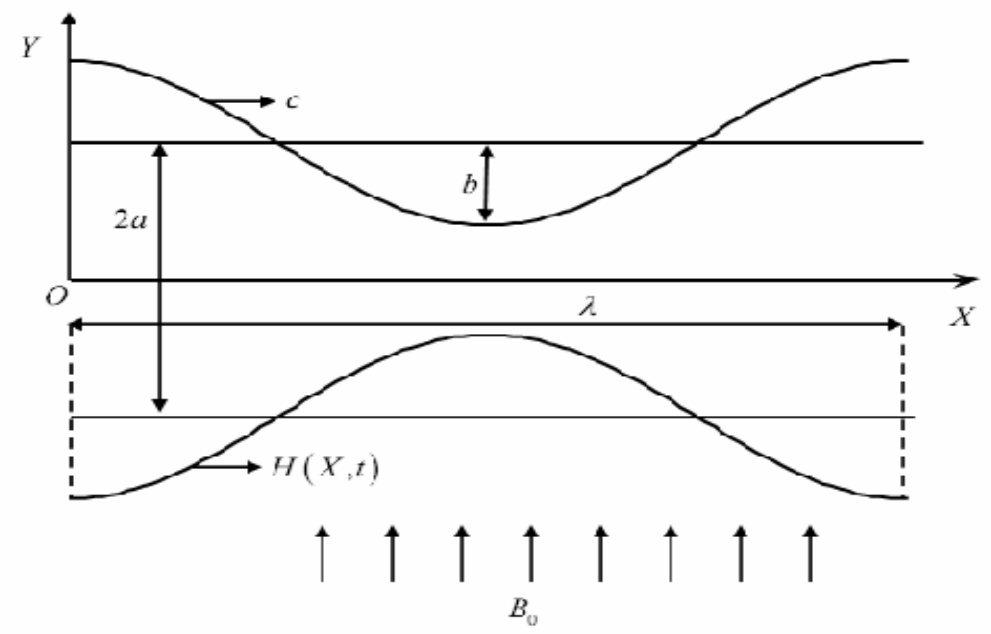

Figure 3.1: Physical model

Using the assumptions mentioned in chapter-1(section 1.7) and along with the basic equations of the movement of the elastic membrane as given in the previous chapter (equations 2.1 to 2.3), the equations that govern the motion of MHD couple stress fluid under peristalsis, for the present problem are given by the Navier-Stokes equations for an incompressible couple stress fluid flow as

$$\frac{\partial u}{\partial x}+\frac{\partial v}{\partial y}=0, \tag{3.1}$$

$$\rho\left(\frac{\partial u}{\partial t}+u\frac{\partial u}{\partial x}+v\frac{\partial u}{\partial y}\right)=-\frac{\partial p}{\partial x}+\mu\nabla^2 u-h\nabla^4 u-\mu\frac{u}{k}-\sigma {B_0}^2 u, \tag{3.2}$$

$$\rho\left(\frac{\partial v}{\partial t}+u\frac{\partial v}{\partial x}+v\frac{\partial v}{\partial y}\right)=-\frac{\partial p}{\partial y}+\mu\nabla^2 v-h\nabla^4 v-\mu\frac{v}{k}\ , \tag{3.3}$$

where σ is the electrical conductivity, B_0 is the magnetic field which is applied normal to the direction of the flow and the components u, v, ρ, k are having usual meanings as mentioned in the previous chapter.

The relevant boundary conditions be

$$\frac{\partial u}{\partial y} = 0, \quad \frac{\partial^3 u}{\partial y^3} = 0, \qquad at \;\; y = 0, \tag{3.4}$$

$$u = -d\frac{\sqrt{Da}}{\beta}\frac{\partial u}{\partial y} \;\; , \quad at \;\; y = \pm\eta(x,t). \tag{3.5}$$

Here β is the slip parameter and Da is the Darcy number.

$$-\left(\frac{\partial^2 v}{\partial x^2} - \frac{\partial^2 u}{\partial x \partial y}\right)\frac{\partial \eta}{\partial x} + \frac{\partial^2 v}{\partial x \partial y} - \frac{\partial^2 u}{\partial y^2} = 0, \qquad at \;\; y = \pm\eta(x,t), \tag{3.6}$$

$$\frac{\partial}{\partial x}L(\eta) = -\rho\left(\frac{\partial u}{\partial t} + u\frac{\partial u}{\partial x} + \; v\frac{\partial u}{\partial y}\right) + \; \mu\nabla^2 u - h\nabla^4 u - \mu\frac{u}{k} - \sigma {B_0}^2 u, \;\; at \;\; y = \pm\eta(x,t), \tag{3.7}$$

where $\frac{\partial}{\partial x}L(\eta) = \frac{\partial p}{\partial x} = \; -T\frac{\partial^3 \eta}{\partial x^3} + \; m\frac{\partial^3 \eta}{\partial x \partial t^2} + C\frac{\partial^2 \eta}{\partial x \partial t}$. (3.8)

Equations 3.1 to 3.7 reduce as follows after making use of the dimensionless quantities mentioned in chapter 2 (equation 2.12).

$$\frac{\partial u}{\partial x} + \frac{\partial v}{\partial y} = \; 0, \tag{3.9}$$

$$R_e\delta\left(\frac{\partial u}{\partial t} + u\frac{\partial u}{\partial x} + \; v\frac{\partial u}{\partial y}\right) = \; -\frac{\partial p}{\partial x} + \left(\delta^2\frac{\partial^2 u}{\partial x^2} + \; \frac{\partial^2 u}{\partial y^2}\right) - \frac{1}{\propto^2}\left(\delta^2\frac{\partial^2}{\partial x^2} + \; \frac{\partial^2}{\partial y^2}\right)\left(\delta^2\frac{\partial^2 u}{\partial x^2} + \; \frac{\partial^2 u}{\partial y^2}\right) - \frac{u}{Da} - {H_0}^2 u, \tag{3.10}$$

$$R_e\delta^3\left(\frac{\partial v}{\partial t} + u\frac{\partial v}{\partial x} + \; v\frac{\partial v}{\partial y}\right) = -\frac{\partial p}{\partial y} + \delta^2\left(\delta^2\frac{\partial^2 v}{\partial x^2} + \; \frac{\partial^2 v}{\partial y^2}\right) - \frac{\delta^2}{\propto^2}\left(\delta^2\frac{\partial^2}{\partial x^2} + \; \frac{\partial^2}{\partial y^2}\right)\left(\delta^2\frac{\partial^2 v}{\partial x^2} + \; \frac{\partial^2 v}{\partial y^2}\right) - \delta^2\frac{v}{Da}\,. \tag{3.11}$$

The corresponding conditions then take the following form:

$$\frac{\partial u}{\partial y} = 0, \quad \frac{\partial^3 u}{\partial y^3} = 0, \qquad at \;\; y = 0, \tag{3.12}$$

$$u = -\frac{\sqrt{Da}}{\beta}\frac{\partial u}{\partial y}, \quad at\ y = \pm\eta(x,t) = \pm\left(1 + \varepsilon sin2\pi(x-t)\right), \tag{3.13}$$

$$-\left(\delta^4\frac{\partial^2 v}{\partial x^2} - \delta^2\frac{\partial^2 u}{\partial x \partial y}\right)\frac{\partial \eta}{\partial x} + \delta^2\frac{\partial^2 v}{\partial x \partial y} - \frac{\partial^2 u}{\partial y^2} = 0,$$

$$at\ y = \pm\eta(x,t) = \pm\left(1 + \varepsilon sin2\pi(x-t)\right) \tag{3.14}$$

and

$$-R_e\delta\left(\frac{\partial u}{\partial t} + u\frac{\partial u}{\partial x} + v\frac{\partial u}{\partial y}\right) + \left(\delta^2\frac{\partial^2 u}{\partial x^2} + \frac{\partial^2 u}{\partial y^2}\right) - \frac{1}{\propto^2}\left(\delta^2\frac{\partial^2}{\partial x^2} + \frac{\partial^2}{\partial y^2}\right)\left(\delta^2\frac{\partial^2 u}{\partial x^2} + \frac{\partial^2 u}{\partial y^2}\right) - \frac{u}{Da} -$$

$${H_0}^2 u = E_1\frac{\partial^3 \eta}{\partial x^3} + E_2\frac{\partial^3 \eta}{\partial x \partial t^2} + E_3\frac{\partial^2 \eta}{\partial x \partial t}, \quad at \quad y = \pm\eta(x,t), \tag{3.15}$$

where $H_0 = B_0 d\sqrt{\frac{\sigma}{\mu}}$ represents the Hartmann number and the other parameters have usual meaning as given in previous chapter.

3.3 Method of Solution

Applying lubrication theory, the equations (3.9) – (3.15) reduce to

$$\frac{\partial u}{\partial x} + \frac{\partial v}{\partial y} = 0, \tag{3.16}$$

$$0 = -\frac{\partial p}{\partial x} + \frac{\partial^2 u}{\partial y^2} - \frac{1}{\alpha^2}\frac{\partial^4 u}{\partial y^4} - \frac{u}{Da} - {H_0}^2 u, \tag{3.17}$$

$$0 = -\frac{\partial p}{\partial y}, \tag{3.18}$$

$$\frac{\partial u}{\partial y} = 0, \quad \frac{\partial^3 u}{\partial y^3} = 0, \qquad at\ y = 0, \tag{3.19}$$

$$u = -\frac{\sqrt{Da}}{\beta}\frac{\partial u}{\partial y}, \quad at\ y = \pm\eta(x,t) = \pm\left(1 + \varepsilon sin2\pi(x-t)\right), \tag{3.20}$$

$$\frac{\partial^2 u}{\partial y^2} = 0,\ at \quad y = \pm\eta(x,t) = \pm\left(1 + \varepsilon sin2\pi(x-t)\right) \tag{3.21}$$

and

$$\frac{\partial^2 u}{\partial y^2} - \frac{1}{\alpha^2}\frac{\partial^4 u}{\partial y^4} - \frac{u}{Da} - {H_0}^2 u = E_1 \frac{\partial^3 \eta}{\partial x^3} + E_2 \frac{\partial^3 \eta}{\partial x \partial t^2} + E_3 \frac{\partial^2 \eta}{\partial x \partial t},$$

$$at \quad y = \pm\eta(x,t). \tag{3.22}$$

Solving equations 3.17 and 3.18 together with the corresponding conditions at the boundary 3.19 – 3.22, gives

$$u(x,y,t) = \frac{E}{M{H_0}^2}\left[\frac{m_1 m_2 - {m_2}^2}{{H_0}^2\alpha^2} + \frac{m_1}{m_2} - M - 1 - \frac{m_2 cosh(\sqrt{m_1}y)}{m_1 T_1} + \frac{cosh(\sqrt{m_2}y)}{T_2}\right]. \tag{3.23}$$

Here

$$E = -8\varepsilon\pi^3 cos2\pi(x-t)(E_1+E_2) + 4\varepsilon\pi^2 E_3 sin2\pi(x-t), \qquad H = \frac{1}{Da} + {H_0}^2,$$

$$M = \frac{m_1 m_2 - {m_2}^2}{{H_0}^2\alpha^2} + \frac{\sqrt{Da}}{\beta} m_2 \left(\frac{T_4}{\sqrt{m_2}} - \frac{T_3}{\sqrt{m_1}}\right),$$

$$m_1 = \frac{\alpha^2 + \alpha\sqrt{\alpha^2 - 4H}}{2}, \qquad m_2 = \frac{\alpha^2 - \alpha\sqrt{\alpha^2 - 4H}}{2},$$

$$T_1 = cosh\left(\sqrt{m_1}\eta\right), \quad T_2 = cosh\left(\sqrt{m_2}\eta\right), \quad T_3 = Tanh\left(\sqrt{m_1}\eta\right), \quad T_4 = Tanh\left(\sqrt{m_2}\eta\right).$$

The time average velocity $\bar{u}(y)$, over a single period of motion, is given by

$$\bar{u}(y) = \int_0^1 u\, dt. \tag{3.24}$$

Following the same procedure as in the previous chapter, the expression for the stream function ψ is obtained as

$$\psi(x,y,t) = \frac{E}{M{H_0}^2}\left[\frac{m_1 m_2 - {m_2}^2}{{H_0}^2\alpha^2} y + \frac{m_1}{m_2} y - My - y - \frac{m_2 sinh(\sqrt{m_1}y)}{{m_1}^{3/2} T_1} + \frac{sinh(\sqrt{m_2}y)}{\sqrt{m_2} T_2}\right]. \tag{3.25}$$

The solution in equation 3.23 under the absence of slip and porosity match with the result mentioned in chapter 8 in the thesis of Sankad [94].

3.4 Results and Discussion

Analytical solutions are obtained using low Reynolds number and long wavelength approximations. The results are graphically analyzed directly with the MATHEMATICA

software package. With reference to equation 3.24, two real valued arbitrary functions m_1 and m_2 are required to determine the results of time average velocity $\bar{u}(y)$.

Here $m_1 = \frac{\alpha^2+\alpha\sqrt{\alpha^2-4H}}{2}$ and $m_2 = \frac{\alpha^2-\alpha\sqrt{\alpha^2-4H}}{2}$, depend on Darcy number Da, Hartmann number (magnetic field) H_0 and couple stress parameter α with $\alpha^2 > 4H$.

This section presents the graphical interpretations to know the effects of parameters involved in presence and absence of stiffness E_2 and damping nature of the wall E_3. The consequences of Hartmann number H_0, couple stress parameter α, slip parameter β, Darcy number Da and elastic parameters E_1, E_2, E_3 on time average velocity $\bar{u}(y)$ from equation 3.24 are presented in Figures 3.2 to 3.10.

For various values of compliant wall parameters E_1, E_2, E_3 Figure 3.2 shows the effect on time average velocity, there by showing decrease in the time average velocity due to increase in the non zero elastic parameters E_1, E_2 and E_3.From Figure 3.3, the time average velocity drops with rise in couple stress parameter under the presence of both stiffness and viscous damping force $E_2 \neq 0, E_3 \neq 0$ at $H_0 = 1$. The negative time average velocity shows that flow reversal takes place. But, in the absence of stiffness and viscous damping force $(E_2 = 0, E_3 = 0)$, increase in the couple stress increases time average velocity for fixed values of other parameters as shown in Figure 3.4. The impact of slip parameter β is presented in Figure 3.5 and Figure 3.6. As the slip parameter β increases we observe a decrease in the time average velocity at non zero elastic parameters and reversal flow is sketched as seen in Figure 3.5. It is noticed from Figure 3.6 that, time average velocity increases with the slip parameter β at $H_0 = 1$ under the conditions of no stiffness and no viscous damping force.

With increase in Darcy number Da, the time average velocity drops under the influence of E_1, E_2 and E_3 as shown in Figure 3.7. The time average velocity increases with increase in Darcy number Da when both stiffness and viscous damping force are zero $E_2 = E_3 = 0$ and is depicted in Figure 3.8. Figure 3.9 and Figure 3.10 depict the effect of Hartman number H_0. Figure 3.9 represents that, under the presence of elastic parameters, there is gain in the time average velocity, with rise in the Hartmann number. This result is an agreement with that of Dheia and Abdulhadi [101]. But when $E_2 = 0$ and $E_3 = 0$ the increase in H_0 decreases time average velocity as plotted in Figure 3.10.

The effects of various parameters on trapping are displayed from Figure 3.11 to Figure 3.17. It is indicated from Figures 3.11(a & b), 3.12(a & b) and 3.13(a & b) that the size of bolus enhances in size as the values of the elastic parameters E_1, E_2 and E_3 increase respectively.

Influence of couple stress parameter on trapping phenomenon is examined from Figures 3.14(a & b). It is noticed that rise in the couple stress parameter reduces the size of trapped bolus. The result of the slip parameter and Darcy number on trapping are drawn in Figures 3.15(a & b) and Figures 3.16(a & b). It clearly indicates that the bolus diminishes in size as the values of slip and Darcy number enhance. The impacts of couple-stress parameter, Darcy number and slip parameter on trapping agree with the results of Hummady and Abdulhadi [103]. The impact of Hartmann number on trapping is shown in Figures 3.17(a & b). It is shown that the size of the bolus increases with rise in Hartmann number. The Darcy number and Hartmann number results agree with the results of Dheia and Abdulhadi [101].

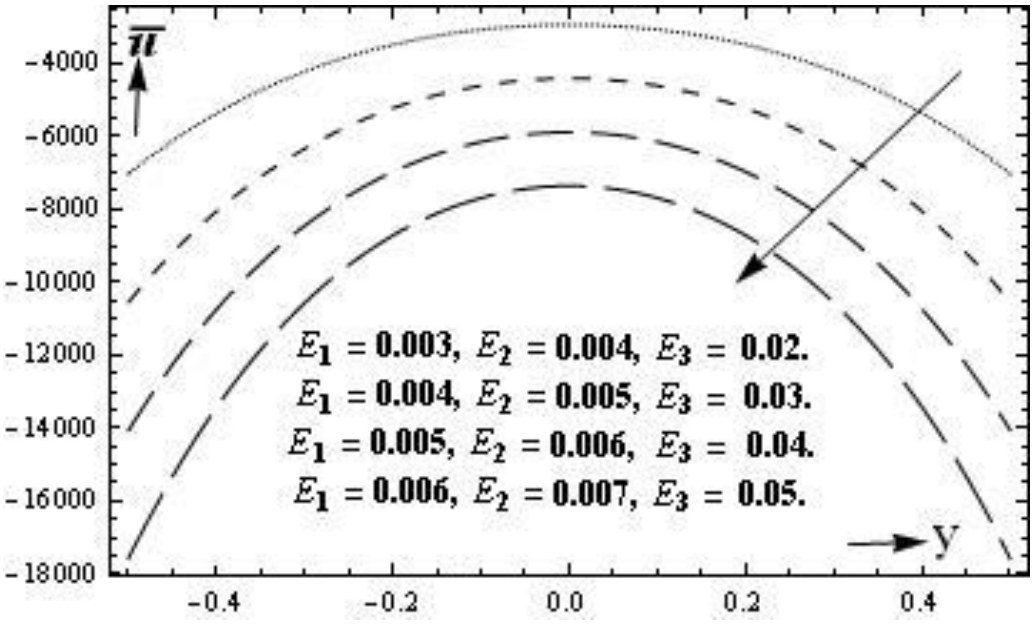

Figure 3.2: Consequences of E_1, E_2, E_3 on average velocity $\bar{u}(y)$.
$(\varepsilon = 0.2; \beta = 0.1; \alpha = 10; Da = 0.1; H_0 = 1)$

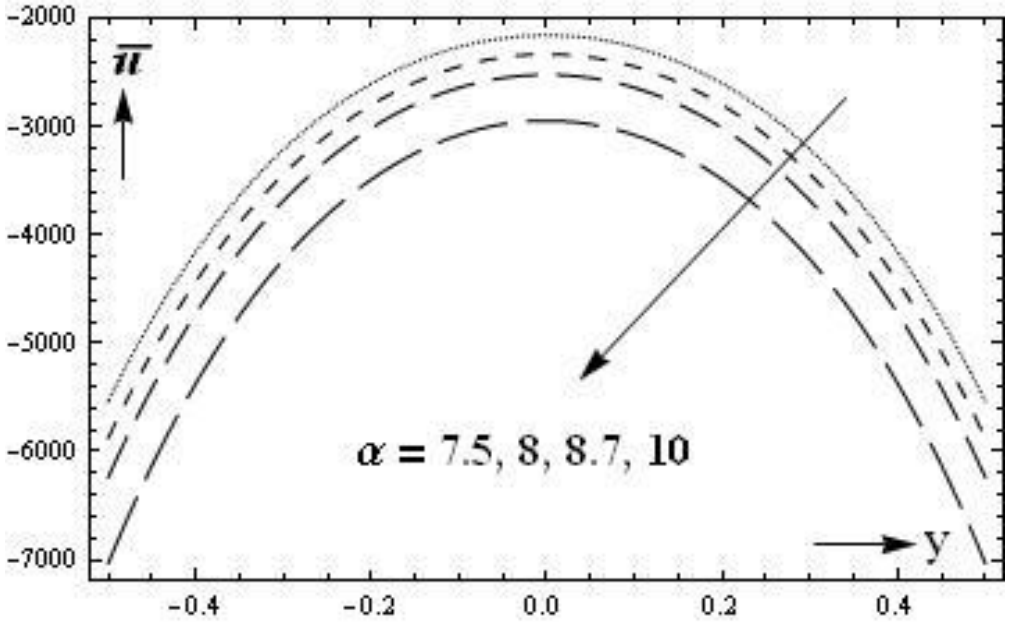

Figure 3.3: Consequences of α on average velocity $\bar{u}(y)$.

$(\varepsilon = 0.2; E_1 = 0.003; E_2 = 0.004; E_3 = 0.02; \beta = 0.1; Da = 0.1; H_0 = 1)$

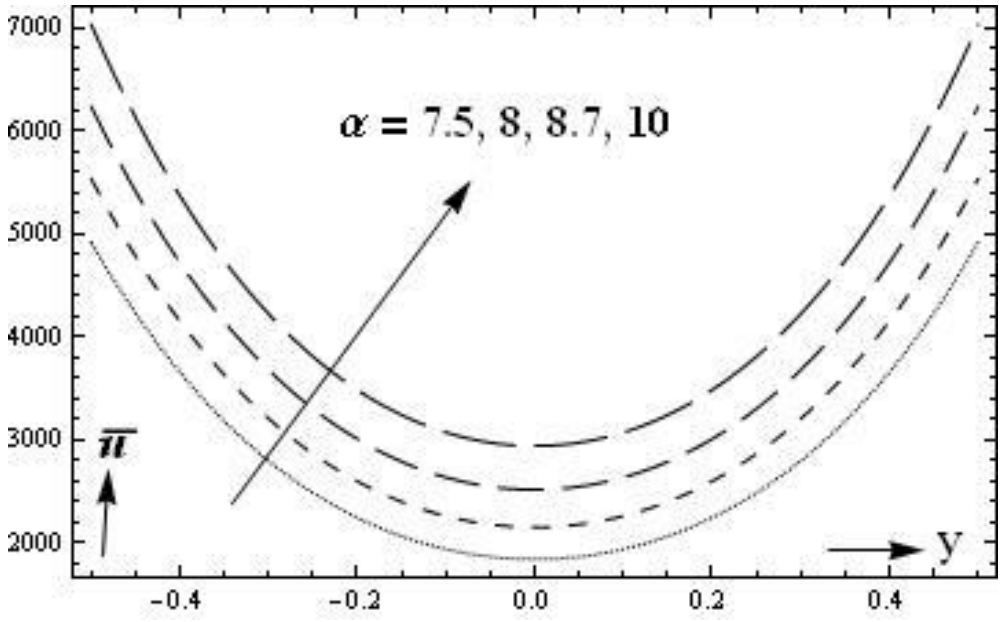

Figure 3.4: Consequences of α on average velocity $\bar{u}(y)$.

$(\varepsilon = 0.2; E_1 = 0.003; E_2 = 0.0; E_3 = 0.0; \beta = 0.1; Da = 0.1; H_0 = 1)$

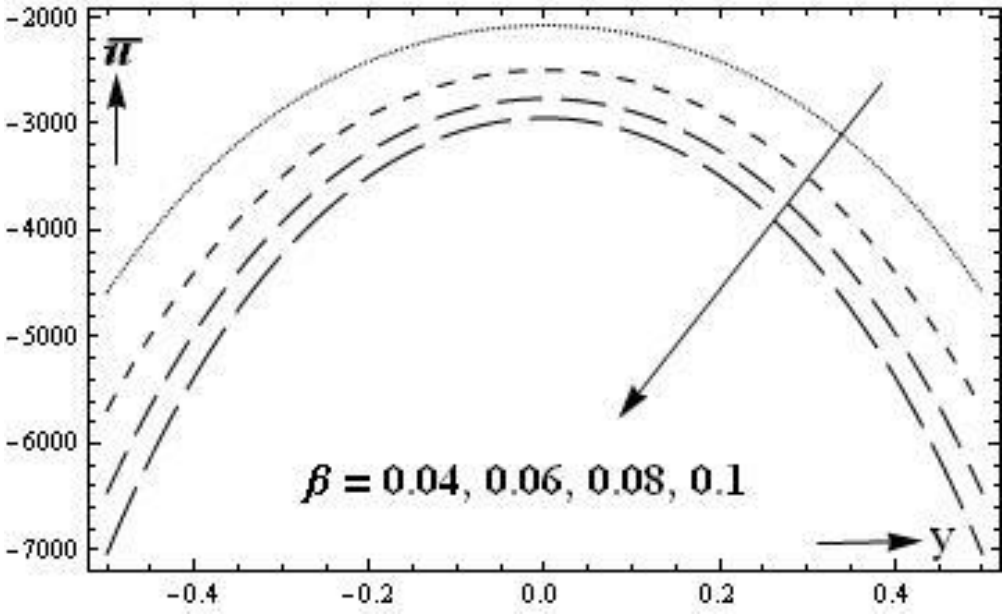

Figure 3.5: Consequences of β on average velocity $\bar{u}(y)$.

$(\varepsilon = 0.2; E_1 = 0.003; E_2 = 0.004; E_3 = 0.02; \alpha = 10; Da = 0.1; H_0 = 1)$

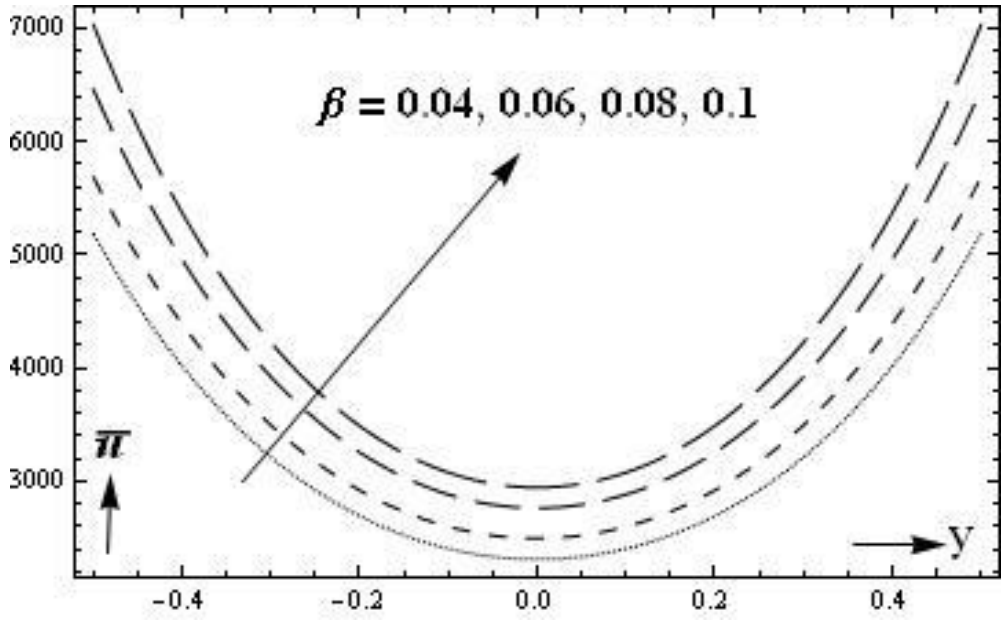

Figure 3.6:Consequences of β on average velocity $\bar{u}(y)$.

$(\varepsilon = 0.2; E_1 = 0.003; E_2 = 0.0; E_3 = 0.0; \alpha = 10; Da = 0.1; H_0 = 1)$

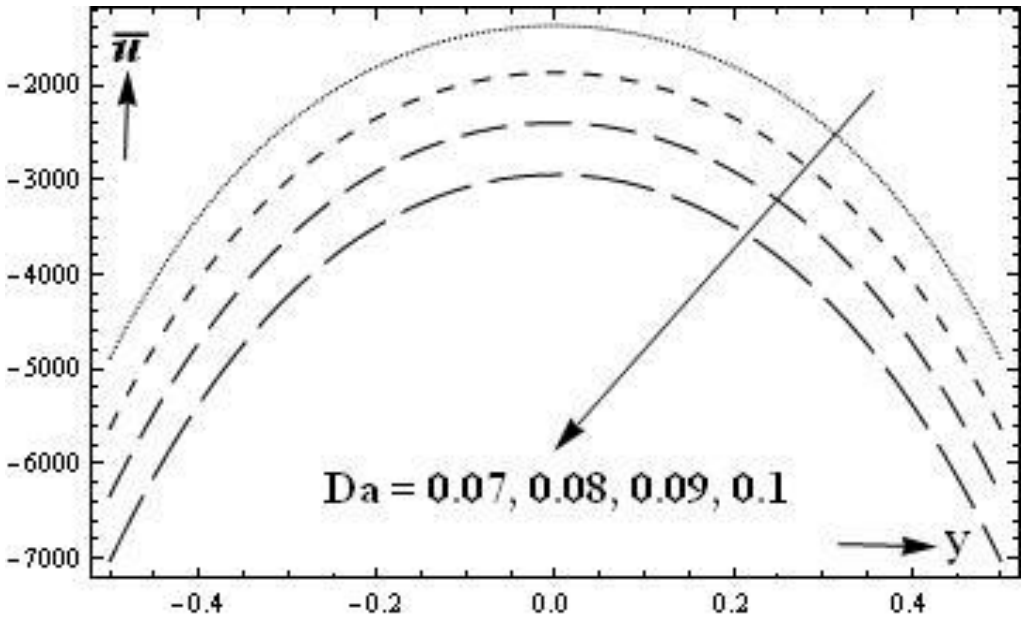

Figure 3.7: Consequences of Da on average velocity $\bar{u}(y)$.

$(\varepsilon = 0.2; E_1 = 0.003; E_2 = 0.004; E_3 = 0.02; \alpha = 10; \beta = 0.1; H_0 = 1)$

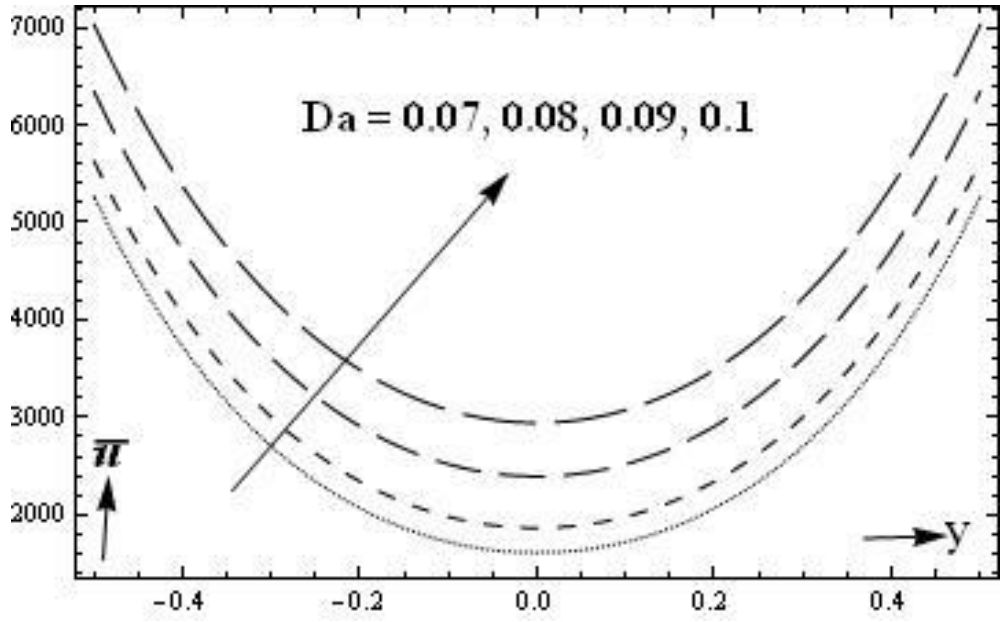

Figure 3.8:Consequences of Da on average velocity $\bar{u}(y)$.

$(\varepsilon = 0.2; E_1 = 0.003; E_2 = 0.0; E_3 = 0.0; \alpha = 10; \beta = 0.1; H_0 = 1)$

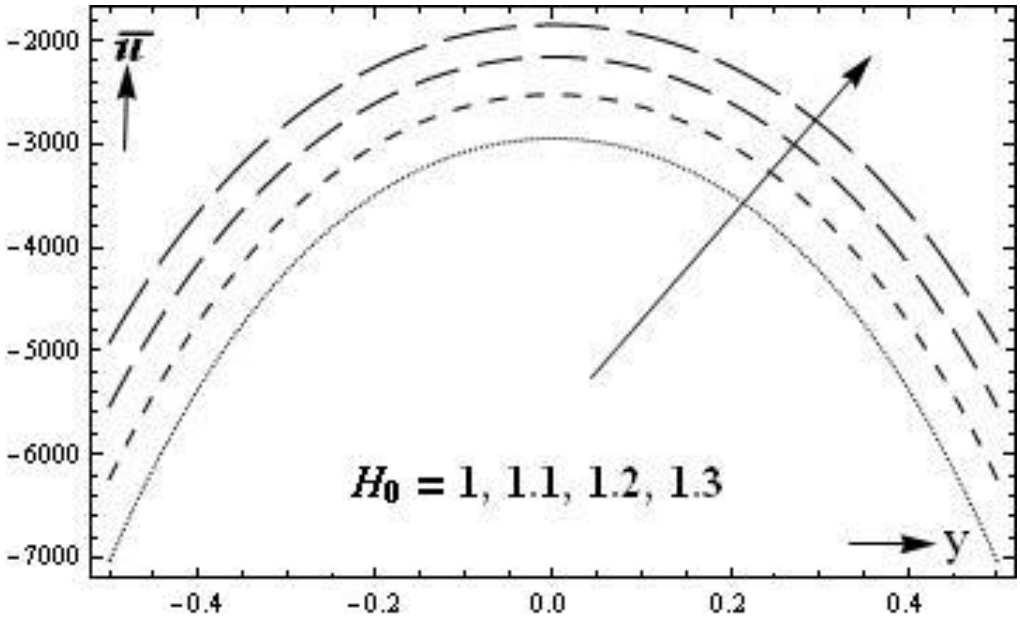

Figure 3.9: Consequences of H_0 on average velocity $\bar{u}(y)$.

$(\varepsilon = 0.2; E_1 = 0.003; E_2 = 0.004; E_3 = 0.02; \alpha = 10; Da = 0.1; \beta = 0.1)$

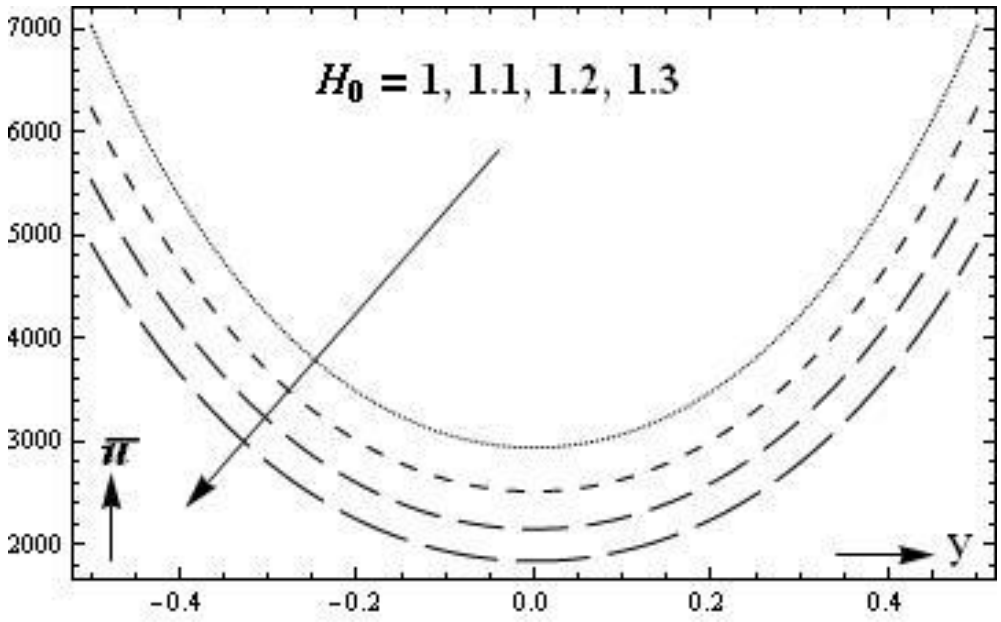

Figure 3.10: Consequences of H_0 on average velocity $\bar{u}(y)$.

$(\varepsilon = 0.2; E_1 = 0.003; E_2 = 0.0; E_3 = 0.0; \alpha = 10; Da = 0.1; \beta = 0.1)$

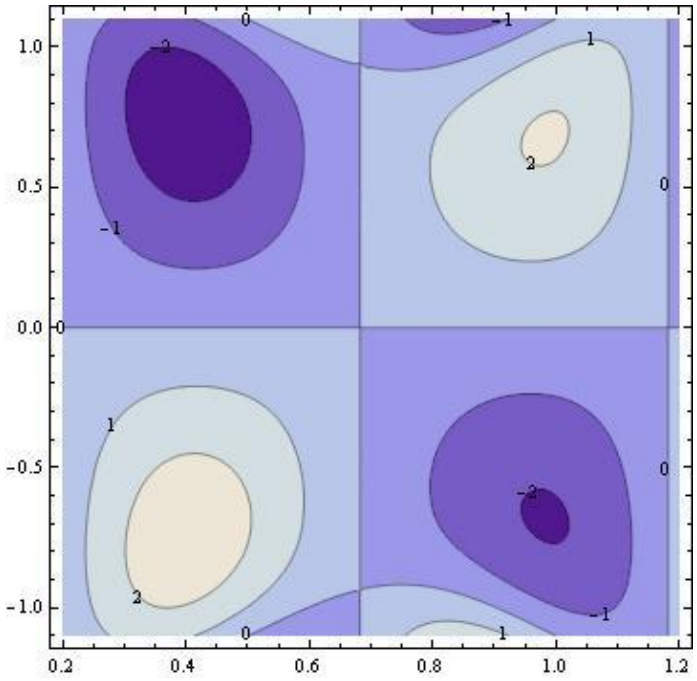

Figure 3.11(a): Stream lines for $E_1 = 0.003$.

$(\varepsilon = 0.1; E_2 = 0.004; E_3 = 0.02; \alpha = 10; Da = 0.1; \beta = 0.1; H_0 = 0.6)$

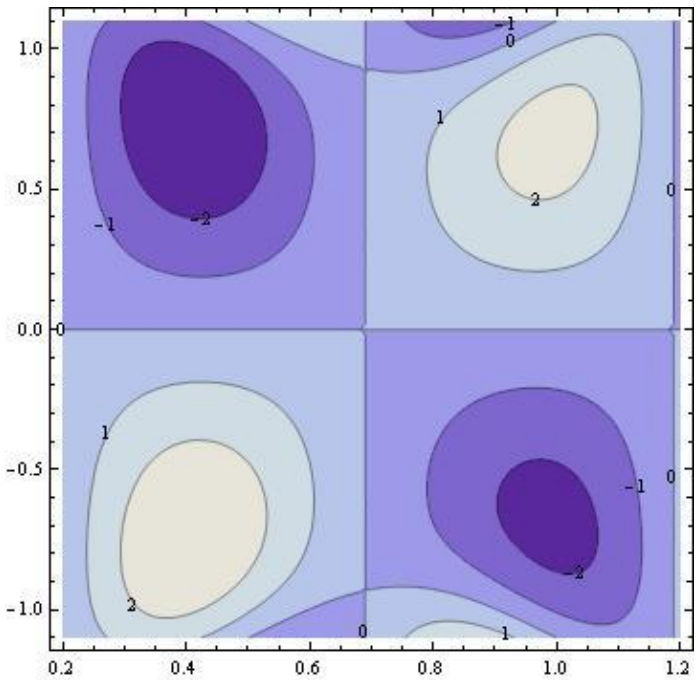

Figure 3.11(b): Stream lines for $E_1 = 0.004$.

$(\varepsilon = 0.1; E_2 = 0.004; E_3 = 0.02; \alpha = 10; Da = 0.1; \beta = 0.1; H_0 = 0.6)$

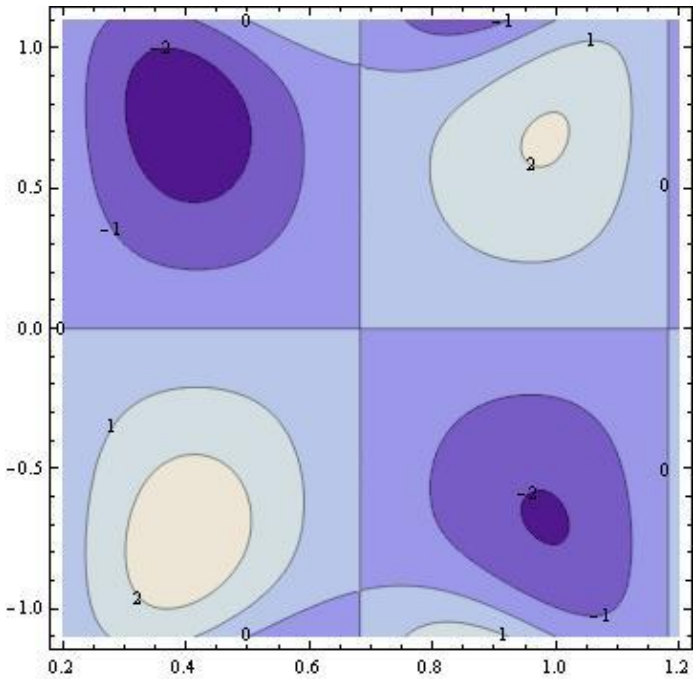

Figure 3.12(a): Stream lines for $E_2 = 0.004$.

$(\varepsilon = 0.1; E_1 = 0.003; E_3 = 0.02; \alpha = 10; Da = 0.1; \beta = 0.1; H_0 = 0.6)$

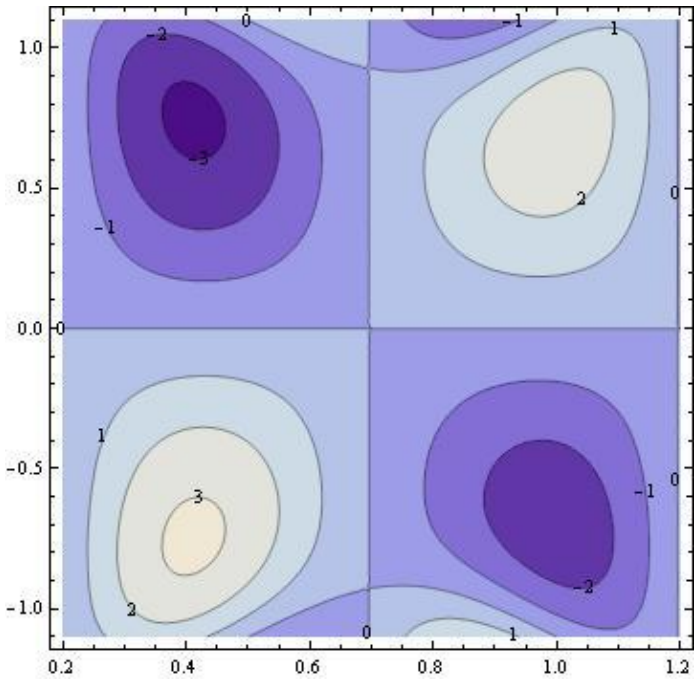

Figure 3.12(b): Stream lines for $E_2 = 0.006$.

$(\varepsilon = 0.1; E_1 = 0.003; E_3 = 0.02; \alpha = 10; Da = 0.1; \beta = 0.1; H_0 = 0.6)$

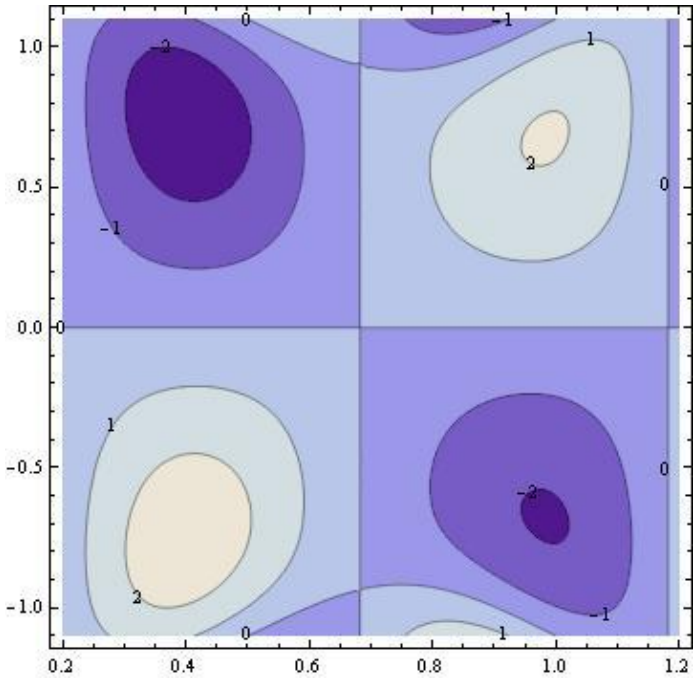

Figure 3.13(a): Stream lines for $E_3 = 0.02$.

($\varepsilon = 0.1; E_1 = 0.003; E_2 = 0.004; \alpha = 10; Da = 0.1; \beta = 0.1; H_0 = 0.6$)

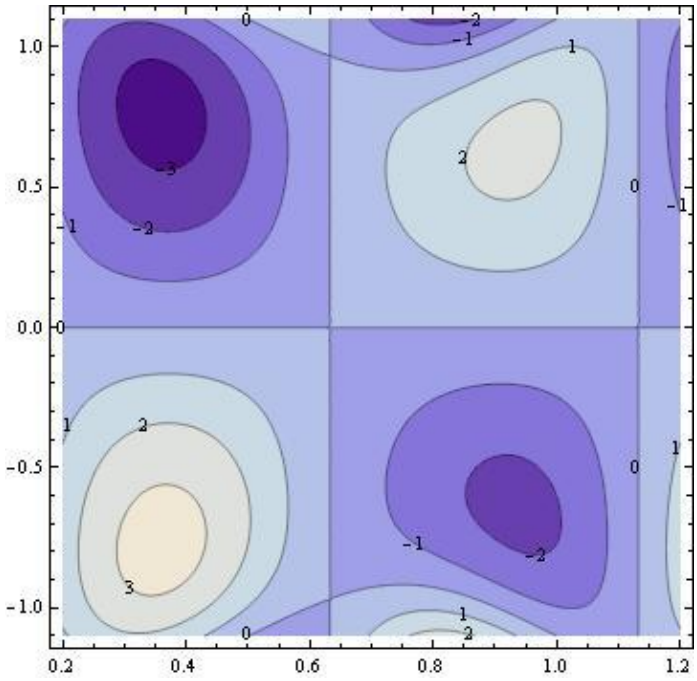

Figure 3.13(b): Stream lines for $E_3 = 0.04$.

($\varepsilon = 0.1; E_1 = 0.003; E_2 = 0.004; \alpha = 10; Da = 0.1; \beta = 0.1; H_0 = 0.6$)

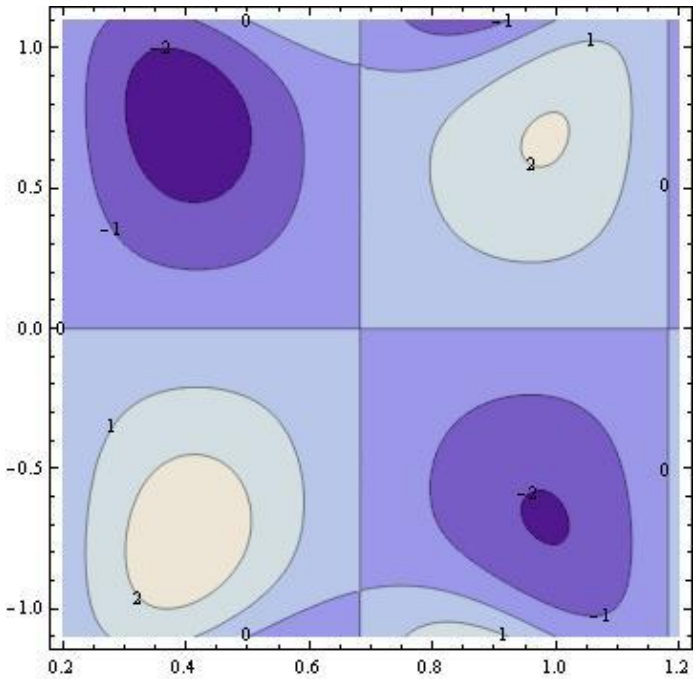

Figure 3.14(a): Stream lines for $\alpha = 10$.

$(\varepsilon = 0.1; E_1 = 0.003; E_2 = 0.004; E_3 = 0.02; Da = 0.1; \beta = 0.1; H_0 = 0.6)$

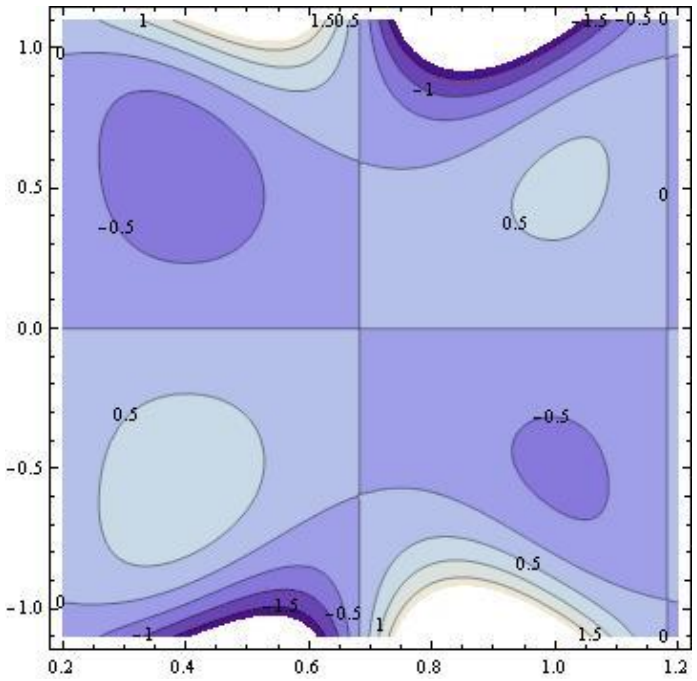

Figure 3.14(b): Stream lines for $\alpha = 10.1$.

$(\varepsilon = 0.1; E_1 = 0.003; E_2 = 0.004; E_3 = 0.02; Da = 0.1; \beta = 0.1; H_0 = 0.6)$

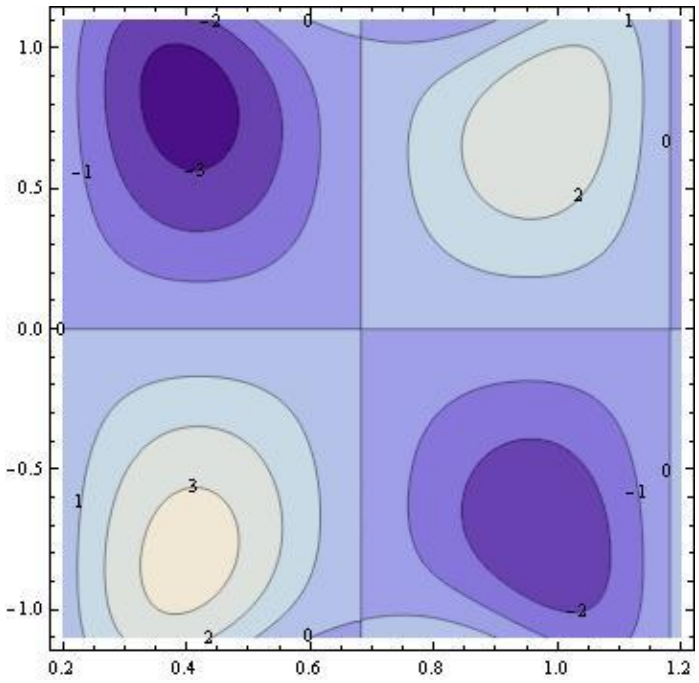

Figure 3.15(a): Stream lines for $\beta = = 0.099$.

$(\varepsilon = 0.1 E_1 = 0.003; E_2 = 0.004; E_3 = 0.02; \alpha = 10; Da = 0.1; H_0 = 0.6)$

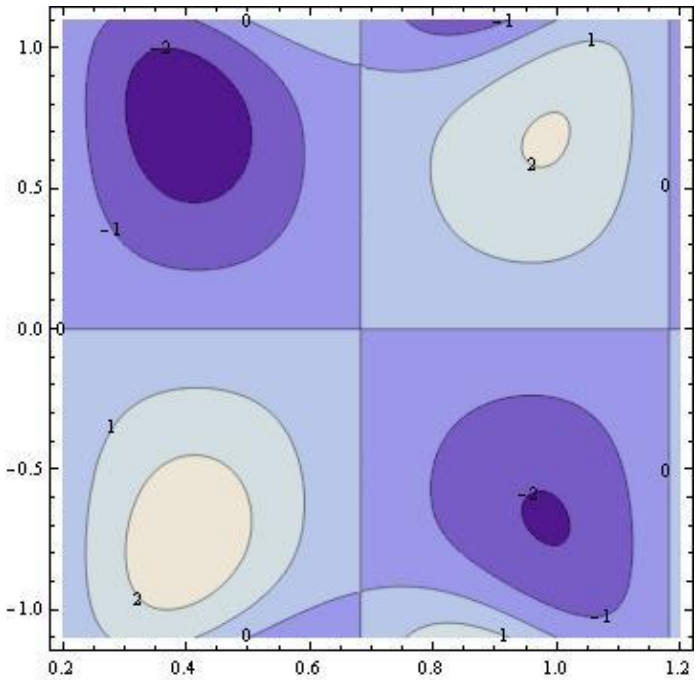

Figure 3.15(b): Stream lines for $\beta = 0.1$.

$(\varepsilon = 0.1; E_1 = 0.003; E_2 = 0.004; E_3 = 0.02; \alpha = 10; Da = 0.1; H_0 = 0.6)$

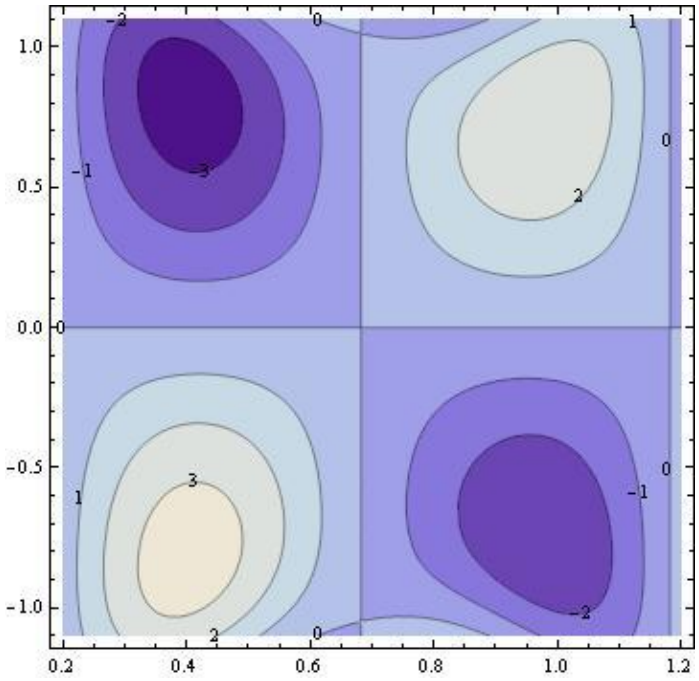

Figure 3.16(a): Stream lines for $Da = 0.099$.

($\varepsilon = 0.1; E_1 = 0.003; E_2 = 0.004; E_3 = 0.02; \alpha = 10; \beta = 0.1; H_0 = 0.6$)

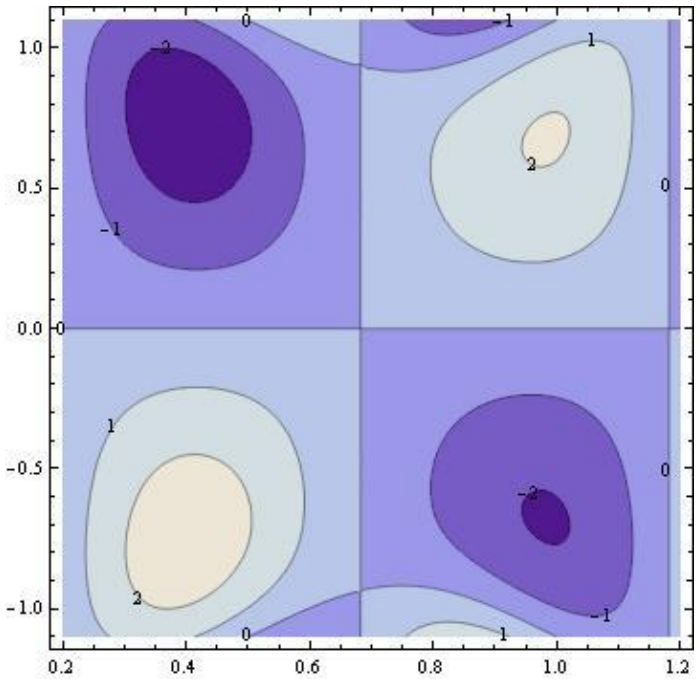

Figure 3.16(b): Stream lines for $Da = 0.1$.

($\varepsilon = 0.1; E_1 = 0.003; E_2 = 0.004; E_3 = 0.02; \alpha = 10; \beta = 0.1; H_0 = 0.6$)

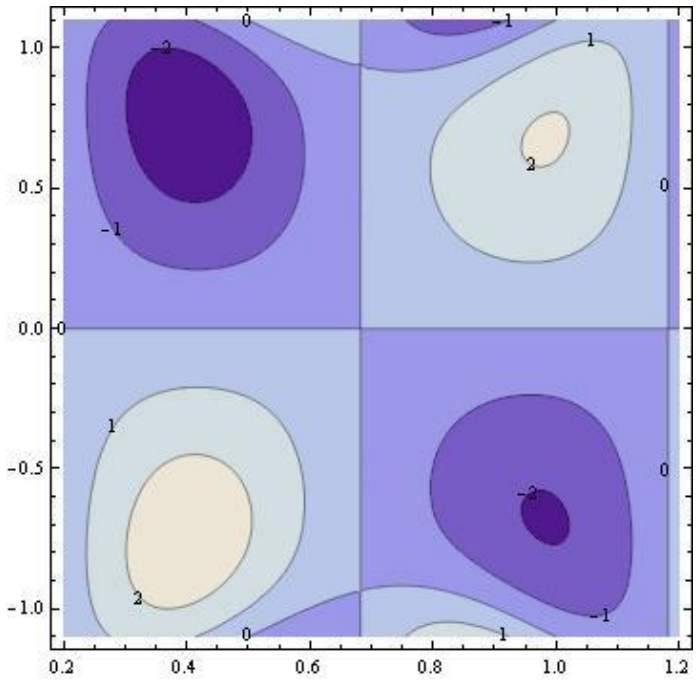

Figure 3.17(a): Stream lines for $H_0 = 0.6$.

$(\varepsilon = 0.1; E_1 = 0.003; E_2 = 0.004; E_3 = 0.02; \alpha = 10; Da = 0.1; \beta = 0.1)$

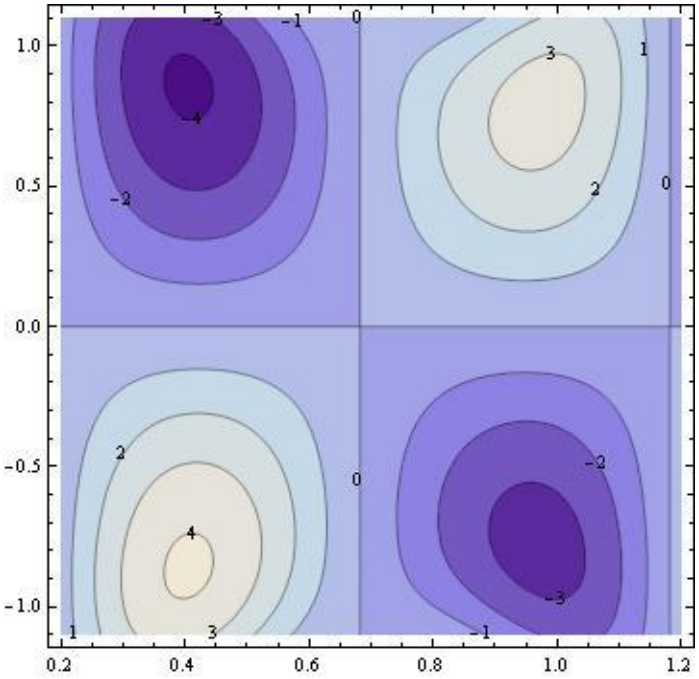

Figure 3.17(b): Stream lines for $H_0 = 0.7$.

$(\varepsilon = 0.1 E_1 = 0.003; E_2 = 0.004; E_3 = 0.02; \alpha = 10; Da = 0.1; \beta = 0.1)$

Chapter 4

Transport of MHD Couple Stress Fluid through Peristalsis in a Porous Medium under the Influence of Heat Transfer and Slip Effects

4.1 Introduction

One of the significant mechanisms used to drive fluids in a variety of ducts is 'Peristalsis' that takes place because of the contraction and expansion of the muscular walls. In the previous two chapters, peristaltic transport of couple stress fluid with elastic wall properties and slip effects in porous uniform channel and under the presence of magnetic field have been discussed. In this chapter the study has been extended to analyze the heat transfer effects.

While blood is inside the body the thermo dynamical aspects of blood seems to be unimportant but are of due importance when blood is taken out of the body. Peristalsis with heat transfer might help in the better perceptive of the flow pattern of blood in bio-medical instruments like hemodialyser, heart-lung machine. Owing to its numerous applications: paper making, food processing and vasodilatation, hemodialyasis, oxygenation, heat transfer study has gained importance.

Srinivas et al. [104] looked into the magnetohydrodynamic peristaltic transport having slip walls to explore the heat transfer effects. Hayat and Mariyam [105] examined significance of the heat transfer and compliant wall effects under the peristaltic motion of a viscous fluid inside a porous channel. Considering the Maxwell fluid the collective effect of the heat transfer, MHD and slip wall, on the flow accompanied by peristalsis through a permeable conduit was analyzed by Das [106]. The viscous couple stress fluid was considered for heat effect and slip analysis in a peristaltic permeable channel by Hummady and Abdulhadi [103]. Javed et al. [107] studied importance of the heat transfer and compliant wall effects under peristaltic flow of Burgers fluid. Considering the couple stress fluid the combined effect of heat transfer and wall effect through porous medium under peristalsis was examined by Eldabe et al. [108]. Laxshiminarayana et al. [109] considered the conducting Bingham fluid for examining the effect of heat transfer in a non-uniform peristaltic conduit. Also the slip and elastic wall properties were considered for analysis.

Present chapter deals with the impressions of heat transfer coefficient and temperature distribution on MHD flow of couple stress fluid under peristalsis with wall and slip effects. The motion has been explored under lubrication approach.

4.2 Physical assumptions of the problem

The peristaltic motion in a uniform magnetohydrodynamic (MHD) channel of a non-Newtonian fluid is considered to flow between the elastic walls under heat transfer as shown in Figure 4.1. The flow geometry and the governing wall equations are explained in chapter 2 (equations 2.1 to 2.3).

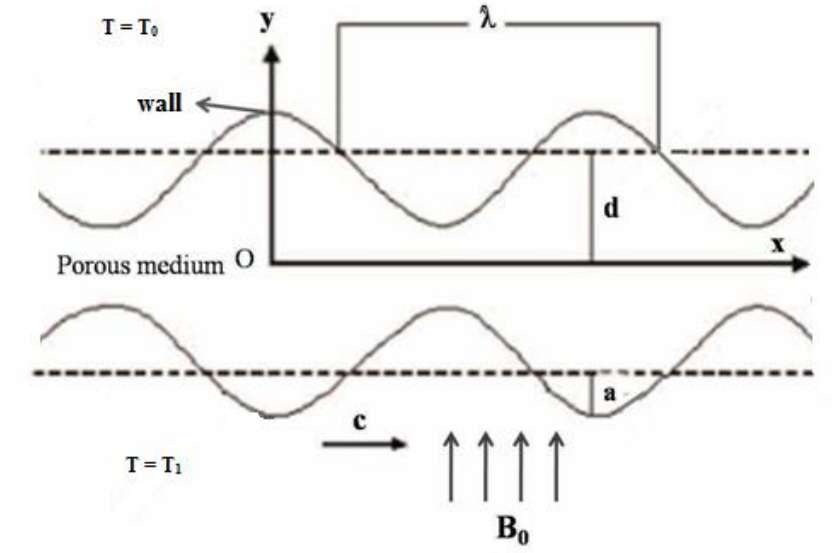

Figure 4.1: Geometry of peristaltic transport.

The flow modeled for the incompressible couple stress fluid has the following governing equations

$$\frac{\partial u}{\partial x}+\frac{\partial u}{\partial y}=0, \tag{4.1}$$

$$\rho\left(\frac{\partial u}{\partial t}+u\frac{\partial u}{\partial x}+v\frac{\partial u}{\partial y}\right)=-\frac{\partial p}{\partial x}+\mu\nabla^2 u-h\nabla^4 u-\mu\frac{u}{k}-\sigma {B_0}^2 u, \tag{4.2}$$

$$\rho\left(\frac{\partial v}{\partial t}+u\frac{\partial v}{\partial x}+v\frac{\partial v}{\partial y}\right)=-\frac{\partial p}{\partial y}+\mu\nabla^2 v-h\nabla^4 v-\mu\frac{v}{k}. \tag{4.3}$$

Energy equation is

$$G\left(\frac{\partial T}{\partial t}+u\frac{\partial T}{\partial x}+v\frac{\partial T}{\partial y}\right)=\frac{K}{\rho}\left(\frac{\partial^2 T}{\partial x^2}+\frac{\partial^2 T}{\partial y^2}\right)+\vartheta\left\{2\left[\left(\frac{\partial u}{\partial x}\right)^2+\left(\frac{\partial v}{\partial y}\right)^2\right]+\left(\frac{\partial v}{\partial x}+\frac{\partial u}{\partial y}\right)^2\right\}. \tag{4.4}$$

Here $T, K, \vartheta \; and \; G$ are respectively the temperature of the fluid, the thermal conductivity of the fluid, the kinematic coefficient of viscosity and the specific heat at constant pressure, along with usual meaning of other parameters as given in chapter 2.

The boundary conditions are correspondingly

$$\frac{\partial u}{\partial y} = 0, \quad \frac{\partial^3 u}{\partial y^3} = 0, \qquad at \;\; y = 0, \tag{4.5}$$

$$u = -d\frac{\sqrt{Da}}{\beta}\frac{\partial u}{\partial y} \;\; , \quad at \;\; y = \pm\eta(x,t), \tag{4.6}$$

$$-\left(\frac{\partial^2 v}{\partial x^2} - \frac{\partial^2 u}{\partial x \partial y}\right)\frac{\partial \eta}{\partial x} + \frac{\partial^2 v}{\partial x \partial y} - \frac{\partial^2 u}{\partial y^2} = 0, \qquad at \;\; y = \pm\eta(x,t), \tag{4.7}$$

$$\frac{\partial}{\partial x}L(\eta) = -\rho\left(\frac{\partial u}{\partial t} + u\frac{\partial u}{\partial x} + v\frac{\partial u}{\partial y}\right) + \mu\nabla^2 u - h\nabla^4 u - \mu\frac{u}{k} - \sigma {B_0}^2 u, at \; y = \pm\eta(x,t), \tag{4.8}$$

where

$$\frac{\partial}{\partial x}L(\eta) = \frac{\partial p}{\partial x} = -T\frac{\partial^3 \eta}{\partial x^3} + m\frac{\partial^3 \eta}{\partial x \partial t^2} + C\frac{\partial^2 \eta}{\partial x \partial t}. \tag{4.9}$$

Non dimensional quantities used are as mentioned in chapter 2 along with $\theta = \frac{T - T_0}{T_1 - T_0}$.

The temperature at the upper wall is T_0 and the temperature at the lower wall is T_1 .

The equations 4.1 to 4.8 then reduce to equations

$$\frac{\partial u}{\partial x} + \frac{\partial u}{\partial y} = 0, \tag{4.10}$$

$$R_e\delta\left(\frac{\partial u}{\partial t} + u\frac{\partial u}{\partial x} + v\frac{\partial u}{\partial y}\right) = -\frac{\partial p}{\partial x} + \left(\delta^2\frac{\partial^2 u}{\partial x^2} + \frac{\partial^2 u}{\partial y^2}\right) - \frac{1}{\propto^2}\left(\delta^2\frac{\partial^2}{\partial x^2} + \frac{\partial^2}{\partial y^2}\right)\left(\delta^2\frac{\partial^2 u}{\partial x^2} + \frac{\partial^2 u}{\partial y^2}\right) - \frac{u}{Da} - {H_0}^2 u \,, \tag{4.11}$$

$$R_e\delta^3\left(\frac{\partial v}{\partial t} + u\frac{\partial v}{\partial x} + v\frac{\partial v}{\partial y}\right) = -\frac{\partial p}{\partial y} + \delta^2\left(\delta^2\frac{\partial^2 v}{\partial x^2} + \frac{\partial^2 v}{\partial y^2}\right) - \frac{\delta^2}{\propto^2}\left(\delta^2\frac{\partial^2}{\partial x^2} + \frac{\partial^2}{\partial y^2}\right)\left(\delta^2\frac{\partial^2 v}{\partial x^2} + \frac{\partial^2 v}{\partial y^2}\right) - \delta^2\frac{v}{Da} \,, \tag{4.12}$$

$$R_e\delta\left(\frac{\partial\theta}{\partial t}+u\frac{\partial\theta}{\partial x}+\ v\frac{\partial\theta}{\partial y}\right)=\ \frac{1}{P_r}\left(\delta^2\frac{\partial^2\theta}{\partial x^2}+\ \frac{\partial^2\theta}{\partial y^2}\right)+\ E_c\left[2\left\{\delta^2\left(\frac{\partial u}{\partial x}\right)^2\right)+\delta^2\left(\frac{\partial v}{\partial y}\right)^2\right\}+$$

$$\left(\delta^2\frac{\partial v}{\partial x}+\ \frac{\partial u}{\partial y}\right)^2\Big]. \tag{4.13}$$

The pertinent peripheral conditions are

$$\frac{\partial u}{\partial y}=0,\quad \frac{\partial^3 u}{\partial y^3}=0,\qquad at\ \ y=0, \tag{4.14}$$

$$u=-\frac{\sqrt{Da}}{\beta}\frac{\partial u}{\partial y},\quad\ \ at\ \ y=\ \pm\eta(x,t)=\ \pm\big(1+\ \varepsilon sin2\pi(x-t)\big), \tag{4.15}$$

$$-\left(\delta^4\frac{\partial^2 v}{\partial x^2}-\delta^2\frac{\partial^2 u}{\partial x\partial y}\right)\frac{\partial\eta}{\partial x}+\delta^2\frac{\partial^2 v}{\partial x\partial y}-\frac{\partial^2 u}{\partial y^2}=0,$$

$$at\ y=\ \pm\eta\ (x,t)=\ \pm\big(1+\ \varepsilon sin2\pi(x-t)\big) \tag{4.16}$$

and

$$-R_e\delta\left(\frac{\partial u}{\partial t}+u\frac{\partial u}{\partial x}+\ v\frac{\partial u}{\partial y}\right)+\left(\delta^2\frac{\partial^2 u}{\partial x^2}+\ \frac{\partial^2 u}{\partial y^2}\right)-\frac{1}{\propto^2}\left(\delta^2\frac{\partial^2}{\partial x^2}+\ \frac{\partial^2}{\partial y^2}\right)\left(\delta^2\frac{\partial^2 u}{\partial x^2}+\ \frac{\partial^2 u}{\partial y^2}\right)-\frac{u}{Da}-$$

$$H_0{}^2u=\ E_1\ \frac{\partial^3\eta}{\partial x^3}+\ E_2\ \frac{\partial^3\eta}{\partial x\partial t^2}+\ E_3\ \frac{\partial^2\eta}{\partial x\partial t}\ ,\ at\ \ y=\ \pm\eta(x,t). \tag{4.17}$$

Here, $P_r=\frac{\rho\vartheta G}{K}$, $E_c=\frac{c^2}{G(T_1-T_0)}$ correspondingly represent the Prandtl number and the Eckert number. The parameters δ, ε, Da, $\beta,\propto$, H_0 and E_1, E_2, E_3 are as given in chapter 2.

4.3. Method of Solution

Using the non dimensional quantities, Equations (4.10) – (4.13) reduce to

$$\frac{\partial u}{\partial x}+\frac{\partial u}{\partial y}=\ 0\ , \tag{4.18}$$

$$0=-\frac{\partial p}{\partial x}+\ \frac{\partial^2 u}{\partial y^2}-\frac{1}{\alpha^2}\frac{\partial^4 u}{\partial y^4}-\frac{u}{Da}-H_0{}^2u\ , \tag{4.19}$$

$$0 = -\frac{\partial p}{\partial y}, \tag{4.20}$$

$$E_c\left(\frac{\partial u}{\partial y}\right)^2 + \frac{1}{P_r}\frac{\partial^2 \theta}{\partial y^2} = 0. \tag{4.21}$$

The boundary conditions 4.14 – 4.17 become

$$\frac{\partial u}{\partial y} = 0, \quad \frac{\partial^3 u}{\partial y^3} = 0, \qquad at\ y = 0, \tag{4.22}$$

$$u = -\frac{\sqrt{Da}}{\beta}\frac{\partial u}{\partial y}, \quad at\ \ y = \pm\eta(x,t) = \pm\big(1 + \varepsilon sin2\pi(x-t)\big), \tag{4.23}$$

$$\frac{\partial^2 u}{\partial y^2} = 0, \qquad at\ \ y = \pm\eta(x,t) = \pm\big(1 + \varepsilon sin2\pi(x-t)\big) \tag{4.24}$$

and

$$\frac{\partial^2 u}{\partial y^2} - \frac{1}{\alpha^2}\frac{\partial^4 u}{\partial y^4} - \frac{u}{Da} - {H_0}^2 u = E_1\frac{\partial^3 \eta}{\partial x^3} + E_2\frac{\partial^3 \eta}{\partial x \partial t^2} + E_3\frac{\partial^2 \eta}{\partial x \partial t}, at\ y = \pm\eta(x,t). \tag{4.25}$$

Further,

$$\theta = 0\ \ at\ \ y = -\eta(x,t)\,, \tag{4.26}$$

$$\theta = 1\ \ at\ y = \eta(x,t)\,. \tag{4.27}$$

Solving equations 4.19 and 4.20, using the boundary conditions 4.22 – 4.25,

$$u(x,y,t) = \frac{E}{M{H_0}^2}\left[\frac{m_1 m_2 - {m_2}^2}{{H_0}^2 \propto^2} + \frac{m_2}{m_1} - 1 - M - \frac{m_2 cosh(\sqrt{m_1}y)}{m_1 T_1} + \frac{cosh(\sqrt{m_2}y)}{T_2}\right]. \tag{4.28}$$

Solving equation 4.21, with boundary conditions 4.26 and 4.27 we get

$$\theta = P\left[\frac{{m_2}^2}{4m_1{T_1}^2}\left\{\frac{cosh2\sqrt{m_1}y}{2m_1} - \frac{M_3}{2m_1} - y^2 + \eta^2\right\} + \frac{m_2}{4{T_2}^2}\left\{\frac{cosh2\sqrt{m_2}y}{2m_2} - \frac{M_4}{2m_2} - y^2 + \eta^2\right\} - \right.$$

$$\left.\frac{{m_2}^{\frac{3}{2}}}{T_1 T_2\sqrt{m_1}}\left\{\frac{coshM_1 y}{{M_1}^2} - \frac{coshM_2 y}{{M_2}^2} - \frac{M_5}{M1^2} + \frac{M_6}{{M_2}^2}\right\}\right] + \frac{y}{2\eta} + \frac{1}{2}. \tag{4.29}$$

Here

$$E = -8\varepsilon\pi^3 cos2\pi(x-t)(E_1 + E_2) + 4\varepsilon\pi^2 E_3 sin2\pi(x-t),$$

$$M = \frac{m_1 m_2 - {m_2}^2}{{H_0}^2 \propto^2} + \frac{\sqrt{Da}}{\beta} m_2 \left(\frac{T_4}{\sqrt{m_2}} - \frac{T_3}{\sqrt{m_1}}\right),$$

$$m_1 = \frac{\alpha^2 + \alpha\sqrt{\alpha^2 - 4H}}{2}, \qquad m_2 = \frac{\alpha^2 - \alpha\sqrt{\alpha^2 - 4H}}{2}, \qquad H = \frac{1}{Da} + {H_0}^2,$$

$$T_1 = \cosh\sqrt{m_1}\eta, \qquad T_2 = \cosh\sqrt{m_2}\eta, \qquad T_3 = Tanh(\sqrt{m_1}\eta),$$

$$T_4 = Tanh(\sqrt{m_2}\eta), \qquad M_1 = \sqrt{m_1} + \sqrt{m_2}\,, \qquad M_2 = \sqrt{m_1} - \sqrt{m_2},$$

$$M_3 = \cosh 2\sqrt{m_1}\eta\,, \qquad M_4 = \cosh 2\sqrt{m_2}\eta\,, \qquad M_5 = \cosh M_1\eta,$$

$$M_6 = \cosh M_2\eta, \qquad P = \frac{-Br\,E^2}{M^2 H 0^4}, \qquad Br = E_c p_r,$$

where Br is the Brinkman number.

At the wall, the heat transfer coefficient is

$$H = \eta_x \theta_y(\eta). \tag{4.30}$$

$$H = [2\pi\varepsilon\, cos 2\pi(x-t)]\left[P\left\{\frac{{m_2}^2}{4m_1{T_1}^2}\left(\frac{sinh 2\sqrt{m_1}\eta}{4{m_1}^{3/2}} - 2\eta\right) + \frac{m_2}{4{T_2}^2}\left(\frac{sinh 2\sqrt{m_2}\eta}{4{m_2}^{3/2}} - 2\eta\right) - \right.\right.$$

$$\left.\left.\frac{{m_2}^{\frac{3}{2}}}{T_1 T_2\sqrt{m_1}}\left(\frac{sinh M_1\eta}{M1^3} - \frac{sinh M_2\eta}{M2^3}\right)\right\} + \frac{1}{2\eta}\right]. \tag{4.31}$$

4.4 Results and Discussion

For equation 4.29, graphs are put forth as in Figures 4.2-4.7, to know the effects of various parameters. Observing Figure 4.2 makes clear that temperature enhances by increasing the values of elastic parameters. From Figure 4.3, it is seen that as the couple stress parameter increases, the temperature decreases. Observing Figure 4.4 it is seen that that temperature increase with rise in the slip parameter β. Figure 4.5 shows that temperature increases with Da. Figure 4.6 reveals that as there is decrease in temperature, Hartmann number H_0 increases. This result is in agreement with that of Das [106]. Enhancing the values of Br, results in gain of temperature as depicted in Figure 4.7. This result validates with the result of Lakshminarayana et al. [109].

Variations in the heat transfer coefficient H at the wall of the channel are illustrated from Figure 4.8 to Figure 4.13 for analyzing the effects α, β, H_0, Da, Br, E_1, E_2 and E_3 with

preset values of parameters from equation 4.31. Graphical observations are discussed by taking the magnitudinal value of the heat transfer coefficient into consideration. Figure 4.8 clarifies that with gain in elastic parameters E_1, E_2 and E_3 magnitudinally reduces the coefficient of heat transfer H. Small variations are noticed in the coefficient of heat transfer for change in the values of couple stress parameter α and slip parameter β as observed from Figure 4.9 and Figure 4.10. The magnitude of H increases by raising the Darcy number Da as seen in Figure 4.11.This result is in agreement with that of Das [106]. Rise in the value of H_0 and Br result in reduction of absolute value of heat transfer coefficient H as represented in Figure 4.12 and Figure 4.13.

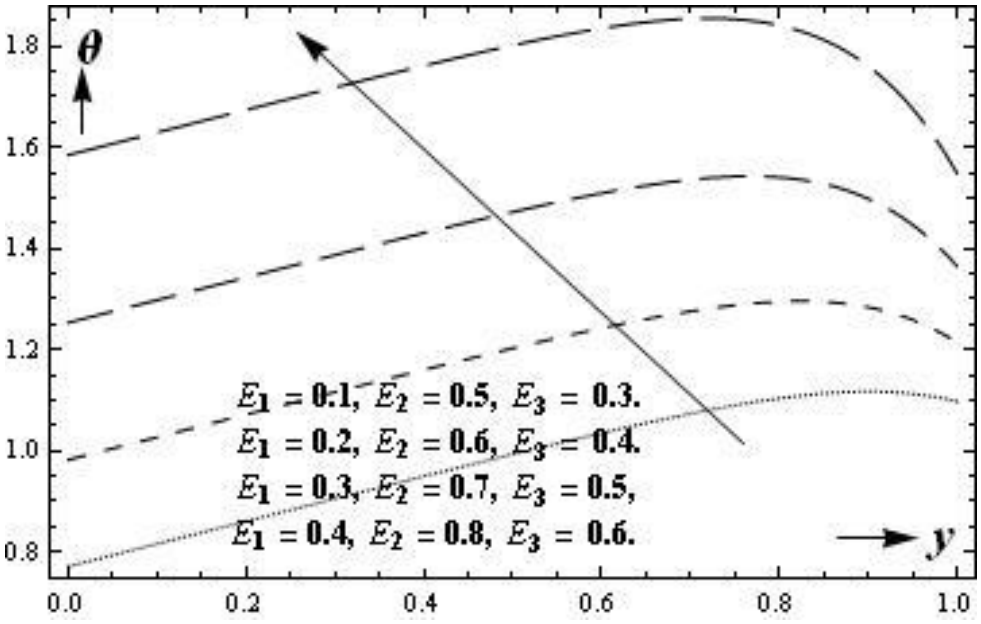

Figure 4.2: Consequences of E_1, E_2, E_3 on temperature distribution θ.

($\epsilon = 0.2$; $\alpha = 10$; $Da = 0.1$; $\beta = 1.1$; $H_0 = 2$; $Br = 1$)

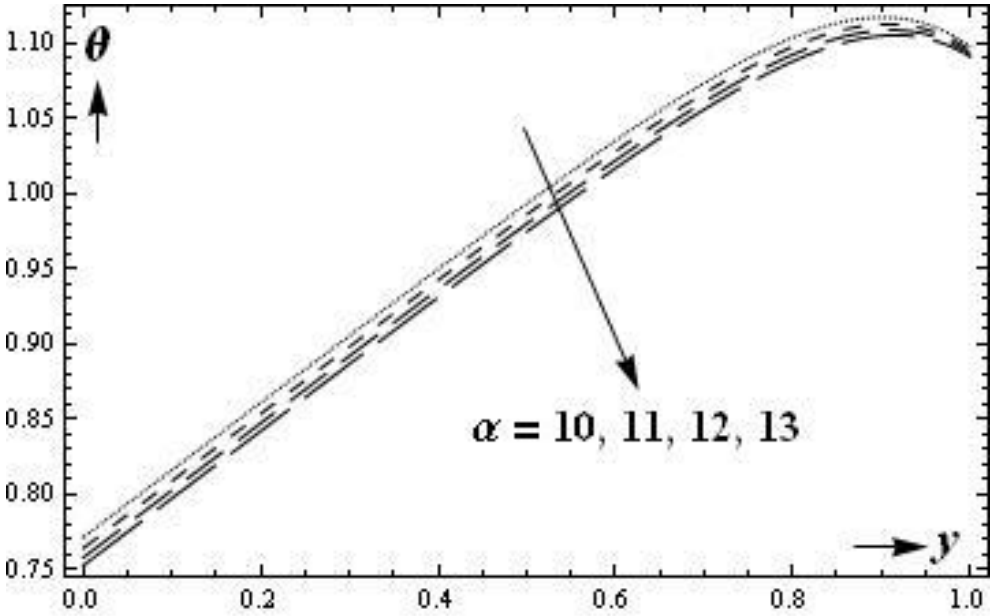

Figure 4.3: Consequences of α on temperature distribution θ.

($\epsilon = 0.2$; $E_1 = 0.1$; $E_2 = 0.5$; $E_3 = 0.3$; $Da = 0.1$; $\beta = 1.1$; $H_0 = 2$; $Br = 1$)

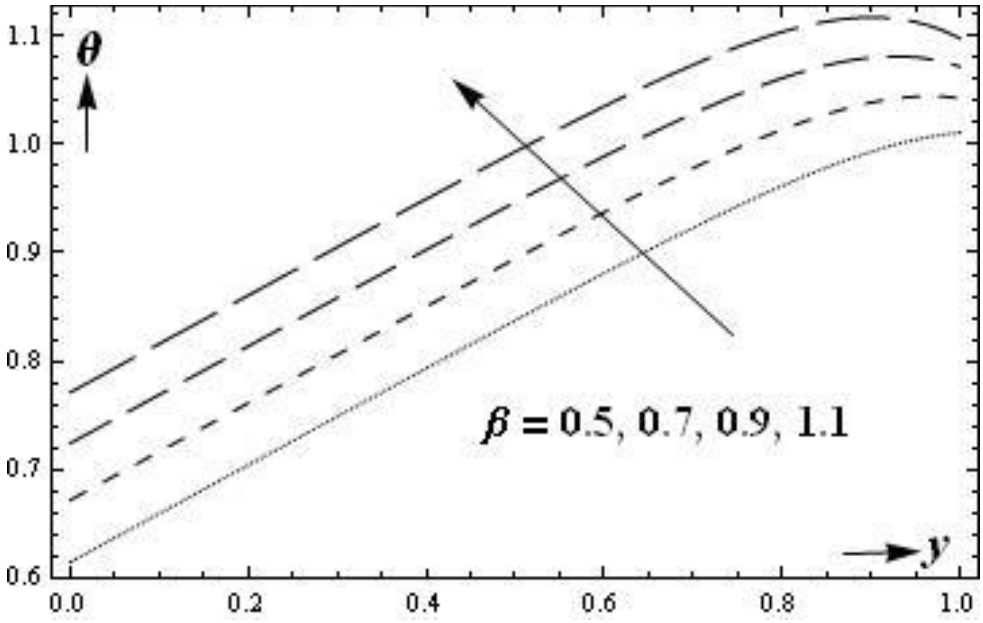

Figure 4.4: Consequences of β on temperature distribution θ.

($\epsilon = 0.2;\ E_1 = 0.1; E_2 = 0.5; E_3 = 0.3; \alpha = 10; Da = 0.1; H_0 = 2; Br = 1$)

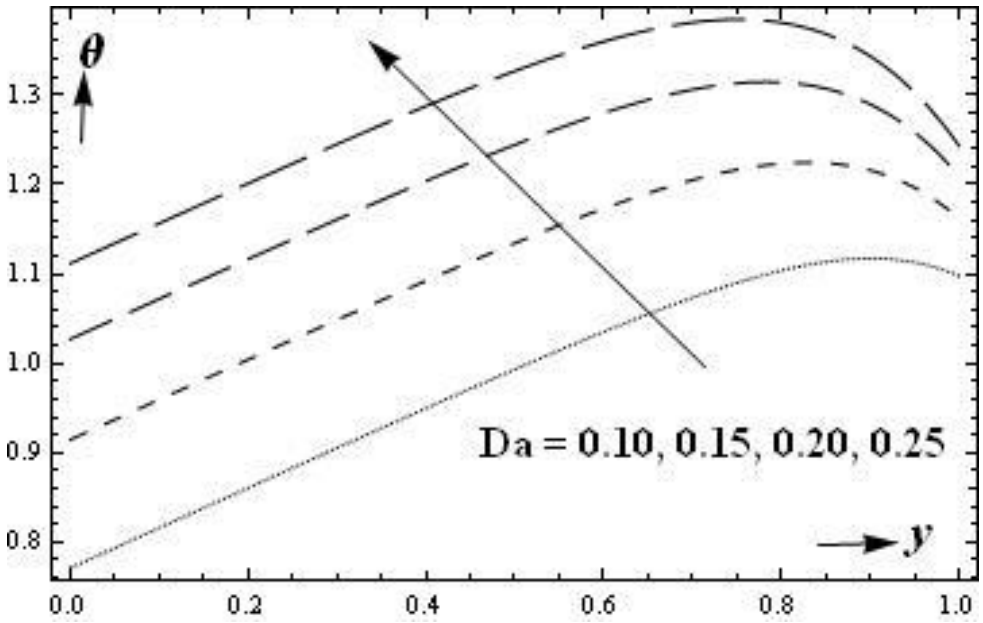

Figure 4.5: Consequences of Da temperature distribution θ.

($\epsilon = 0.2;\ E_1 = 0.1; E_2 = 0.5; E_3 = 0.3; \alpha = 10; \beta = 1.1; H_0 = 2; Br = 1$)

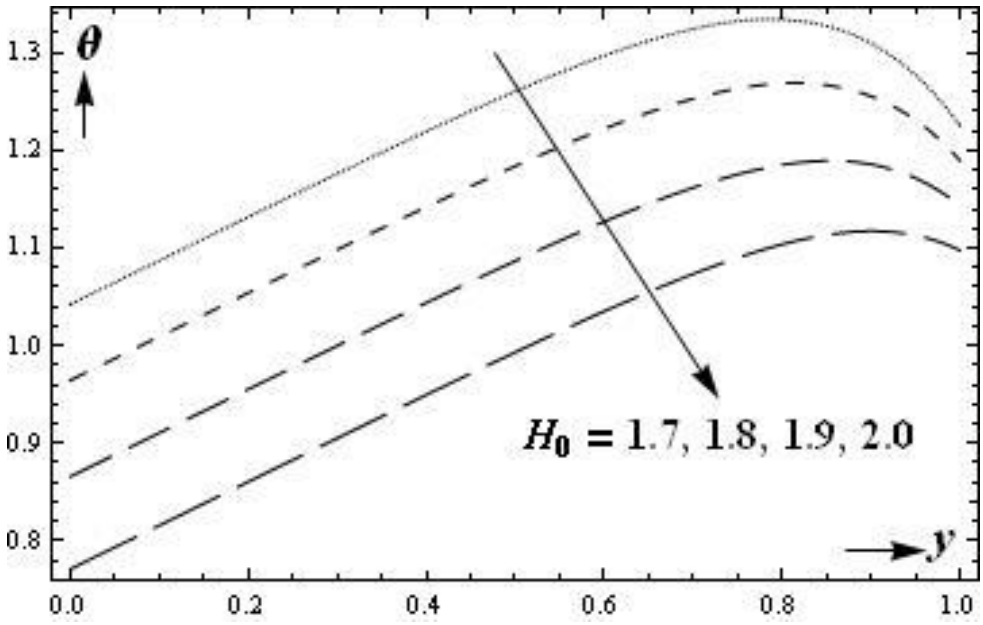

Figure 4.6: Consequences of H_0 on temperature distribution θ.

$(\epsilon = 0.2;\ E_1 = 0.1; E_2 = 0.5; E_3 = 0.3; \alpha = 10; Da = 0.1; \beta = 1.1; Br = 1)$

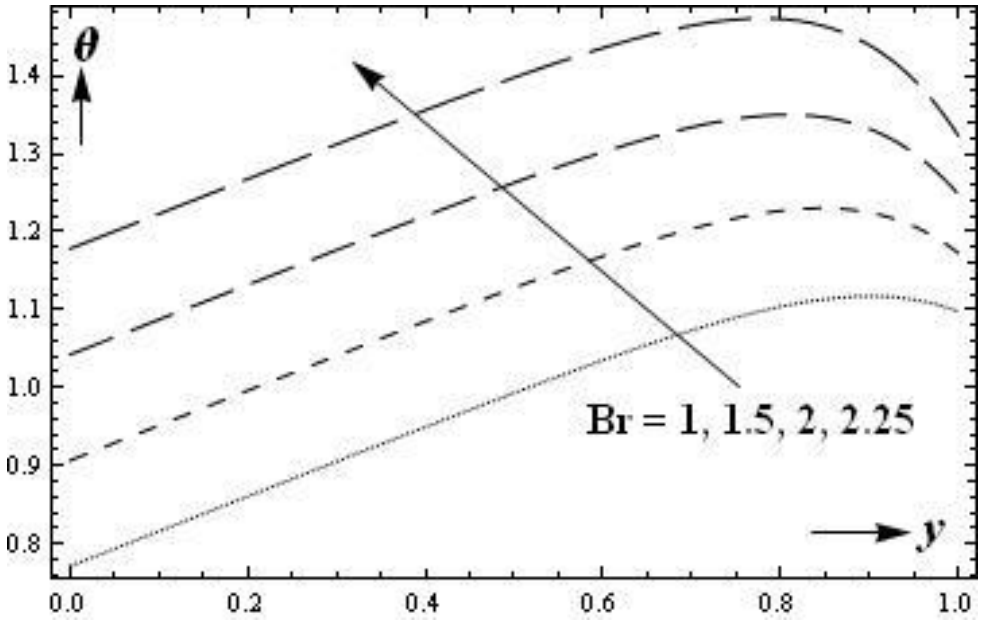

Figure 4.7: Consequences of Br temperature distribution θ.

$(\epsilon = 0.2;\ E_1 = 0.1; E_2 = 0.5; E_3 = 0.3; \alpha = 10; Da = 0.1; \beta = 1.1; H_0 = 2)$

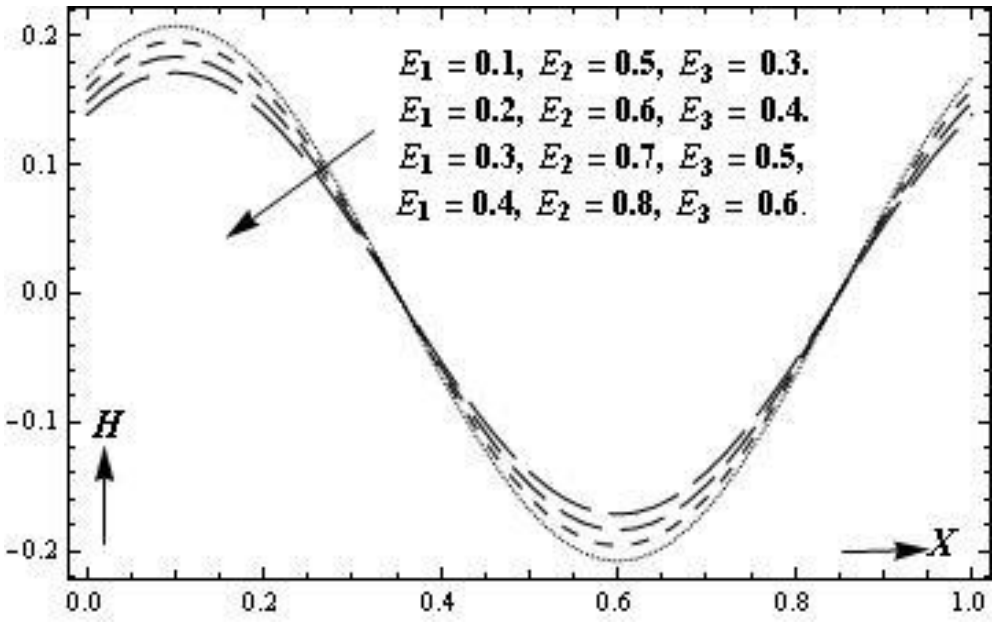

Figure 4.8: Consequences of E_1, E_2, E_3 on Heat transfer coefficient for H.

$(\epsilon = 0.2;\ \alpha = 10; Da = 0.1; \beta = 1.1; H_0 = 2; Br = 1)$

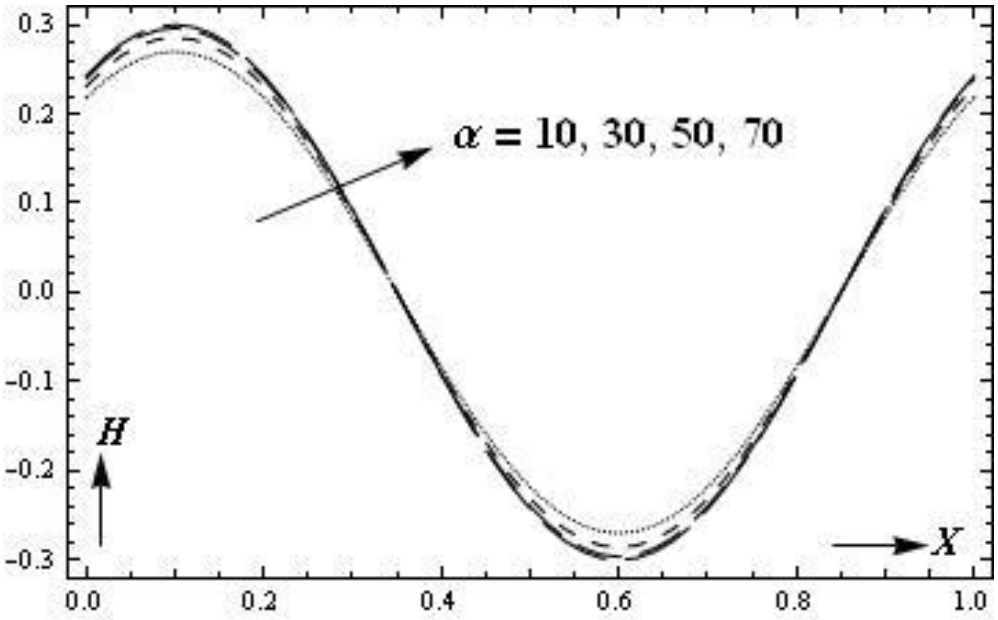

Figure 4.9: Consequences of α on Heat transfer coefficient H.

$(\epsilon = 0.2; E_1 = 0.1; E_2 = 0.5; E_3 = 0.3;\ Da = 0.1; \beta = 1.1; H_0 = 2; Br = 1)$

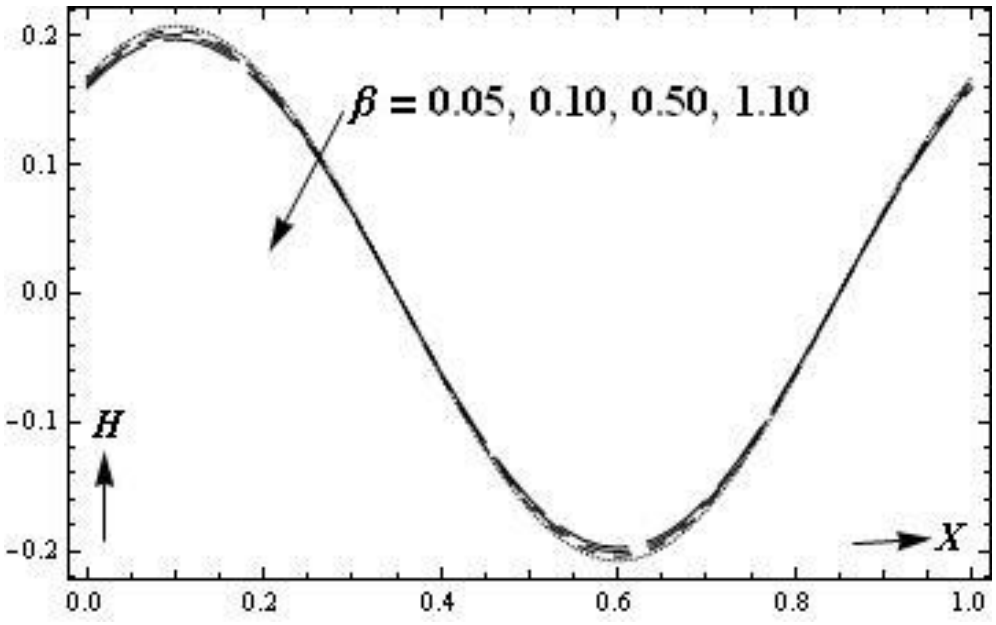

Figure 4.10: Consequences of β on Heat transfer coefficient H.

($\epsilon = 0.2;\ E_1 = 0.1; E_2 = 0.5; E_3 = 0.3; \alpha = 10; Da = 0.1; H_0 = 2; Br = 1$)

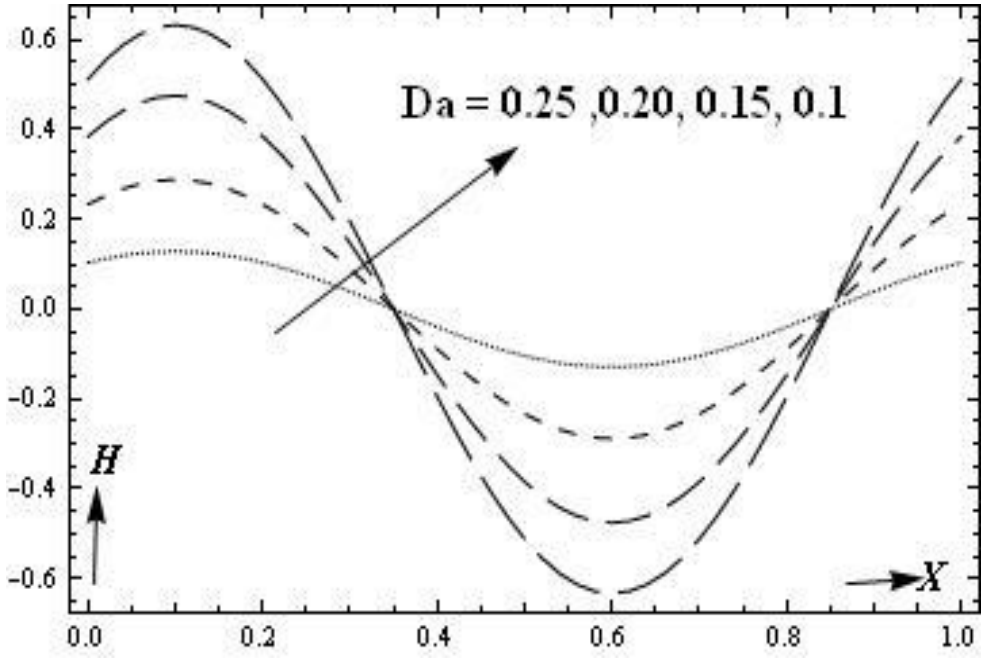

Figure 4.11: Consequences of Da on Heat transfer coefficient H.

($\epsilon = 0.2;\ E_1 = 0.1; E_2 = 0.5; E_3 = 0.3; \alpha = 10; \beta = 1.1; H_0 = 2; Br = 1$)

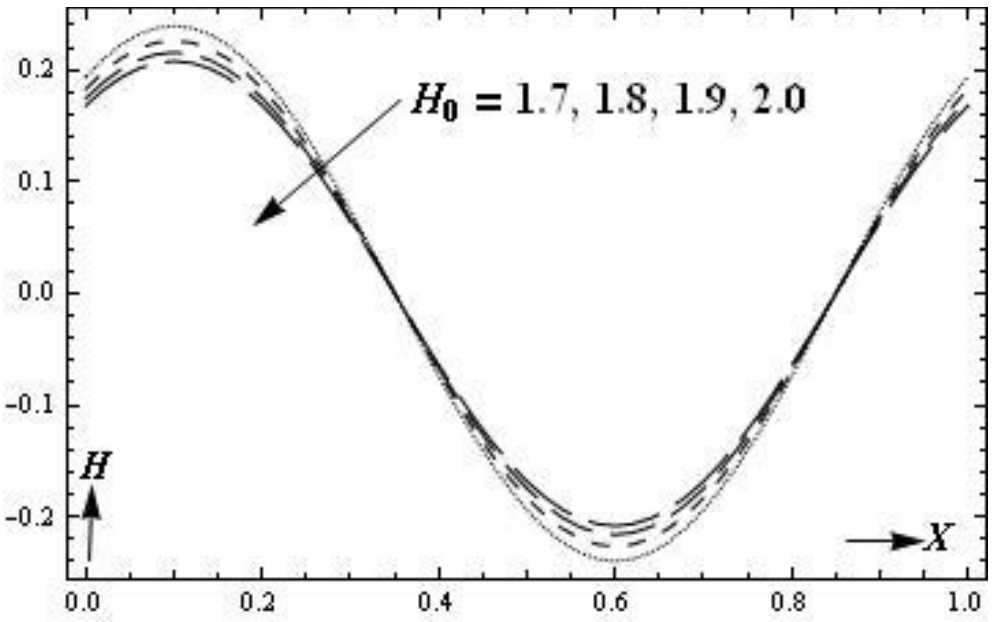

Figure 4.12: Consequences of H_0 on Heat transfer coefficient H.

$(\epsilon = 0.2;\ E_1 = 0.1; E_2 = 0.5; E_3 = 0.3; \alpha = 10; Da = 0.1; \beta = 1.1; Br = 1)$

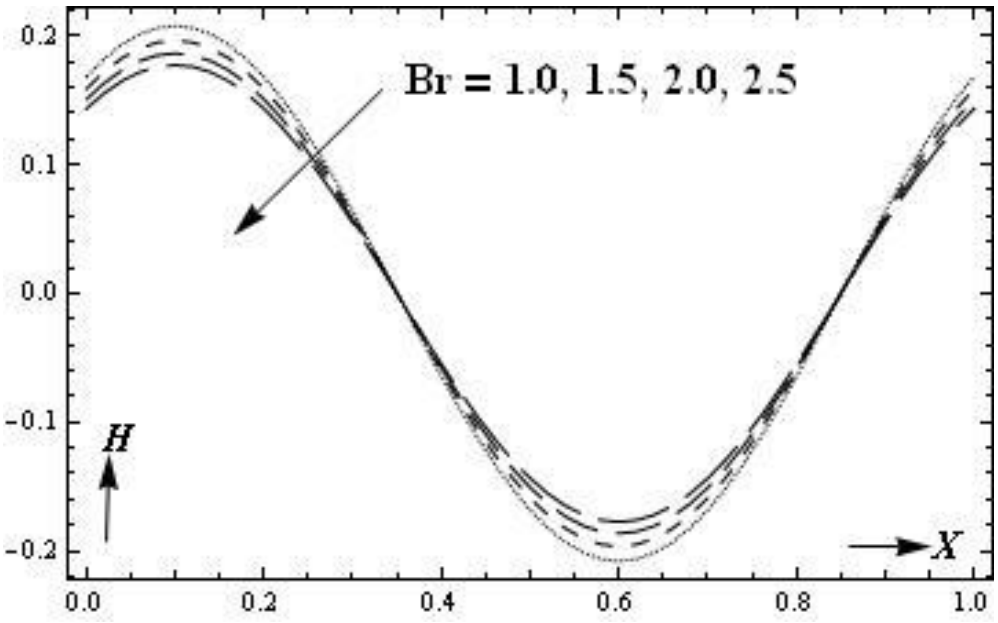

Figure 4.13: Consequences of Br on Heat transfer coefficient H.

$(\epsilon = 0.2; E_1 = 0.1; E_2 = 0.5; E_3 = 0.3;\ \alpha = 10; Da = 0.1; \beta = 1.1; H_0 = 2)$

Chapter 5

Effects of Slip on the Peristaltic Motion of a Jeffrey Fluid in Porous Medium with Wall Effects

5.1 Introduction

The analysis of peristaltic pumping has fascinated many engineering and scientific researchers in the recent years. The phenomenon of peristalsis is defined as a sequence of waves that compress and clasp through the conduit at the peripheral walls. It is a natural phenomenon observed in several human organs having tubular structure. Peristalsis displays a vital role in moving fluids within living bodies, and many biomechanical and engineering devices. For example, the heart-lung machine and other pump instruments. Peristalsis is a means of locomotion for some of the worms.

Recent experimental observations suggest that slip also plays a role in the formation of enhanced concentration fluctuations in entangled polymer solutions. Several experiments clearly show that the slip velocity and the critical shear stress for slip depend upon the polymer/die wall interface.

Chapters 2, 3 and 4 are based on the peristaltic transport inside a symmetric channel having uniform cross section. The flow modeled considered a couple stress fluid to study the slip and wall effects, magnetic and heat transfer effects in porous medium. In this chapter, the peristaltic flow of a Jeffrey fluid with wall properties in uniform porous channel is studied.

Among numerous non-Newtonian models that define the physiological fluids, Jeffrey model is most probably considerable since Newtonian fluid model is easily worked out from the Jeffrey model by taking $\lambda_1 = 0$. Moreover many studies have ensured that blood and other physiological fluids exhibits Newtonian and non-Newtonian nature while it circulates in human body. Also this is a simple linear model that makes use of time derivative as an alternative for convective derivative.

Srinivas and Muthuraj [110] examined the impacts of slip on the Jeffrey fluid flow in an asymmetric inclined peristaltic conduit. Subba Reddy and Prasanth Reddy [111] analyzed peristaltic flow of a Jeffrey fluid in a planar porous channel having variable viscosity. Rathod and Mahadev [112] examined slip effect analysis of a Jeffrey fluid in an inclined conduit under peristaltic motion. Navaneeswara and Viswanatha [113] studied slip effects on pumping of a Jeffrey fluid flow in presence of permeability in an asymmetric peristaltic inclined channel.

The main intention of this chapter is to put forward the wall effects under the peristaltic flow of a Jeffrey fluid in a permeable medium under slip condition using large wavelength approximation and small Reynolds number.

5.2 Physical assumptions of the problem

The motion of an incompressible fluid, namely the Jeffery fluid, moving within a uniform conduit in between the flexible peristaltic walls is considered. Here the channel is considered to be having thickness $2d$, wave amplitude a and wave length λ. x axis is along the direction of wave propagation and y axis transverse to it. The motion is discussed considering only half the width of channel.

The peristaltic wave is propagating with speed c, where c is constant, along the conduit wall. The wall equation is

$$y = \pm\,\eta(x,t) = \pm(d + a\,sin\frac{2\pi}{\lambda}(x - ct)). \tag{5.1}$$

The flexible wall is governed by the equation

$$L(\eta) = p - p_0. \tag{5.2}$$

The operator L used to represent the stretched membrane movement accompanied by viscosity damping force is given by

$$L = -T\frac{\partial^2}{\partial x^2} + m\frac{\partial^2}{\partial t^2} + C\frac{\partial}{\partial t}. \tag{5.3}$$

Here T, C, m respectively represents elastic tension in the membrane, coefficient of viscous damping force and mass per unit area.

The governing equations of the flow field of Jeffrey fluid in porous medium are

The equation of continuity

$$\frac{\partial u}{\partial x} + \frac{\partial v}{\partial y} = 0. \tag{5.4}$$

The equations regarding conservation of momentum

$$\rho\left(\frac{\partial u}{\partial t}+u\frac{\partial u}{\partial x}+v\frac{\partial u}{\partial y}\right)=-\frac{\partial p}{\partial x}+\frac{\mu}{1+\lambda_1}\nabla^2 u-\mu\frac{u}{k}, \tag{5.5}$$

$$\rho\left(\frac{\partial v}{\partial t}+u\frac{\partial v}{\partial x}+v\frac{\partial v}{\partial y}\right)=-\frac{\partial p}{\partial y}+\frac{\mu}{1+\lambda_1}\nabla^2 v-\mu\frac{v}{k}. \tag{5.6}$$

The velocity in the direction of x and y are correspondingly u and v. Due to symmetrical plane the normal velocity is zero. Experimentally it is proved in several physiological situations that flow is accompanied with very small Reynolds number. Hence infinite wavelength is assumed. The ratio of relaxation time to retardation time is λ_1, porous medium permeability is k, time is t, fluid density is ρ, fluid viscosity coefficient is μ and $\nabla^2=\frac{\partial^2}{\partial x^2}+\frac{\partial^2}{\partial y^2}$, $\nabla^4=\nabla^2\nabla^2$, pressure is p. Due to the tension in the muscles, pressure is exerted on the outer surface of the wall and is denoted by p_0. Here we assume $p_0=0$.

The relative peripheral conditions are

$$\frac{\partial u}{\partial y}=0, \quad at\ y=0\ \text{(the regularity condition)}, \tag{5.7}$$

$$u=-d\frac{\sqrt{Da}}{\beta}\frac{\partial u}{\partial y}, \quad at\ y=\pm\eta(x,t),\ \text{(the slip condition)}, \tag{5.8}$$

where Darcy number is Da and slip parameter is β.

The boundary condition with reference to Mittra and Prasad [29] is

$$\frac{\partial}{\partial x}L(\eta)=-\rho\left(\frac{\partial u}{\partial t}+u\frac{\partial u}{\partial x}+v\frac{\partial u}{\partial y}\right)+\frac{\mu}{1+\lambda_1}\nabla^2 u-\mu\frac{u}{k}, \quad at\ \ y=\pm\eta(x,t), \tag{5.9}$$

$$\text{where}\ \ \frac{\partial}{\partial x}L(\eta)=\frac{\partial p}{\partial x}=-T\frac{\partial^3\eta}{\partial x^3}+m\frac{\partial^3\eta}{\partial x\partial t^2}+C\frac{\partial^2\eta}{\partial x\partial t}. \tag{5.10}$$

The non dimensional parameters taken are

$$x'=\frac{x}{\lambda}, y'=\frac{y}{d}, t'=\frac{ct}{\lambda}, u'=\frac{u}{c}, v'=\frac{\lambda v}{cd}, p'=\frac{d^2 p}{\mu\lambda c}, \beta'=\frac{\beta}{d}, \eta'=\frac{\eta}{d}. \tag{5.11}$$

Introducing non dimensional variables in equations 5.4 to 5.9, give

$$\frac{\partial u}{\partial x}+\frac{\partial u}{\partial y}=0, \tag{5.12}$$

$$R_e\delta\left(\frac{\partial u}{\partial t}+u\frac{\partial u}{\partial x}+u\frac{\partial u}{\partial y}\right)=-\frac{\partial p}{\partial x}+\frac{1}{1+\lambda_1}\left(\delta^2\frac{\partial^2 u}{\partial x^2}+\frac{\partial^2 u}{\partial y^2}\right)-\frac{u}{Da}\ , \tag{5.13}$$

$$R_e\delta^3\left(\frac{\partial v}{\partial t}+u\frac{\partial v}{\partial x}+v\frac{\partial v}{\partial y}\right)=-\frac{\partial p}{\partial y}+\frac{\delta^2}{1+\lambda_1}\left(\delta^2\frac{\partial^2 v}{\partial x^2}+\frac{\partial^2 v}{\partial y^2}\right)-\delta^2\frac{v}{Da}\,, \tag{5.14}$$

$$\frac{\partial u}{\partial y}=0,\quad at\ y=0, \tag{5.15}$$

$$u=-\frac{\sqrt{Da}}{\beta}\frac{\partial u}{\partial y},\quad at\ y=\pm\eta(x,t)=\pm\left(1+\varepsilon sin2\pi(x-t)\right) \tag{5.16}$$

and

$$-R_e\delta\left(\frac{\partial u}{\partial t}+u\frac{\partial u}{\partial x}+v\frac{\partial u}{\partial y}\right)+\frac{1}{1+\lambda_1}\left(\delta^2\frac{\partial^2 u}{\partial x^2}+\frac{\partial^2 u}{\partial y^2}\right)-\frac{u}{Da}=E_1\frac{\partial^3\eta}{\partial x^3}+E_2\frac{\partial^3\eta}{\partial x\partial t^2}+$$

$$E_3\frac{\partial^2\eta}{\partial x\partial t}\ ,\quad at\ y=\pm\eta(x,t). \tag{5.17}$$

Here $\varepsilon=\frac{a}{d}$ is the amplitude ratio and $\delta=\frac{d}{\lambda}$ is the wall slope parameter, $R_e=\frac{\rho cd}{\mu}$ is the Reynolds number, $Da=\frac{k}{d^2}$ is the Darcy number. The elastic parameters are defined as $E_1=\frac{-\tau d^3}{c\mu\lambda^3}$, $E_2=\frac{mcd^3}{\mu\lambda^3}$, $E_3=\frac{Cd^3}{\mu\lambda^2}$. The parameter E_1 represents the inflexibility (rigidity), E_2 stiffness (mass characterizing parameter) and E_3 viscous damping force (damping nature of the membrane).

5.3 Method of Solution

Usually the analytic solution of the governing equations is not possible in general; hence long wavelength approximation and small Reynolds number assumptions are made to solve equations 5.12 to 5.17.

Equations 5.12 to 5.14 yield the compatibility equations as

$$\frac{\partial u}{\partial x}+\frac{\partial u}{\partial y}=0\,, \tag{5.18}$$

$$0=-\frac{\partial p}{\partial x}+\frac{1}{1+\lambda_1}\frac{\partial^2 u}{\partial y^2}-\frac{u}{Da}\ , \tag{5.19}$$

$$0 = -\frac{\partial p}{\partial y}. \tag{5.20}$$

The boundary conditions 5.15 to 5.17 become

$$\frac{\partial u}{\partial y} = 0, \ \ at \ \ y = 0, \tag{5.21}$$

$$u = \ -\frac{\sqrt{Da}}{\beta}\frac{\partial u}{\partial y}, \quad at \ \ y = \ \pm\eta(x,t) = \ \pm\big(1 + \ \varepsilon sin2\pi(x-t)\big), \tag{5.22}$$

$$\frac{1}{1+\lambda_1}\frac{\partial^2 u}{\partial y^2} - \frac{u}{Da} = \ E_1 \ \frac{\partial^3 \eta}{\partial x^3} + E_2 \ \frac{\partial^3 \eta}{\partial x \partial t^2} + E_3 \ \frac{\partial^2 \eta}{\partial x \partial t}, \ \ at \ \ y \pm \eta(x,t). \tag{5.23}$$

Solving equations 5.19 and 5.20 along with the conditions 5.21 to 5.23, we get

$$u(x,y,t) = \ \frac{E}{N^2}\left[-1 - \frac{cosh(Ny)}{T_1}\right], \tag{5.24}$$

here

$$E = -\varepsilon[(2\pi)^3 cos2\pi(x-t)\ (E_1 \ + E_2 \ ) - E_3 \ (2\pi)^2 sin2\pi(x-t)],$$

$$T_1 = DN\text{sinhN}\eta - \text{sinhN}\eta, \qquad D = \ -\frac{\sqrt{Da}}{\beta}, \qquad N = \ \sqrt{\frac{1+\lambda_1}{Da}}.$$

The time average velocity $\bar{u}(y)$ is

$$\bar{u}(y) = \ \int_0^1 u \ dt. \tag{5.25}$$

Stream function ψ is defined by

$$u = \ \frac{\partial \psi}{\partial y} \ \ and \ v = -\frac{\partial \psi}{\partial x} \ . \tag{5.26}$$

Using equation 5.24 in $u = \frac{\partial \psi}{\partial y}$ and integrating it along with the condition that $\psi = 0 \ at \ y = 0$, we obtain

$$\psi = \ \ \frac{E}{N^2}\left[-y - \frac{sinh(Ny)}{NT_1}\right]. \tag{5.27}$$

5.4. Results and Discussion

The effect of elastic wall properties is examined and the nonlinear governing equations are solved using large wavelength approximation and low Reynolds number assumptions. The consequences of the parameters under consideration on the time mean velocity profile $\bar{u}(y)$ are obtained using MATHEMATICA software. From equation 5.25 graphs are plotted and depicted in Figure 5.1 to Figure 5.4 to observe the consequences of the physical parameters, say Jaffrey parameter λ_1, slip parameter β, elastic parameters E_1, E_2, E_3 and Darcy number Da on time average velocity $\bar{u}(y)$.

Figure 5.1 shows the variations in $\bar{u}(y)$ under the effect of elastic parameters E_1, E_2, E_3 It is concluded that with enhancement in the elastic parameters, the time average velocity $\bar{u}(y)$ reduces. Figure 5.2 presents the flow structure of time average velocity $\bar{u}(y)$ for different values of Jeffrey parameter λ_1. This Figure indicates that rise in λ_1, results gradual increase in the time average velocity $\bar{u}(y)$.This result is in agreement with that of Dheia [114]. The time average velocity $\bar{u}(y)$ reduces by gain in the slip parameter β and Darcy parameter Da as depicted in Figure 5.3 and Figure 5.4.

Families of curves representing the streamlines of the flow are instantaneously tangential to the velocity vector that explains the path of a fluid particle travelling at any instance, resulting into an attractive phenomenon in peristalsis called trapping. The creation of the bolus of the fluid circulating internally, enclosed by stream line patterns for various values of Jaffrey parameter λ_1, slip parameter β, Darcy number Da and elastic parameters E_1, E_2, E_3 are shown in Figure 5.5 to Figure 5.10 using equation 5.27. Figures 5.5(a & b), Figures 5.6(a & b) and Figures 5.7 (a & b) reveals that the trapped bolus enhances in size as there is rise in E_1, E_2 and E_3 respectively. The bolus size decreases by gain in the Jeffrey parameter as depicted in Figures 5.8(a & b).It is shown from Figures 5.9(a & b) that as the slip parameter is enhanced the bolus size reduces. Size of the bolus enhances with Darcy number as shown in Figures 5.10(a & b).

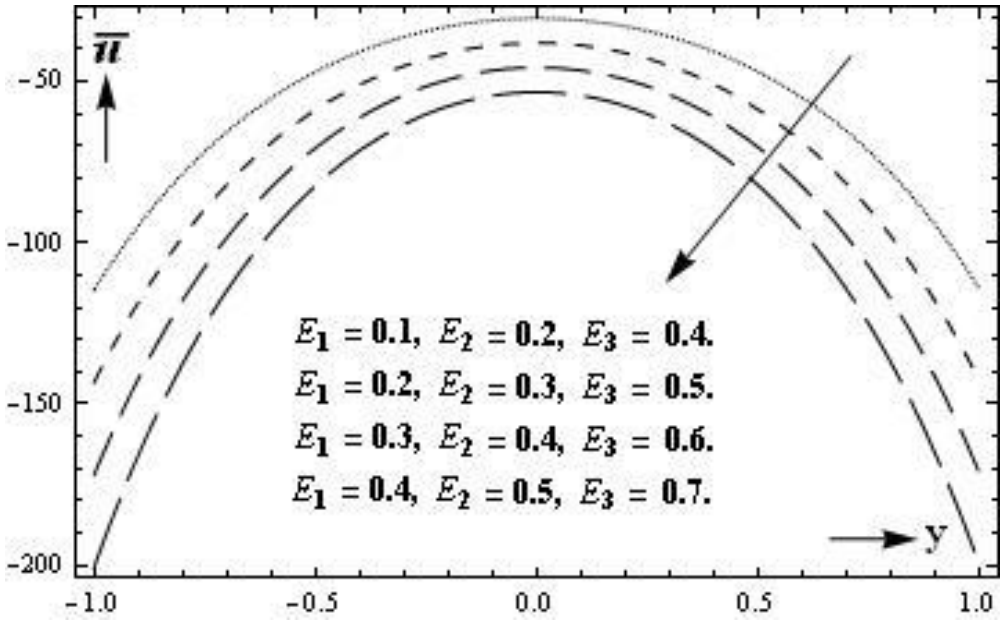

Figure 5.1: Consequences of E_1, E_2, E_3 on average velocity $\bar{u}(y)$.

$(\epsilon = 0.2;\ Da = 0.5; \beta = 0.1; \lambda_1 = 1)$

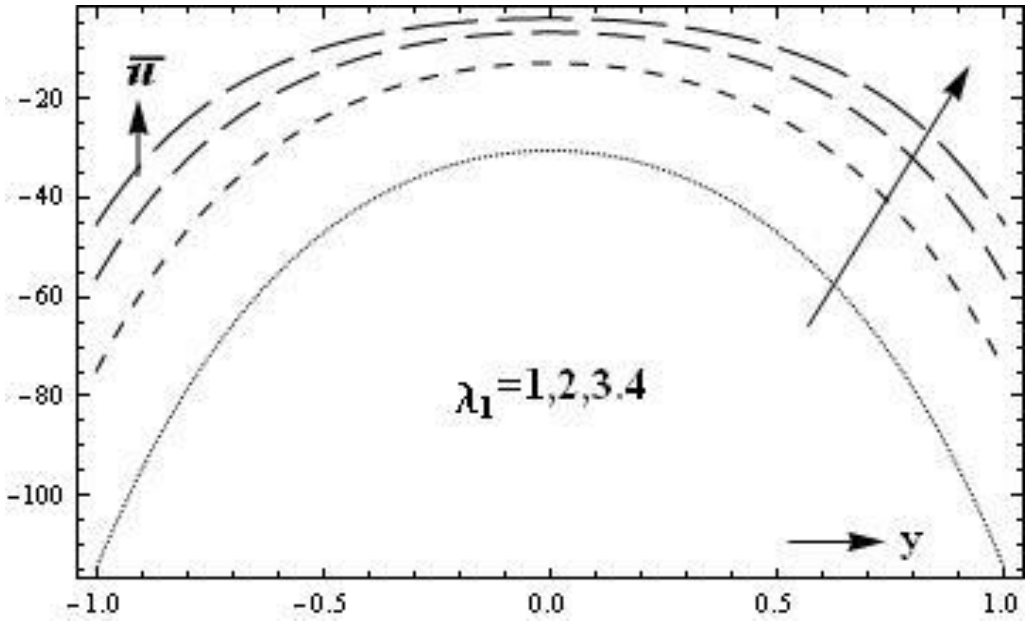

Figure 5.2: Consequences of λ_1 on average velocity $\bar{u}(y)$.

$(\epsilon = 0.2;\ E_1 = 0.1; E_2 = 0.2; E_3 = 0.4; Da = 0.5; \beta = 0.1)$

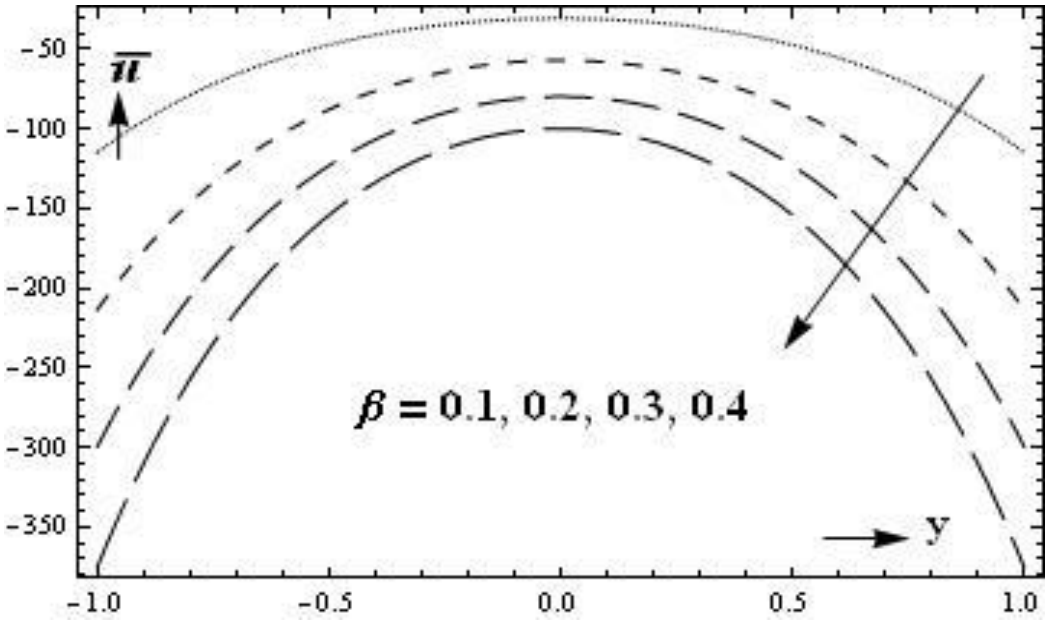

Figure 5.3: Consequences of β on average velocity $\bar{u}(y)$.

$(\epsilon = 0.2;\ E_1 = 0.1; E_2 = 0.2; E_3 = 0.4; Da = 0.5;\ \lambda_1 = 1)$

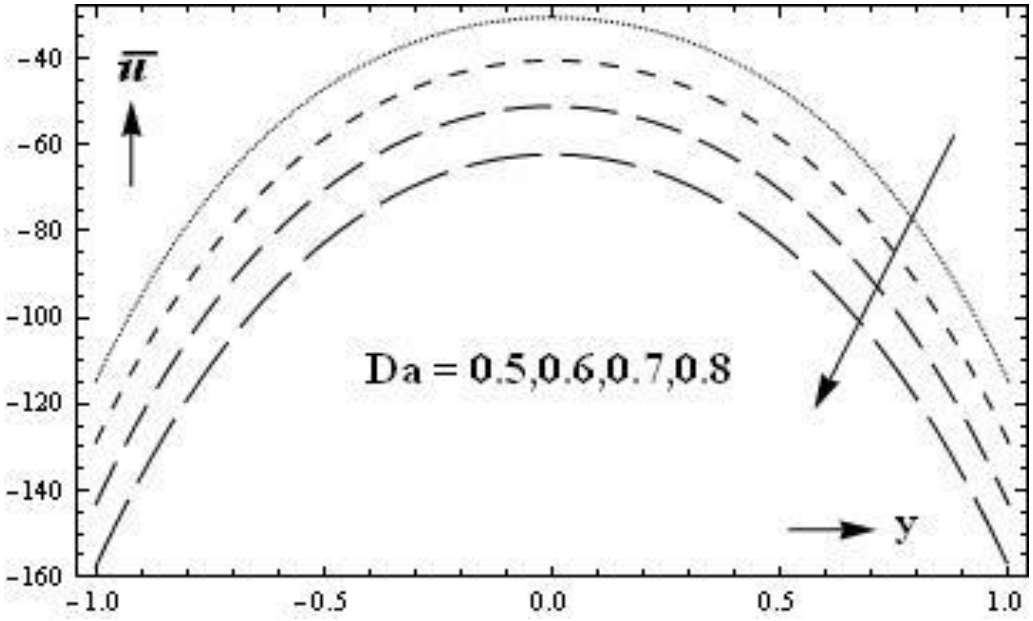

Figure 5.4: Consequences of a on average velocity $\bar{u}(y)$.

$(\epsilon = 0.2;\ E_1 = 0.1; E_2 = 0.2; E_3 = 0.4; \beta = 0.1; \lambda_1 = 1)$

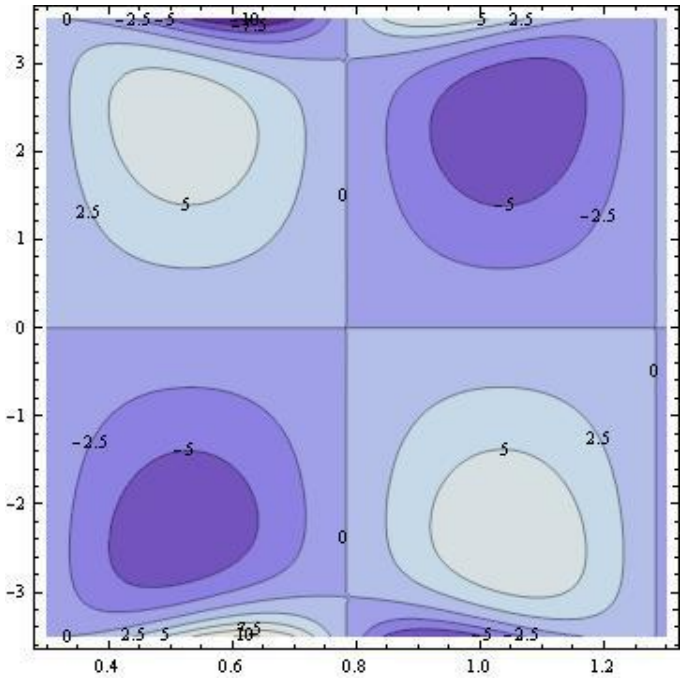

Figure 5.5(a): Effect of Stream lines for E_1 = 0.1.

($\epsilon = 0.2;\ E_2 = 0.2; E_3 = 0.4; Da = 0.5; \beta = 0.1; \lambda_1 = 1$)

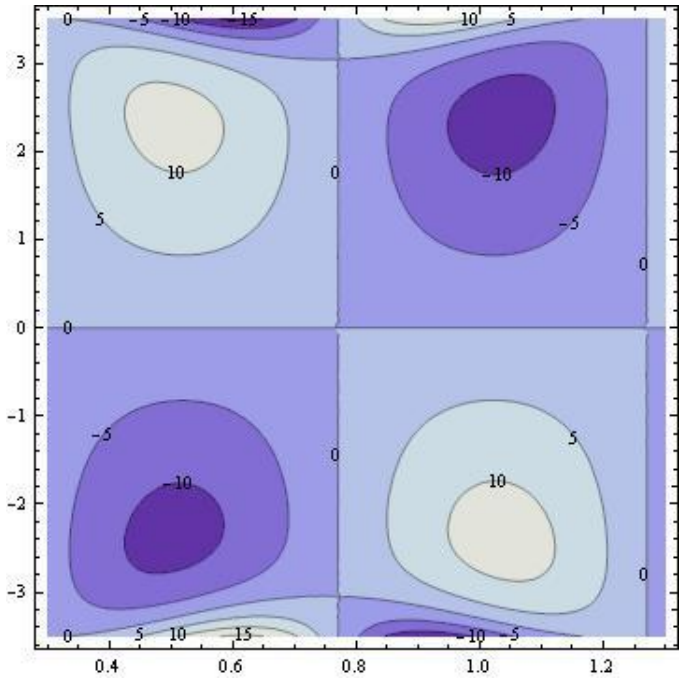

Figure 5.5(b): Effect of Stream lines for E_1 = 0.3.

($\epsilon = 0.2;\ E_2 = 0.2; E_3 = 0.4; Da = 0.5; \beta = 0.1; \lambda_1 = 1$)

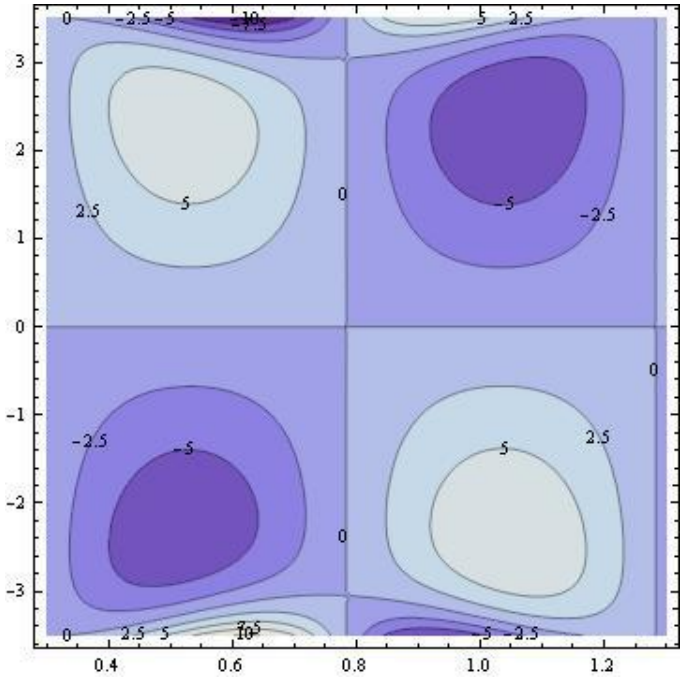

Figure 5.6(a): Effect of Stream lines for E_2 = 0.2.

($\epsilon = 0.2;\ E_1 = 0.1; E_3 = 0.4; Da = 0.5; \beta = 0.1; \lambda_1 = 1$)

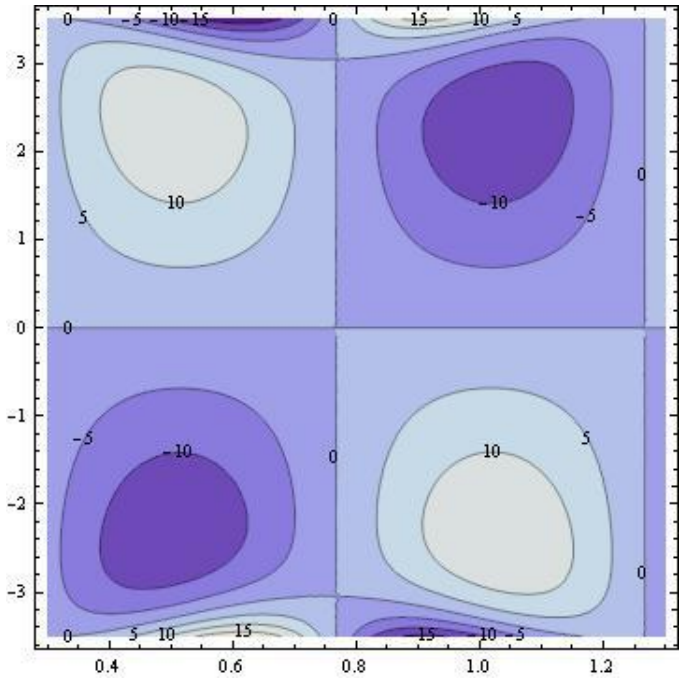

Figure 5.6(b): Effect of Stream lines for E_2 = 0.5.

($\epsilon = 0.2;\ E_1 = 0.1; E_3 = 0.4; Da = 0.5; \beta = 0.1; \lambda_1 = 1$)

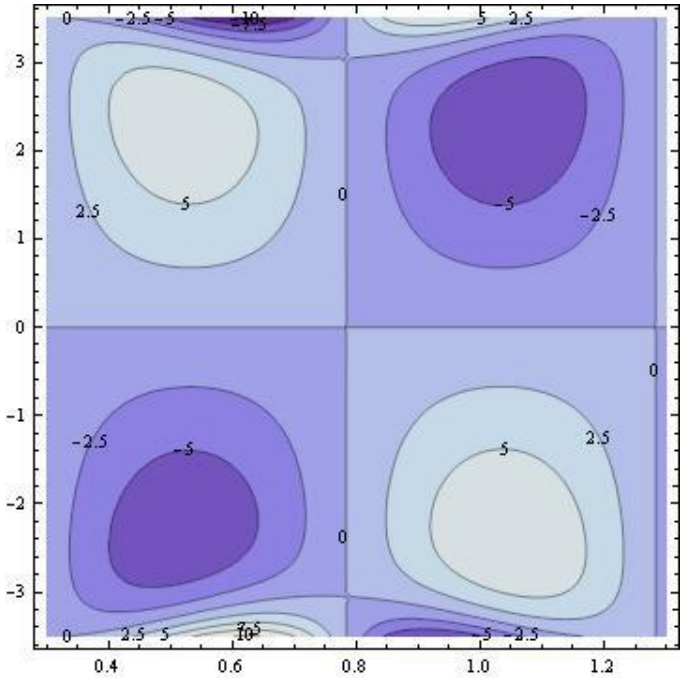

Figure 5.7(a): Effect of Stream lines for E_3 = 0.4.

$(\epsilon = 0.2;\ E_1 = 0.1; E_2 = 0.2; Da = 0.5; \beta = 0.1; \lambda_1 = 1)$

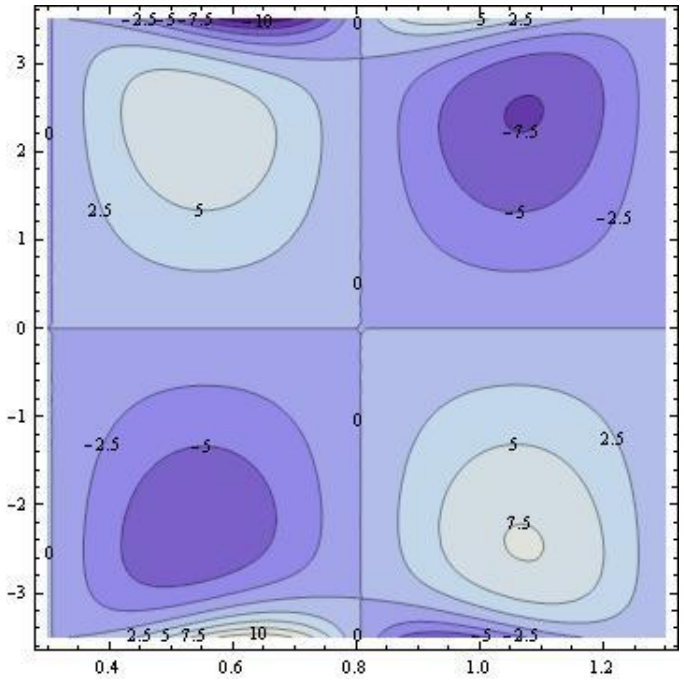

Figure 5.7(b): Stream lines for E_3 = 0.7.

$(\epsilon = 0.2;\ E_1 = 0.1; E_2 = 0.2; Da = 0.5; \beta = 0.1; \lambda_1 = 1)$

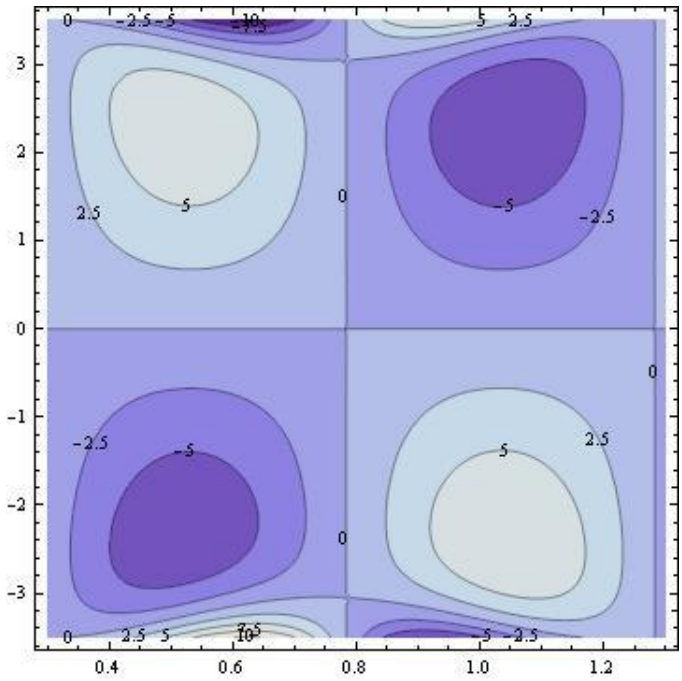

Figure 5.8(a): Stream lines for λ_1 = 1.

$(\epsilon = 0.2;\ E_1 = 0.1; E_2 = 0.2; E_3 = 0.4; Da = 0.5; \beta = 0.1)$

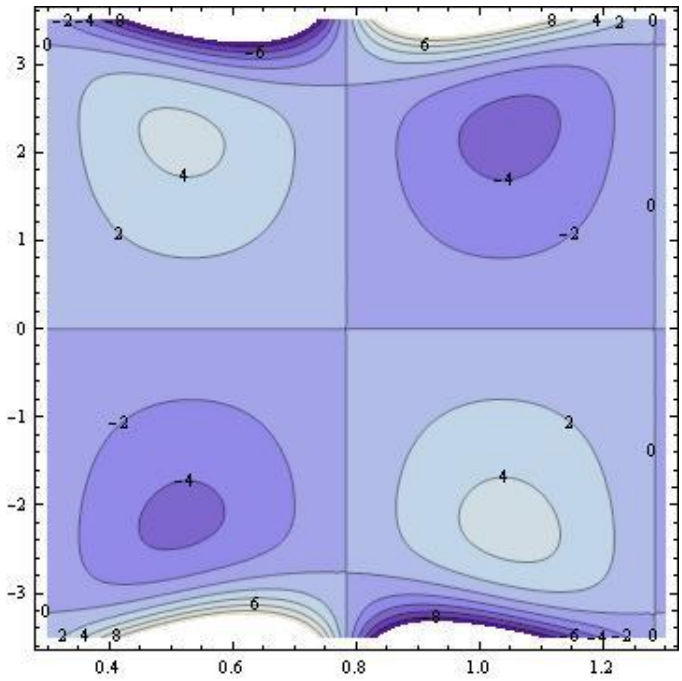

Figure 5.8 (b) Stream lines for λ_1= 2.

$(\epsilon = 0.2;\ E_1 = 0.1; E_2 = 0.2; E_3 = 0.4; Da = 0.5; \beta = 0.1)$

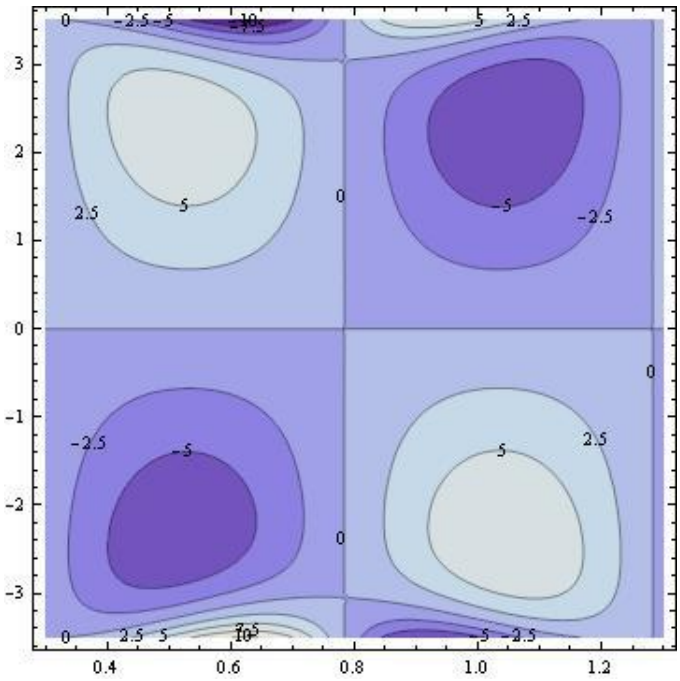

Figure 5.9 (a): Stream lines for β = 0.1.

$(\epsilon = 0.2;\ E_1 = 0.1; E_2 = 0.2; E_3 = 0.4; Da = 0.5;\ \lambda_1 = 1)$

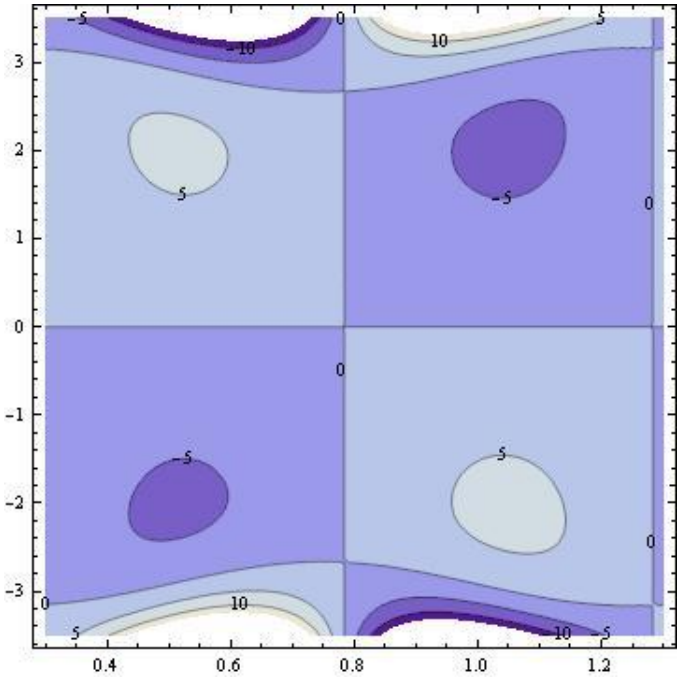

Figure 5.9(b): Stream lines for β = 0.2.

$(\epsilon = 0.2;\ E_1 = 0.1; E_2 = 0.2; E_3 = 0.4; Da = 0.5;\ \lambda_1 = 1)$

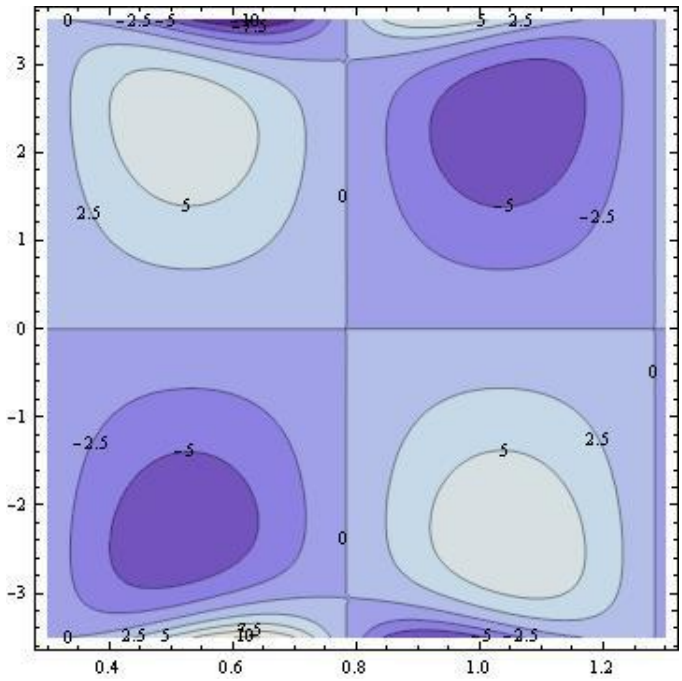

Figure 5.10 (a): Stream lines for *Da* = 0.5.

$(\epsilon = 0.2;\ E_1 = 0.1; E_2 = 0.2; E_3 = 0.4; \beta = 0.1; \lambda_1 = 1)$

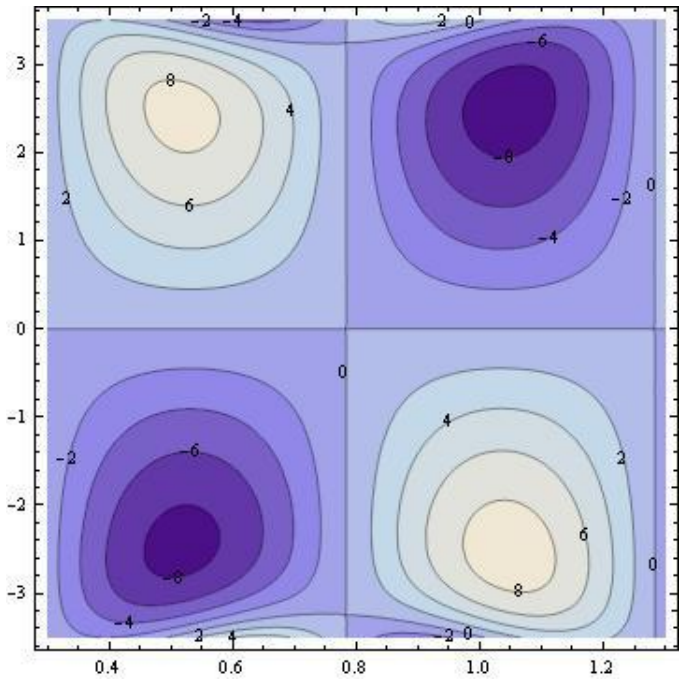

Figure 5.10(b): Stream lines for $Da = 0.6$.

$(\epsilon = 0.2;\ E_1 = 0.1; E_2 = 0.2; E_3 = 0.4; \beta = 0.1; \lambda_1 = 1)$

Chapter 6

Unsteady Magnetohydrodynamic Flow of Jeffrey Fluid due to Peristaltic Motion of Uniform Channel with Slip in Porous Medium

6.1 Introduction

In the last chapter, the effects of wall on the two dimensional peristaltic flow of an incompressible Jeffrey fluid in a porous medium channel with slip condition has been reported.

Magnetohydrodynamics (MHD) is that discipline of dynamics which studies the movement of conducting fluids under the existence of a magnetic field. MHD is concerned with the mutual interaction of fluid flow and magnetic field. Magnetic fields are used to heat, mix, pump and mount liquid metals in industries. Researchers have developed a magnetic navigation system for medical instruments such as catheters and guide wires. In view of this discussion the study has been extended for analyzing the magnetic field effect in the present chapter.

Hayat et al. [115] studied magnetic field and compliant wall effects on the flow of a Jeffrey fluid through a peristaltic porous channel. Mahmouda et al. [116] looked into the transport of a Jeffrey fluid within a permeable space under peristalsis having magnetic effect. Hayat et al. [117] observed wall impact analysis of MHD Jeffrey fluid under peristalsis. Peristaltic pumping motion of a Jeffrey fluid under the influence of magnetic field through a channel inclined to the horizontal has been studied by Krishna Kumari et al. [118]. The peristaltic pumping flow subjected to a magnetic field on the flow of a Jeffrey fluid in a conduit with variable viscosity was examined by Jayarami Reddy and Subba Reddy [119]. Subba Reddy et al. [120] have examined the influence of magnetic field on a stream of the Jeffrey fluid flowing inside a peristaltic channel considered to be asymmetric, porous and having slip effects. Influence of MHD and slip effects on peristaltic motion considering blood as Jeffrey fluid model through a porous medium was examined by Bhatti and Abbas [121].

The objective of this chapter is to examine the effects of magnetic field on time average velocity and stream lines under lubrication approach. The peristaltic transport of an electrically conducting Jeffrey fluid in a porous uniform channel under wall effect is considered.

6.2 Physical assumptions of the problem

Motion of incompressible Jeffrey fluid within an elastic channel influenced by magnetic field with the flow geometry as mentioned in chapter 5 is considered.

Using Maxwell's equation and assumptions regarding magnetic field as given in chapter 1 and same governing equations 5.1 to 5.3 as given in the previous chapter, the equation of motion and boundary conditions considered are

$$\frac{\partial u}{\partial x}+\frac{\partial v}{\partial y}=0, \tag{6.1}$$

$$\rho\left(\frac{\partial u}{\partial t}+u\frac{\partial u}{\partial x}+v\frac{\partial u}{\partial y}\right)=-\frac{\partial p}{\partial x}+\frac{\mu}{1+\lambda_1}\nabla^2 u-\mu\frac{u}{k}-\sigma {B_0}^2 u\ , \tag{6.2}$$

$$\rho\left(\frac{\partial v}{\partial t}+u\frac{\partial v}{\partial x}+v\frac{\partial v}{\partial y}\right)=-\frac{\partial p}{\partial y}+\frac{\mu}{1+\lambda_1}\nabla^2 v-\mu\frac{v}{k}, \tag{6.3}$$

where σ is the electrical conductivity, B_0 is the magnetic field is considered vertical to the direction of flow and the components $\rho,\ p, u, v, \lambda_1, k, \mu$ are having usual meaning as mentioned in previous chapter 5.

Correspondingly the boundary conditions are,

$$\frac{\partial u}{\partial y}=0\ , \qquad at \quad y=0 \ \text{(the regularity condition)}, \tag{6.4}$$

$$u=-d\frac{\sqrt{Da}}{\beta}\frac{\partial u}{\partial y} \quad at \ \ y=\pm\eta(x,t) \ \ \text{(the slip condition)}. \tag{6.5}$$

Here β denotes slip parameter.

$$\frac{\partial}{\partial x}L(\eta)=-\rho\left(\frac{\partial u}{\partial t}+u\frac{\partial u}{\partial x}+v\frac{\partial u}{\partial y}\right)+\frac{\mu}{1+\lambda_1}\nabla^2 u-\mu\frac{u}{k}-\sigma {B_0}^2 u, \ \text{at y}=\pm\eta(x,\text{t}), \tag{6.6}$$

where

$$\frac{\partial}{\partial x}L(\eta)=\frac{\partial p}{\partial x}=-T\frac{\partial^3\eta}{\partial x^3}+m\frac{\partial^3\eta}{\partial x\partial t^2}+C\frac{\partial^2\eta}{\partial x\partial t}. \tag{6.7}$$

Using same dimensionless quantities as in previous chapter and substituting in equations 6.1 to 6.6 give,

$$\frac{\partial u}{\partial x}+\frac{\partial v}{\partial y}=0, \tag{6.8}$$

$$R_e\delta\left(\frac{\partial u}{\partial t}+u\frac{\partial u}{\partial x}+v\frac{\partial u}{\partial y}\right)=-\frac{\partial p}{\partial x}+\frac{1}{1+\lambda_1}\left(\delta^2\frac{\partial^2 u}{\partial x^2}+\frac{\partial^2 u}{\partial y^2}\right)-\frac{u}{Da}-H_0 u\,, \tag{6.9}$$

$$R_e\delta^3\left(\frac{\partial v}{\partial t}+u\frac{\partial v}{\partial x}+v\frac{\partial v}{\partial y}\right)=-\frac{\partial p}{\partial y}+\frac{\delta^2}{1+\lambda_1}\left(\delta^2\frac{\partial^2 v}{\partial x^2}+\frac{\partial^2 v}{\partial y^2}\right)-\delta^2\frac{v}{Da}\,, \tag{6.10}$$

$$\frac{\partial u}{\partial y}=0,\quad at\quad y=0, \tag{6.11}$$

$$u=-\frac{\sqrt{Da}}{\beta}\frac{\partial u}{\partial y},\ at\ y=\pm\eta(x,t)=\pm\left(1+\varepsilon sin2\pi(x-t)\right) \tag{6.12}$$

and

$$-R_e\delta\left(\frac{\partial u}{\partial t}+u\frac{\partial u}{\partial x}+v\frac{\partial u}{\partial y}\right)+\frac{1}{1+\lambda_1}\left(\delta^2\frac{\partial^2 u}{\partial x^2}+\frac{\partial^2 u}{\partial y^2}\right)-\frac{u}{Da}-{H_0}^2u=E_1\frac{\partial^3\eta}{\partial x^3}+E_2\frac{\partial^3\eta}{\partial x\partial t^2}+$$

$$E_3\frac{\partial^2\eta}{\partial x\partial t}\,,\ at\ y=\pm\eta(x,t), \tag{6.13}$$

where $H_0=\sqrt{\frac{\sigma}{\mu}}B_0 d$ is the Hartmann number along with usual meaning of other elastic and geometric parameters as given in previous chapter.

6.3 Method of Solution

Under lubrication approach, equations 6.8 to 6.13 reduce to

$$\frac{\partial u}{\partial x}+\frac{\partial v}{\partial y}=0, \tag{6.14}$$

$$0=-\frac{\partial p}{\partial x}+\frac{1}{1+\lambda_1}\frac{\partial^2 u}{\partial y^2}-\left({H_0}^2+\frac{1}{Da}\right)u, \tag{6.15}$$

$$0=-\frac{\partial p}{\partial y}\,, \tag{6.16}$$

$$\frac{\partial u}{\partial y}=0,\ at\ y=0, \tag{6.17}$$

$$u = -\frac{\sqrt{Da}}{\beta}\frac{\partial u}{\partial y}, \quad at\ y = \pm\eta(x,t) = \pm\big(1 + \varepsilon sin2\pi(x-t)\big), \tag{6.18}$$

$$\frac{1}{1+\lambda_1}\frac{\partial^2 u}{\partial y^2} - \left({H_0}^2 + \frac{1}{Da}\right)u = E_1\frac{\partial^3\eta}{\partial x^3} + E_2\frac{\partial^3\eta}{\partial x\partial t^2} + E_3\frac{\partial^2\eta}{\partial x\partial t},\ at\ y \pm \eta(x,t). \tag{6.19}$$

The solution of equations 6.15 and 6.16 subject to the boundary conditions 6.17 to 6.19 reduce to the form

$$u = \frac{E}{N^2}\left[-1 - \frac{cosh(Ny)}{T_1}\right], \tag{6.20}$$

where

$$E = -\varepsilon[(2\pi)^3 cos2\pi(x-t)\ (E_1 + E_2) - E_3(2\pi)^2 sin2\pi(x-t)],$$

$$T_1 = DN\text{sinhN}\,\eta - \text{sinhN}\,\eta, \qquad D = -\frac{\sqrt{Da}}{\beta}, \qquad N = \sqrt{\left({H_0}^2 + \frac{1}{Da}\right)(1+\lambda_1)}\,.$$

The time average velocity $\bar{u}(y)$ is,

$$\bar{u}(y) = \int_0^1 u\ dt. \tag{6.21}$$

Referring the same stream condition ψ as in previous chapter, we obtain

$$\psi(x,y,t) = \frac{E}{N^2}\left[-y - \frac{sinh(Ny)}{NT_1}\right]. \tag{6.22}$$

6.4 Results and Discussion

The graphs for mean velocity $\bar{u}(y)$ using equation 6.21 and the stream lines using equation 6.22 are drawn. The flow is governed by the non dimensional parameters: Jeffrey parameter λ_1, Hartmann number H_0, Darcy number Da, slip parameter β, and the elastic parameters E_1, E_2, E_3.

Figure 6.1 represents the behavior of time average velocity against y axis for various values of elastic parameters E_1, E_2, E_3. It is inspected closely from Figure 6.1 that time average velocity reduces as there is rise in elastic parameters. Observations from Figure 6.2 show that as λ_1 rise, the time average velocity enhances. It is observe that the time

average velocity reduces with an enhancement in β and Da in Figure 6.3 and Figure 6.4.The time average velocity enhance as the Hartmann number H_0 increases as shown in Figure 6.5. This result is in agreement with that of Hayat et al. [117].

Generally the stream lines are a contour analogous to the walls, as the walls are stationary, to surround a bolus of fluid particles inside the closed stream lines. Figure 6.6 to Figure 6.12 illustrate the trapping for various values of β, Da, H_0, λ_1 and E_1, E_2, E_3. Figures 6.6(a & b), Figures 6.7(a & b) and Figures 6.8(a & b) depict that the bolus enhances with rise in elastic parameters E_1, E_2 and E_3 respectively. It observed that the bolus reduces in size as there is increase in λ_1 as shown in Figures 6.9(a & b). From Figures 6.10(a & b) it is revealed that the bolus shrinks as the slip parameter rises. Figures 6.11(a & b) confirms that the bolus enhances in size with rise in Darcy number Da. Size of the bolus reduces with Hartmann number as shown in Figures 6.12(a & b),

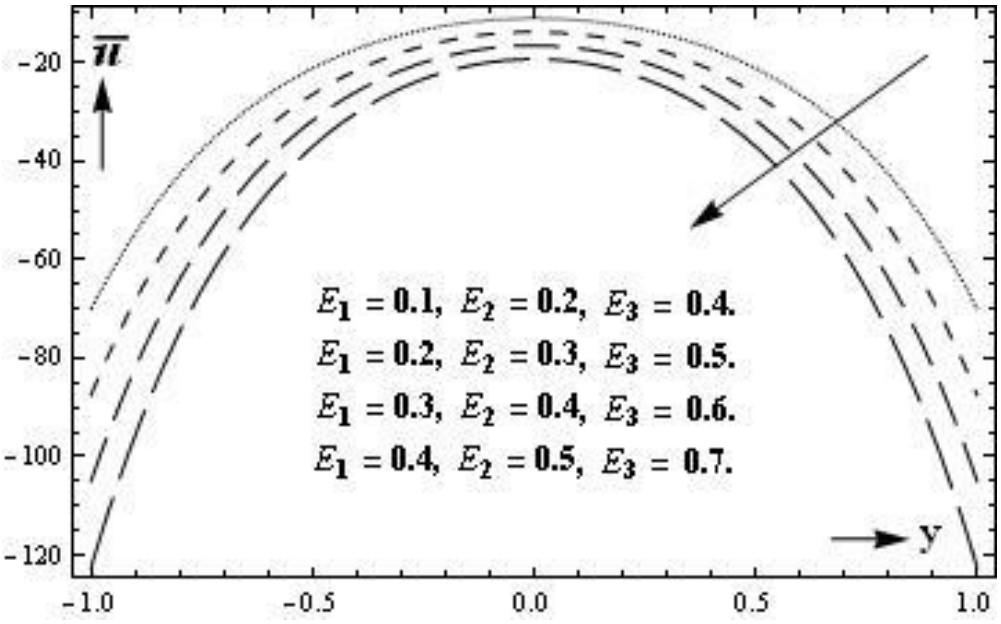

Figure 6.1: Consequences of E_1, E_2, E_3 on average velocity $\overline{u}(y)$.

$(\epsilon = 0.2; \beta = 0.1; \text{Da} = 0.5;\ \lambda_1 = 1; H_0 = 1)$

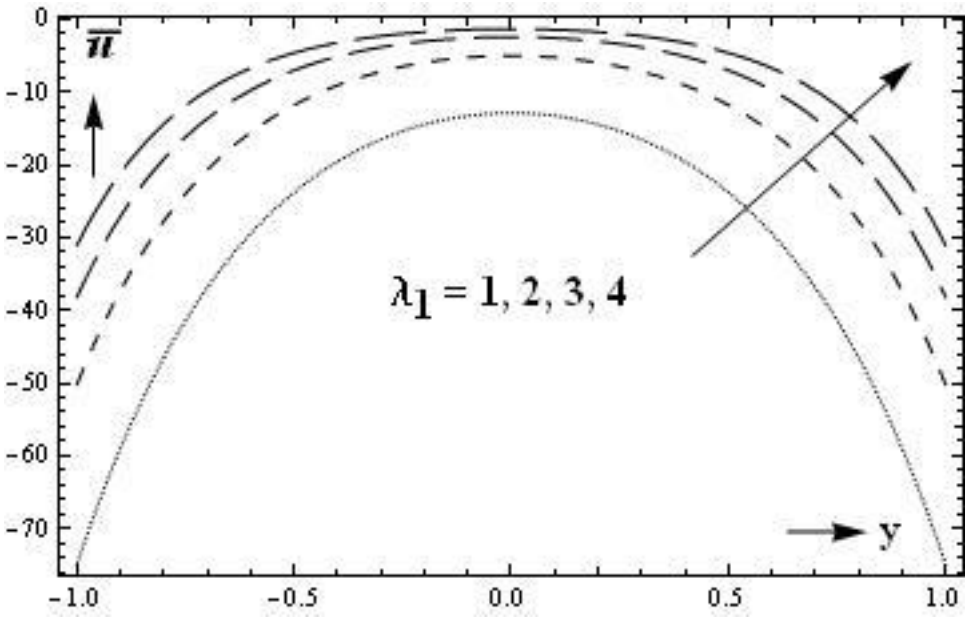

Figure 6.2: Consequences of λ_1 on average velocity $\overline{u}(y)$.

$(\epsilon = 0.2; E_1 = 0.1; E_2 = 0.2; E_3 = 0.4; \beta = 0.1; \text{Da} = 0.5;\ H_0 = 1)$

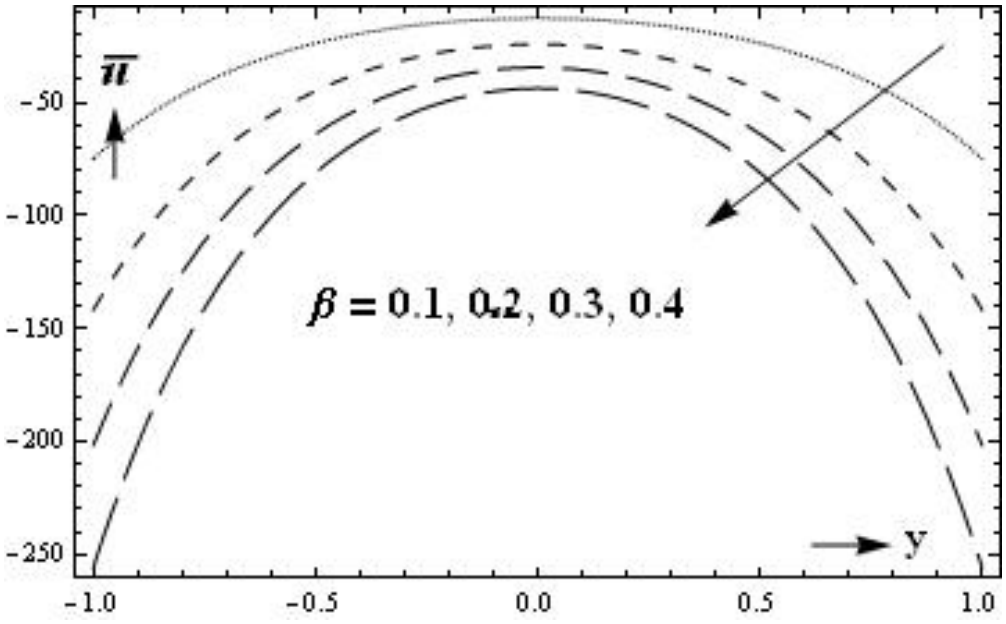

Figure 6.3: Consequences of β on average velocity $\bar{u}(y)$.

$(\epsilon = 0.2; E_1 = 0.1; E_2 = 0.2; E_3 = 0.4; \mathrm{Da} = 0.5;\ \lambda_1 = 1; H_0 = 1)$

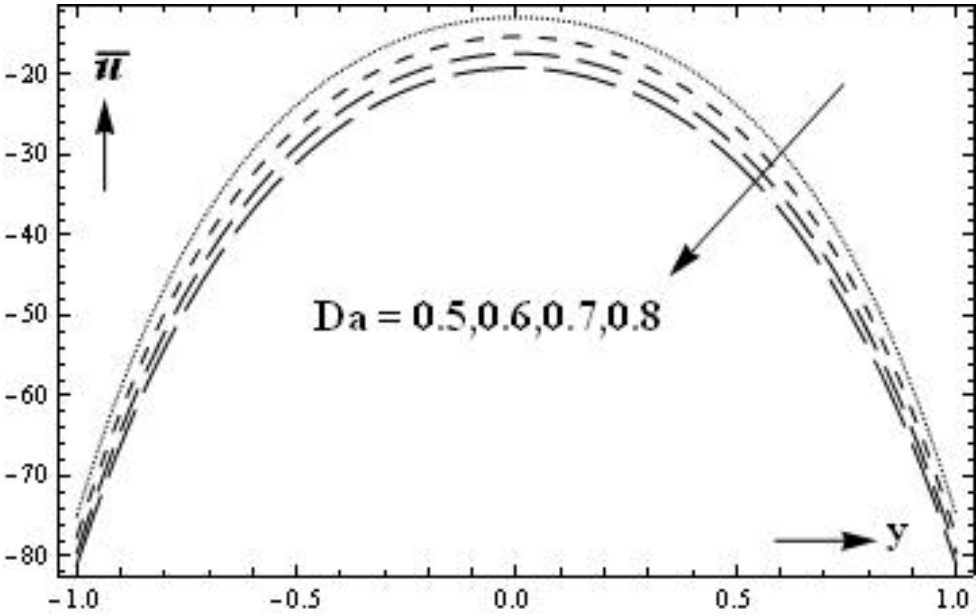

Figure 6.4: Consequences of Da on average velocity $\bar{u}(y)$.

$(\epsilon = 0.2; E_1 = 0.1; E_2 = 0.2; E_3 = 0.4; \beta = 0.1;\ \lambda_1 = 1; H_0 = 1)$

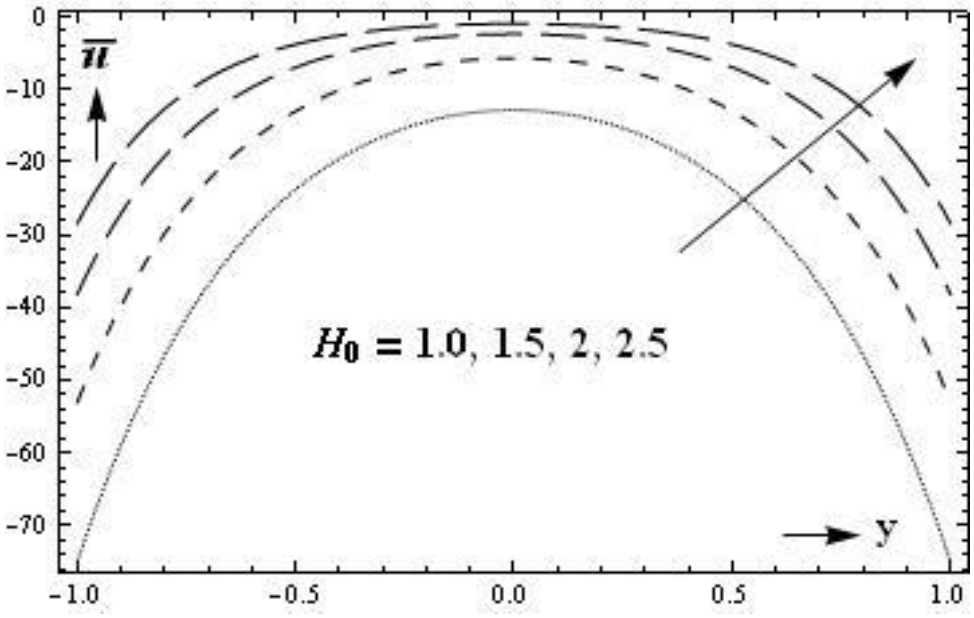

Figure 6.5: Consequences of H_0 on average velocity $\overline{u}(y)$.

$(\epsilon = 0.2; E_1 = 0.1; E_2 = 0.2; E_3 = 0.4; \beta = 0.1; \mathrm{Da} = 0.5;\ \lambda_1 = 1)$

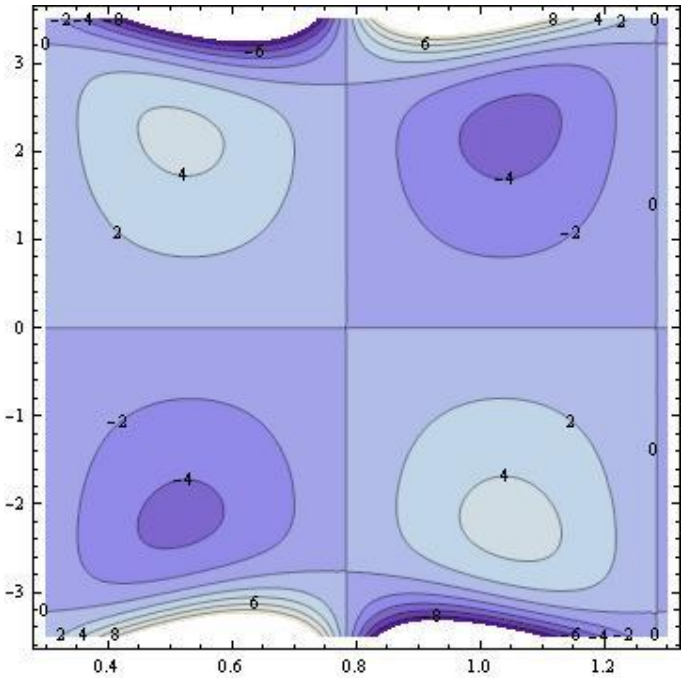

Figure 6.6(a): Stream lines for $E_1 = 0.1$.

($\epsilon = 0.2; E_2 = 0.2; E_3 = 0.4; \beta = 0.1;$ Da $= 0.5;\ \lambda_1 = 1; H_0 = 1$)

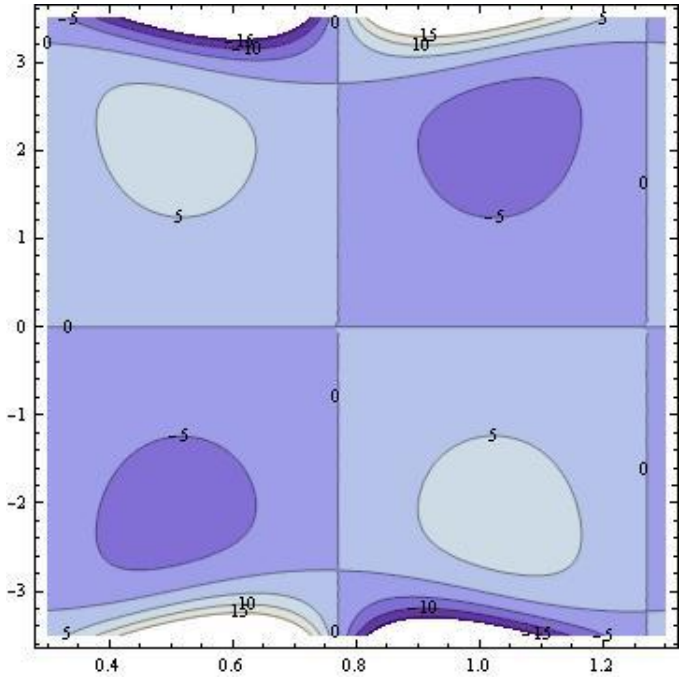

Figure 6.6(b): Stream lines for $E_1 = 0.2$.

($\epsilon = 0.2; E_2 = 0.2; E_3 = 0.4; \beta = 0.1;$ Da $= 0.5;\ \lambda_1 = 1; H_0 = 1$)

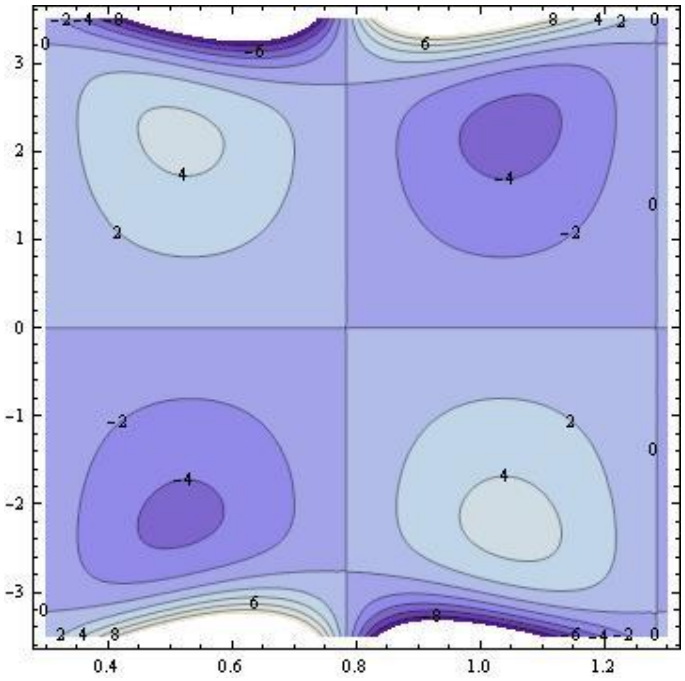

Figure 6.7(a): Stream lines for $E_2 = 0.2$.

$(\epsilon = 0.2; E_1 = 0.1; E_3 = 0.4; \beta = 0.1; \mathrm{Da} = 0.5;\ \lambda_1 = 1; H_0 = 1)$

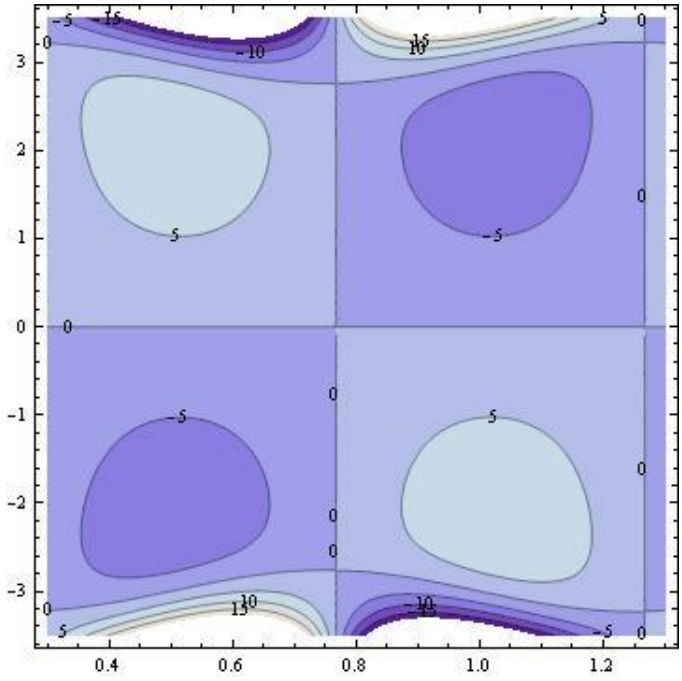

Figure 6.7(b): Stream lines for $E_2 = 0.5$.

$(\epsilon = 0.2; E_1 = 0.1; E_3 = 0.4; \beta = 0.1; \mathrm{Da} = 0.5;\ \lambda_1 = 1; H_0 = 1)$

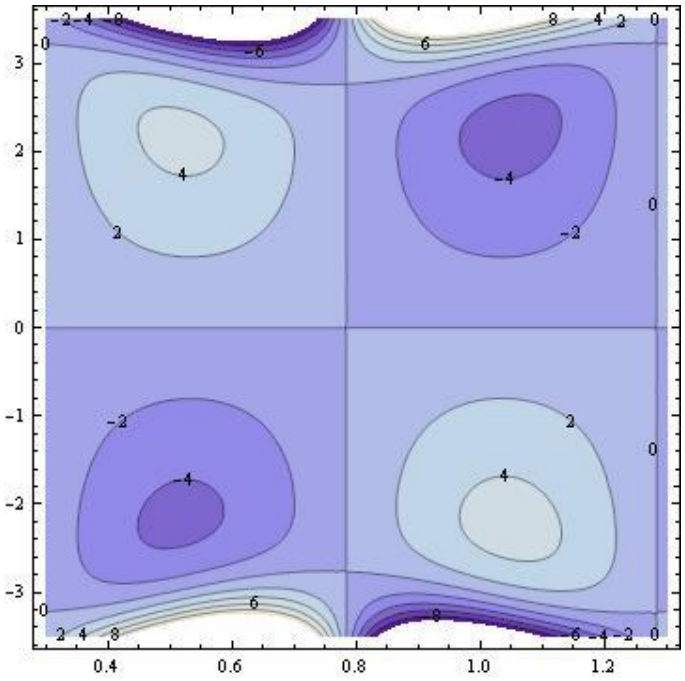

Figure 6.8(a): Stream lines for $E_3 = 0.4$.

$(\epsilon = 0.2; E_1 = 0.1; E_2 = 0.2; \beta = 0.1; \mathrm{Da} = 0.5;\ \lambda_1 = 1; H_0 = 1)$

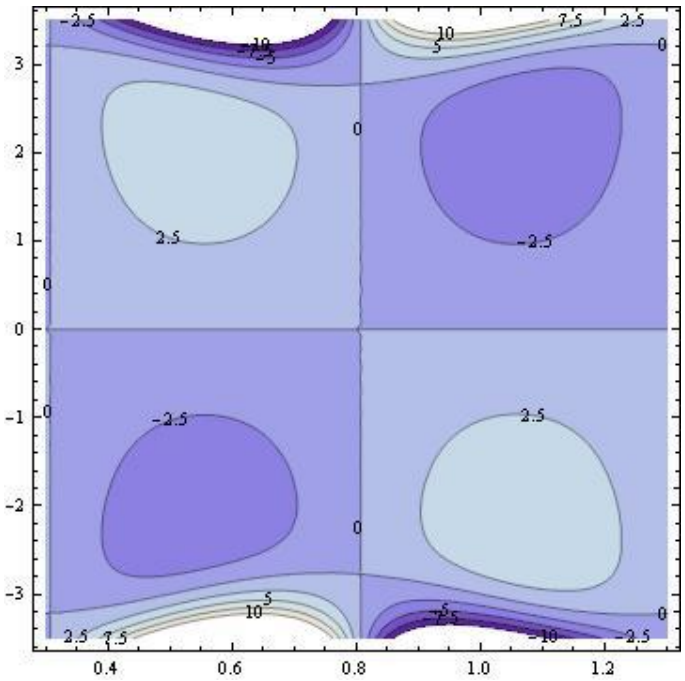

Figure 6.8(b): Stream lines for $E_3 = 0.7$.

$(\epsilon = 0.2; E_1 = 0.1; E_2 = 0.2; \beta = 0.1; \mathrm{Da} = 0.5;\ \lambda_1 = 1; H_0 = 1)$

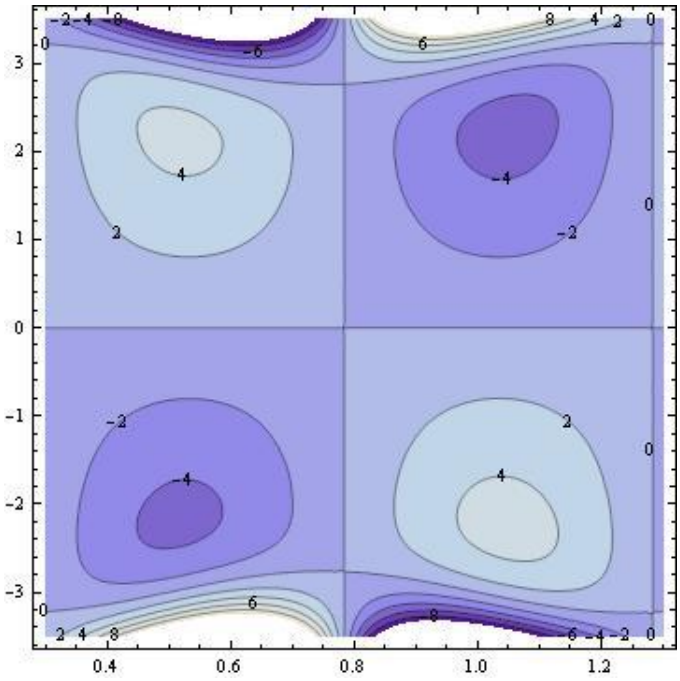

Figure 6.9(a): Stream lines for λ_1= 1
$(\epsilon = 0.2; E_1 = 0.1; E_2 = 0.2; E_3 = 0.4; \beta = 0.1; \mathrm{Da} = 0.5;\ H_0 = 1)$

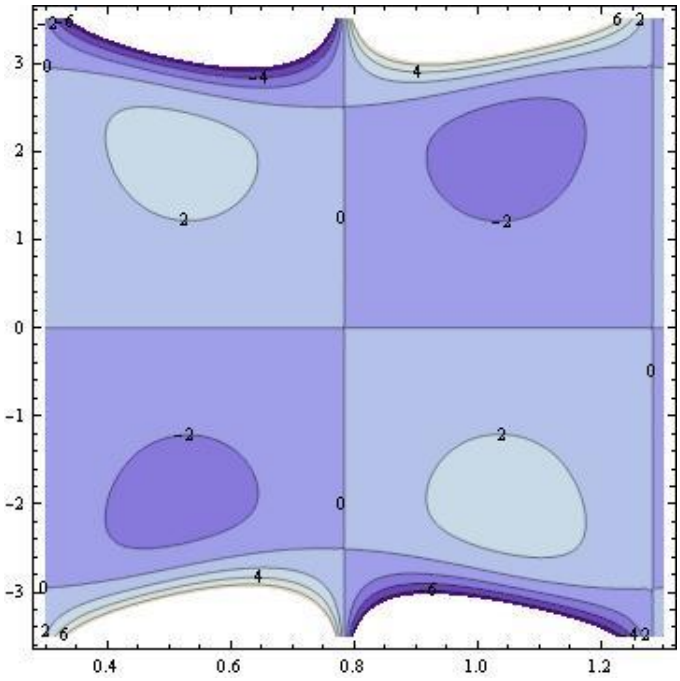

Figure 6.9(b): Stream lines for λ_1= 2.
$(\epsilon = 0.2; E_1 = 0.1; E_2 = 0.2; E_3 = 0.4; \beta = 0.1; \mathrm{Da} = 0.5;\ H_0 = 1)$

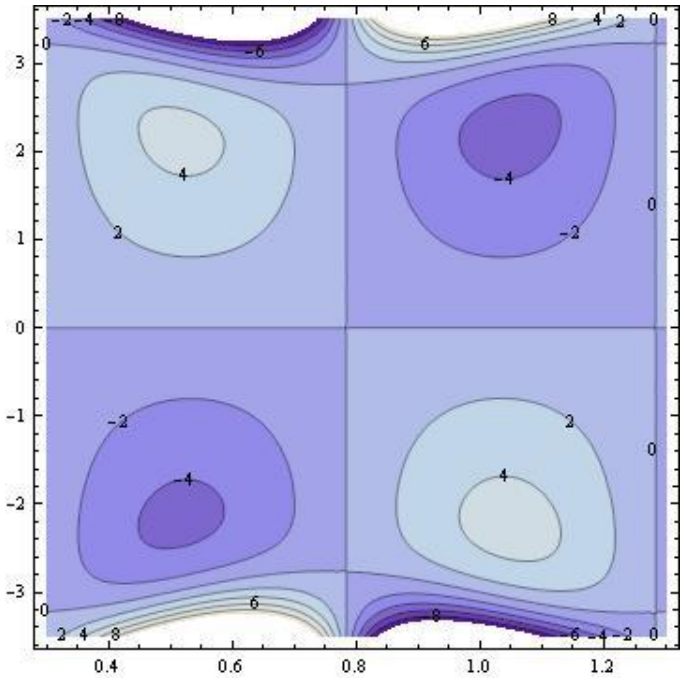

Figure 6.10(a): Stream lines for β =0.1.

($\epsilon = 0.2; E_1 = 0.1; E_2 = 0.2; E_3 = 0.4;$ Da $= 0.5;\ \lambda_1 = 1; H_0 = 1$)

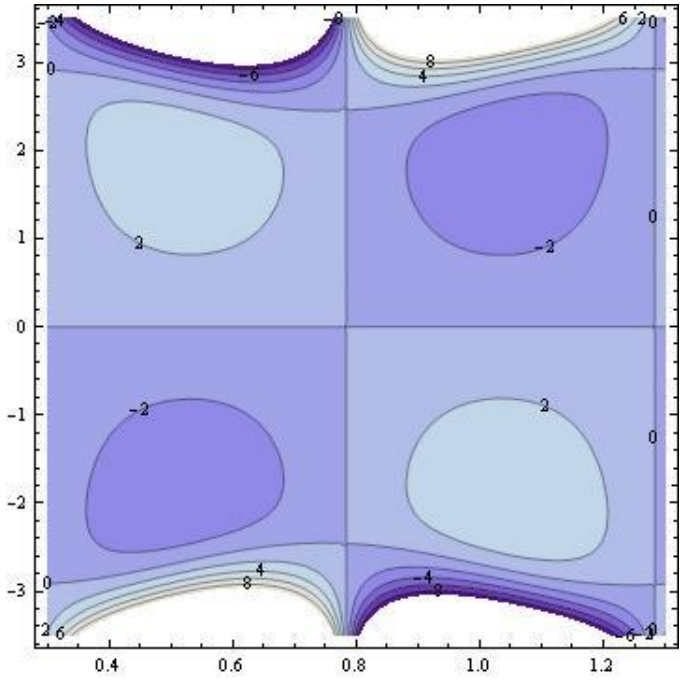

Figure 6.10(b): Stream lines for β = 0.2.

($\epsilon = 0.2; E_1 = 0.1; E_2 = 0.2; E_3 = 0.4;$ Da $= 0.5;\ \lambda_1 = 1; H_0 = 1$)

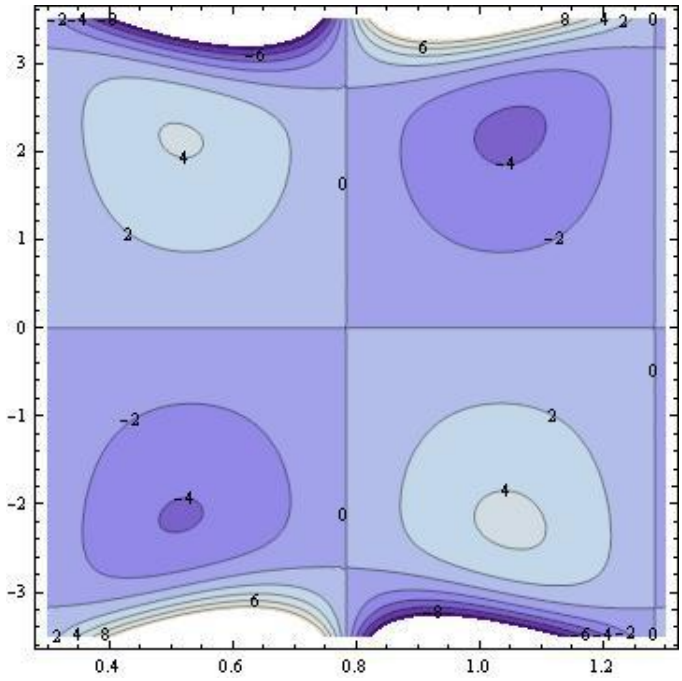

Figure 6.11 (a): Stream lines for Da = 0.5.
$(\epsilon = 0.2; E_1 = 0.1; E_2 = 0.2; E_3 = 0.4; \beta = 0.1;\ \lambda_1 = 1; H_0 = 1)$

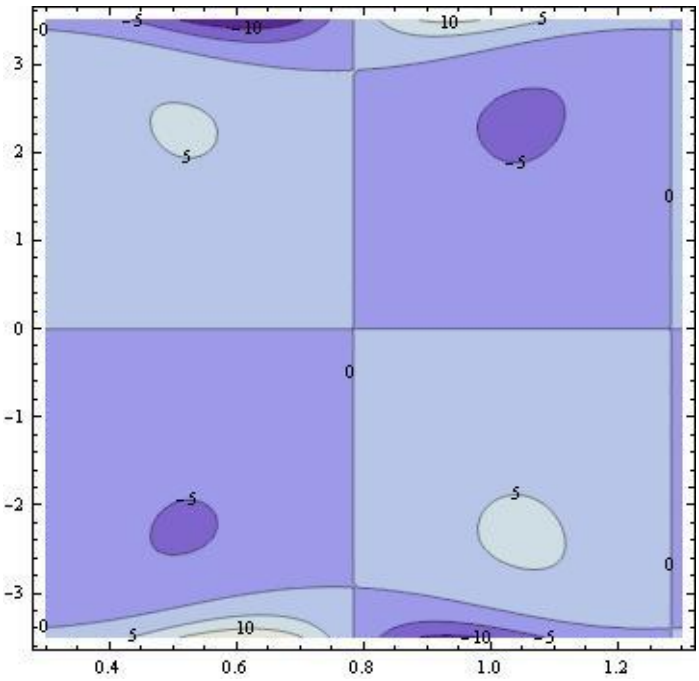

Figure 6.11(b): Stream lines for Da = 0.7
$(\epsilon = 0.2; E_1 = 0.1; E_2 = 0.2; E_3 = 0.4; \beta = 0.1;\ \lambda_1 = 1; H_0 = 1)$

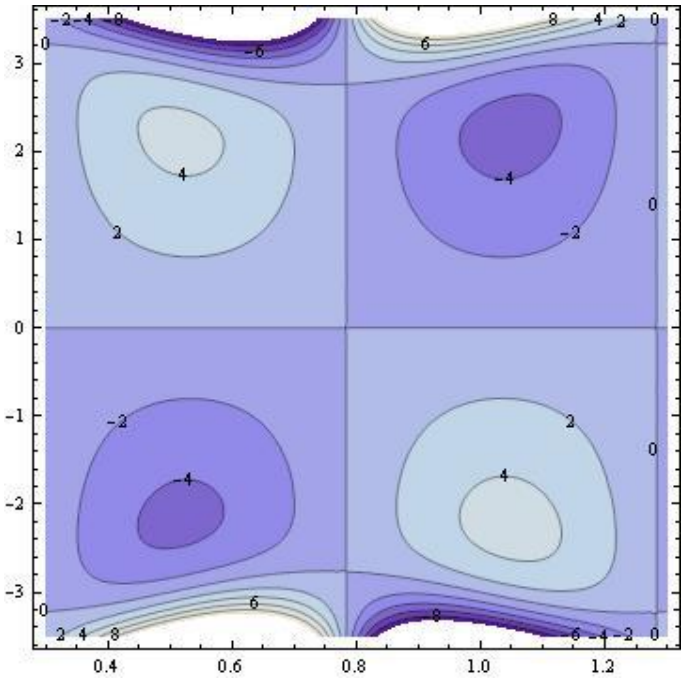

Figure 6.12(a): Stream lines for H_0= 1.
($\epsilon = 0.2; E_1 = 0.1; E_2 = 0.2; E_3 = 0.4; \beta = 0.1; \mathrm{Da} = 0.5;\ \lambda_1 = 1$)

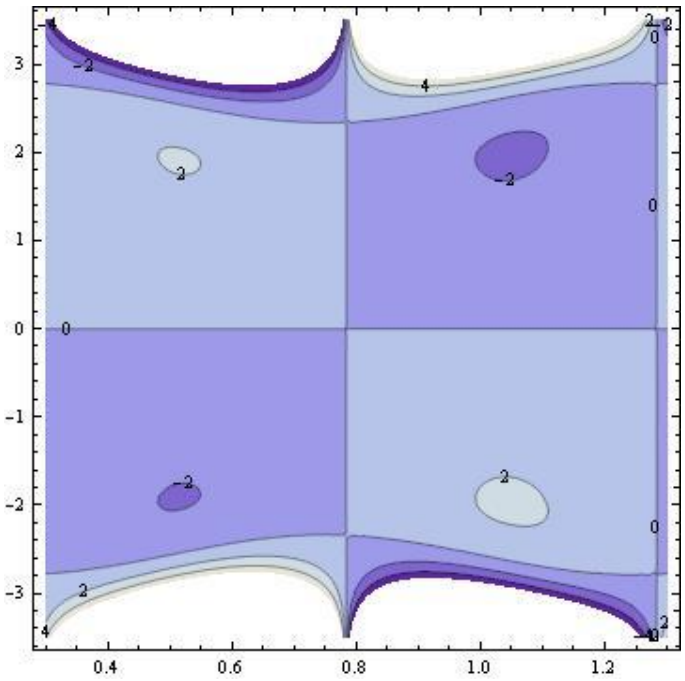

Figure 6.12(b). Stream lines for H_0= 1.5.
($\epsilon = 0.2; E_1 = 0.1; E_2 = 0.2; E_3 = 0.4; \beta = 0.1; \mathrm{Da} = 0.5;\ \lambda_1 = 1$)

Chapter 7

Influence of Wall Properties on the Peristaltic Flow of a Jeffrey Fluid in a Uniform Porous Channel under Heat Transfer

Chapter 7

7.1 Introduction

In view of the role played by peristalsis in biological and engineering systems, we have studied, in the last two chapters, the effects of peristalsis of a Jeffrey fluid in uniform channel taking porous, slip condition and wall properties in the presence of magnetic field. As the study of peristalsis under heat transfer gives a better perceptive of the flows in physiological systems, in the present chapter the study is carried on to know the heat transfer effects.

In oxygenation processes peristalsis accompanied by heat transfer is useful. Further applications of this concept are transport of corrosive materials and sanitary fluid transport. Heat transfer in medical applications is seen in fields of hyper and hypothermic ranges. Many more applications are skin burns, heating of body tissues and organs, heat and mass transmission in the human respiratory system, electro surgery, preservation of tissues by freezing and the application of cryosurgery, heat transfer in teeth, temperature measurement and thermograph.

Sudhakar Reddy et al. [122] discussed the heat transfer in Jeffery fluid moving under peristaltic action in a uniform tube travelling with the velocity as that of the wave in the laborotary frame, having variable viscosity. Influence of heat transfer on the peristaltic motion of a Jeffrey fluid in a channel having wall properties is studied by Arun Kumar et al. [123]. Dheia et al. [114] studied the impacts of wall and heat on the bolus, believed as Jeffrey fluid, moving in the esophagus. Their results depict that velocity enhances with rise in Jeffrey parameter, Darcy number, thermal conductivity and Grashoff number. Hariprabakaran et al. [124] investigated the peristaltic motion under long wavelength and low Reynolds number presumptions to know the influence of heat and MHD peristaltic flow of Jeffrey fluid in a permeable channel. They obtained the analytic results for the stream function, velocity field and temperature profile. Hussain et al. [125] examined MHD peristaltic flow of a Jeffrey fluid with variable thermal conductivity under heat transfer.

Hence the analysis of the wall effects and heat transfer on the peristaltic flow of a MHD Jeffrey fluid in a two dimensional porous channel with slip condition is inspected in this chapter.

7.2 Physical assumptions of the problem

A uniform permeable channel under heat transfer is considered to be held fixed wherein the peristaltic transport of a non-Newtonian MHD Jeffrey fluid is moving under slip conditions. The flow geometry and governing wall equations are mentioned in chapter 5 (Equations 5.1 to 5.3).

The fundamental equations are:

The mass conservation equation is

$$\frac{\partial u}{\partial x}+\frac{\partial v}{\partial y}=0. \tag{7.1}$$

The momentum equations are

$$\rho\left(\frac{\partial u}{\partial t}+u\frac{\partial u}{\partial x}+v\frac{\partial u}{\partial y}\right)=\frac{\mu}{1+\lambda_1}\nabla^2 u-\mu\frac{u}{k}-\sigma {B_0}^2 u-\frac{\partial p}{\partial x}, \tag{7.2}$$

$$\rho\left(\frac{\partial v}{\partial t}+u\frac{\partial v}{\partial x}+v\frac{\partial v}{\partial y}\right)=\frac{\mu}{1+\lambda_1}\nabla^2 v-\mu\frac{v}{k}-\frac{\partial p}{\partial y}. \tag{7.3}$$

Energy equation is

$$G\left(\frac{\partial T}{\partial t}+u\frac{\partial T}{\partial x}+v\frac{\partial T}{\partial y}\right)=\frac{K}{\rho}\left(\frac{\partial^2 T}{\partial x^2}+\frac{\partial^2 T}{\partial y^2}\right)+\vartheta\left\{\left(\frac{\partial v}{\partial x}+\frac{\partial u}{\partial y}\right)^2+2\left[\left(\frac{\partial u}{\partial x}\right)^2+\left(\frac{\partial v}{\partial y}\right)^2\right]\right\}, \tag{7.4}$$

where $K, \vartheta, T, G,$ are respectively the thermal conductivity of the fluid, the kinematic coefficient of viscosity, the temperature and the specific heat at constant pressure.

The corresponding conditions are

$$\frac{\partial u}{\partial y}=0, \qquad at\ y=0 \quad \text{(the regularity condition)}, \tag{7.5}$$

$$u=-d\,\frac{\sqrt{Da}}{\beta}\,\frac{\partial u}{\partial y}, \quad at\ \ y=\pm\eta(x,t), \ \ \text{(the slip condition)}, \tag{7.6}$$

The dynamic boundary conditions at the flexible walls are,

$$\frac{\partial}{\partial x}L(\eta)=-\rho\left(\frac{\partial u}{\partial t}+u\frac{\partial u}{\partial x}+v\frac{\partial u}{\partial y}\right)+\frac{\mu}{1+\lambda_1}\nabla^2 u-{B_0}^2 u-\mu\frac{u}{k},$$

$$at\ \ y=\pm\eta(x,t), \tag{7.7}$$

where $\frac{\partial}{\partial x}L(\eta) = \frac{\partial p}{\partial x} = -T\frac{\partial^3 \eta}{\partial x^3} + m\frac{\partial^3 \eta}{\partial x \partial t^2} + C\frac{\partial^2 \eta}{\partial x \partial t}$. (7.8)

Using the same dimensionless quantities as in the chapter 5 along with $\theta = \frac{T-T_0}{T_1-T_0}$. The equations 7.1 to 7.7, then reduce to the equations

$$\frac{\partial u}{\partial x} + \frac{\partial v}{\partial y} = 0, \tag{7.9}$$

$$R_e\delta\left(\frac{\partial u}{\partial t} + u\frac{\partial u}{\partial x} + v\frac{\partial u}{\partial y}\right) = \frac{1}{1+\lambda_1}\left(\delta^2\frac{\partial^2 u}{\partial x^2} + \frac{\partial^2 u}{\partial y^2}\right) - \frac{u}{Da} - {H_0}^2 u - \frac{\partial p}{\partial x}, \tag{7.10}$$

$$R_e\delta^3\left(\frac{\partial v}{\partial t} + u\frac{\partial v}{\partial x} + v\frac{\partial v}{\partial y}\right) = \frac{\delta^2}{1+\lambda_1}\left(\delta^2\frac{\partial^2 v}{\partial x^2} + \frac{\partial^2 v}{\partial y^2}\right) - \delta^2\frac{v}{Da} - \frac{\partial p}{\partial y}, \tag{7.11}$$

$$R_e\delta\left(\frac{\partial \theta}{\partial t} + u\frac{\partial \theta}{\partial x} + v\frac{\partial \theta}{\partial y}\right) = \frac{1}{P_r}\left(\delta^2\frac{\partial^2 \theta}{\partial x^2} + \frac{\partial^2 \theta}{\partial y^2}\right) + E_c\left[2\left\{\delta^2\left(\frac{\partial u}{\partial x}\right)^2 + \delta^2\left(\frac{\partial v}{\partial y}\right)^2\right\} + \left(\delta^2\frac{\partial v}{\partial x} + \frac{\partial u}{\partial y}\right)^2\right]. \tag{7.12}$$

Boundary conditions after dropping primes are

$$\frac{\partial u}{\partial y} = 0, \quad at\ y = 0, \tag{7.13}$$

$$u = -\frac{\sqrt{Da}}{\beta}\frac{\partial u}{\partial y}, \quad at\ y = \pm\eta(x,t) = \pm\left(1 + \varepsilon sin2\pi(x-t)\right) \tag{7.14}$$

and

$$-R_e\delta\left(\frac{\partial u}{\partial t} + u\frac{\partial u}{\partial x} + v\frac{\partial u}{\partial y}\right) + \frac{1}{1+\lambda_1}\left(\delta^2\frac{\partial^2 u}{\partial x^2} + \frac{\partial^2 u}{\partial y^2}\right) - \frac{u}{Da} - {H_0}^2 u = E_1\frac{\partial^3 \eta}{\partial x^3} + E_2\frac{\partial^3 \eta}{\partial x \partial t^2} + E_3\frac{\partial^2 \eta}{\partial x \partial t} \quad at\ y = \pm\eta(x,t), \tag{7.15}$$

where $P_r = \frac{\rho\vartheta G}{K}$ denotes Prandtl number and $E_c = \frac{c^2}{G(T_1-T_0)}$ denotes Eckert number along with usual meaning of other parameters as mentioned in chapter 5.

7.3 Method of solution

The solution of the governing equations is not possible in general, hence we assume long wavelength approximation and low Reynolds number to solve equations 7.9 – 7.15

Equations 7.9 – 7.12 yield the compatibility equation as

$$\frac{\partial u}{\partial x}+\frac{\partial v}{\partial y}=0, \tag{7.16}$$

$$0=-\frac{\partial p}{\partial x}+\frac{1}{1+\lambda_1}\frac{\partial^2 u}{\partial y^2}-\left({H_0}^2+\frac{1}{Da}\right)u, \tag{7.17}$$

$$0=-\frac{\partial p}{\partial y}, \tag{7.18}$$

$$E_c\left(\frac{\partial u}{\partial y}\right)^2+\frac{1}{P_r}\frac{\partial^2\theta}{\partial y^2}=0. \tag{7.19}$$

The dimensionless boundary conditions 7.13 – 7.15 become

$$\frac{\partial u}{\partial y}=0,\ \ at\ y=0, \tag{7.20}$$

$$u=-\frac{\sqrt{Da}}{\beta}\frac{\partial u}{\partial y},\quad at\ \ y=\pm\eta(x,t)=\pm\big(1+\varepsilon sin2\pi(x-t)\big), \tag{7.21}$$

$$\frac{1}{1+\lambda_1}\frac{\partial^2 u}{\partial y^2}-\left({H_0}^2+\frac{1}{Da}\right)u=E_1\frac{\partial^3\eta}{\partial x^3}+E_2\frac{\partial^3\eta}{\partial x\partial t^2}+E_3\frac{\partial^2\eta}{\partial x\partial t}, at\ y=\pm\eta(x,t). \tag{7.22}$$

Further,

$$\theta=0\ \ at\ \ y=-\eta(x,t), \tag{7.23}$$

$$\theta=1\ \ at\ \ y=\eta(x,t). \tag{7.24}$$

Solving equations 7.17 and 7.18 with boundary conditions 7.20 – 7.22, we get

$$u(x,y,t)=\frac{E}{N^2}\left[-1-\frac{cosh(Ny)}{T_1}\right]. \tag{7.25}$$

Solving equation 7.19, with boundary conditions 7.23 and 7.24, we get

$$\theta=B\left(\frac{cosh(2Ny)}{4N^2}-\frac{y^2}{2}\right)+\frac{y}{2\eta}+\frac{1}{2}-\frac{B}{2}\left(\frac{cosh(2N\eta)}{2N^2}-\eta^2\right). \tag{7.26}$$

Here

$$E = -\varepsilon[(2\pi)^3 cos2\pi(x-t)\,(E_1+E_2) - E_3(2\pi)^2 sin2\pi(x-t)],$$

$$D = \frac{\sqrt{Da}}{\beta}, \qquad T_1 = DN\text{sinhN}\eta - \text{sinhN}\eta, \qquad B_r = E_c p_r,$$

$$B = -\frac{B_r E^2}{2(1+\lambda_1){T_1}^2}, \qquad N = \sqrt{\left({H_0}^2 + \frac{1}{Da}\right)(1+\lambda_1)}.$$

Thus it is obvious that Brinkman number B_r signifies the relative importance between dissipation effects and the fluid conduction.

The heat transfer coefficient that defines the flux at the walls is

$$H = [\eta_x]\left[\theta_y(\eta)\right], \tag{7.27}$$

$$H = [2\pi\varepsilon cos2\pi(x-t)]\left[\left\{B\left(\frac{sinh2N\eta}{2N} - \eta\right)\right\} + \frac{1}{2\eta}\right]. \tag{7.28}$$

The solutions in equations 7.26 and 7.28 match with the results of Saravana et al [126] for k = 0.

7.4 Results and Discussion

The uniform motion of an incompressible Jeffrey fluid inside a porous medium channel having slip on its surface is considered. This investigation has been carried out to study the wall effect and slip factors which influence the flow in porous uniform channel. The non-Newtonian fluid of Jeffrey model has been considered in the analysis. Heat transfer coefficient H and temperature distribution θ equations have been analytically derived using momentum and energy equations. Results are analyzed through graphical plots to study the behavior of various parameters of temperature distribution and heat transfer coefficient.

The analytical solution for temperature distribution, using equation 7.26, is analyzed for various values of Hartmann number H_0, Darcy number Da, Brinkman number Br, slip parameter β, Jeffrey parameter λ_1, the elastic parameters E_1, E_2, E_3 to study their behavior. Figure 7.1 illustrates the temperature distribution for changing E_1, E_2 and E_3

with constant values of other parameters. It is clear from the graphical illustration that temperature distribution reduces with the rise of elastic parameters. Figure 7.2 depicts the effect of Jaffrey parameter on temperature distribution. One can see that the temperature distribution decreases with rise in the Jeffrey parameter. This result is in agreement with that of Hari prabakaran et al. [124]. Figure 7.3 depicts the effects of slip parameter on the temperature distribution for the peristaltic flow. It demonstrates that temperature distribution diminishes with increasing slip parameter. Temperature distribution enhances with increasing Darcy number as in Figure 7.4. The consequences of various values of Hartmann number upon temperature distribution is drawn in Figure 7.5. Interestingly it can be noted that the impact of enhancing Hartmann number leads to a drop in the temperature in the conduit. A similar result can be seen in Figure 7.6 for Brinkman number.

The effect of $H_0, Da, \beta, Br, \lambda_1$ and elastic parameters on the heat transform coefficient H in the symmetric porous channel are plotted in Figure 7.7 to Figure 7.12 using equation 7.28. The significant characteristic of uniform peristaltic motion of Jeffrey fluid through the channel having porosity under heat transfer and magnetic field effects is explored through these Figures. It is noticed that, peristaltic motion in the conduit gives rise to a periodical oscillatory behavior for the heat transfer coefficient. The heat transfer coefficient drops as the elastic parameters as shown in Figure 7.7. The absolute value of heat transfer coefficient rises as Jeffrey parameter increase as depicted in Figure 7.8. The heat transfer coefficient reduces as the slip parameter increase as shown in Figure 7.9. One can examine that the heat transfer coefficient enhances with enhancing Darcy number as shown in Figure 7.10. The absolute value of heat transfer coefficient rises as Hartmann number increase as depicted in Figure 7.11. Absolute value of heat transfer coefficient H reduces by enhancing Brinkman number as depicted in Figure 7.12.

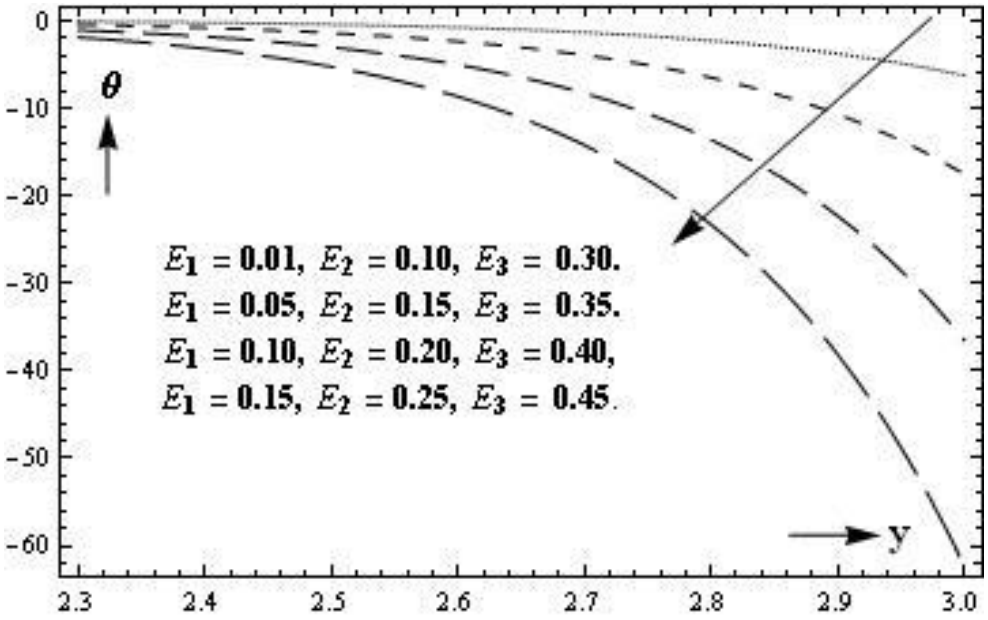

Figure 7.1: Consequences of E_1, E_2, E_3 on temperature distribution θ.

($\epsilon = 0.2;\ H_0 = 1, Br = 3; Da = 0.5; \beta = 0.1; \lambda_1 = 1$)

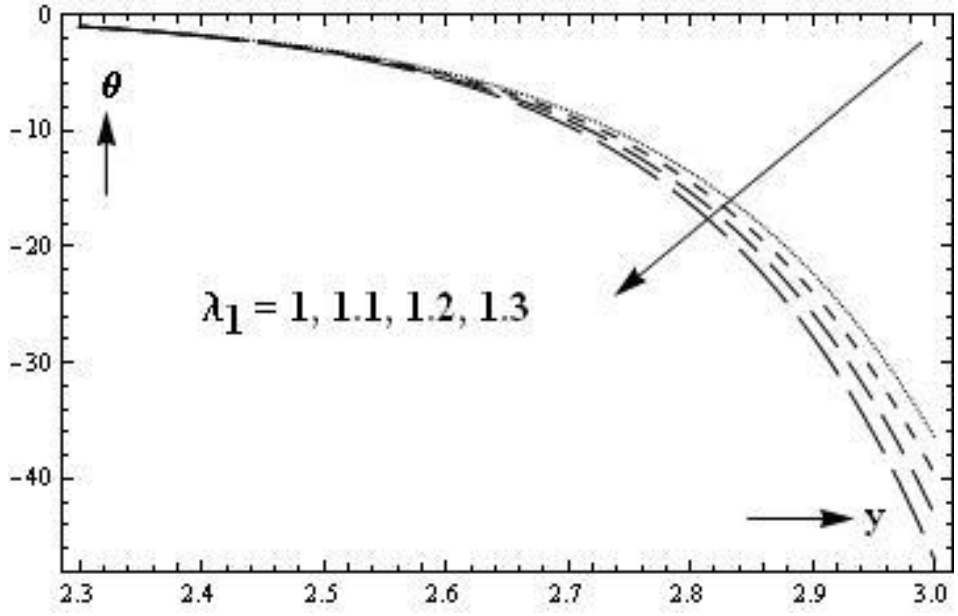

Figure 7.2: Consequences of λ_1 on temperature distribution θ.

($\epsilon = 0.2;\ H_0 = 1, Br = 3; E_1 = 0.1; E_2 = 0.2; E_3 = 0.4; Da = 0.5; \beta = 0.1$)

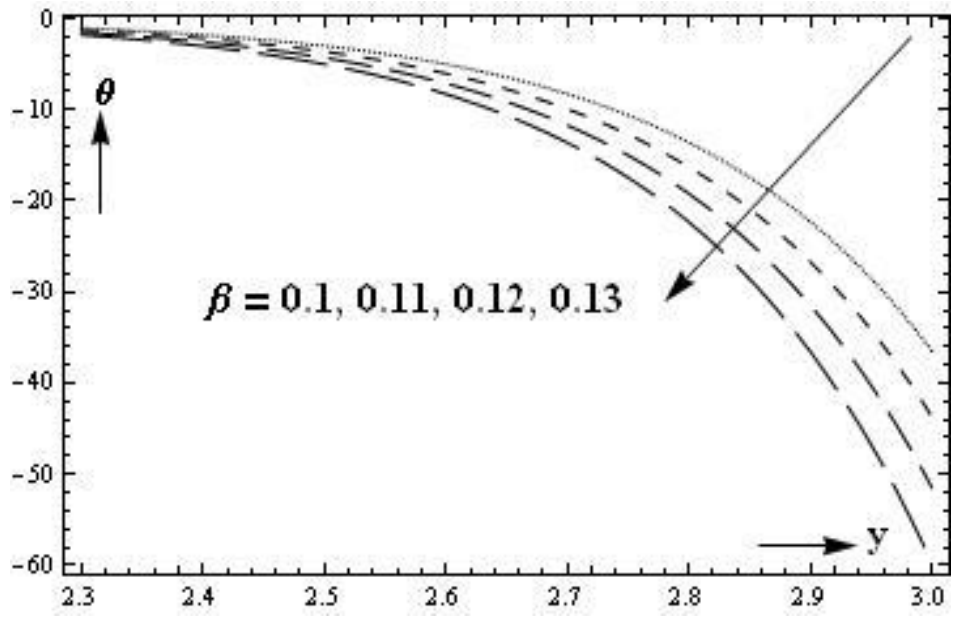

Figure 7.3: Consequences of β on temperature distribution θ.

($\epsilon = 0.2;\ H_0 = 1, Br = 3; E_1 = 0.1; E_2 = 0.2; E_3 = 0.4; Da = 0.5; \lambda_1 = 1$)

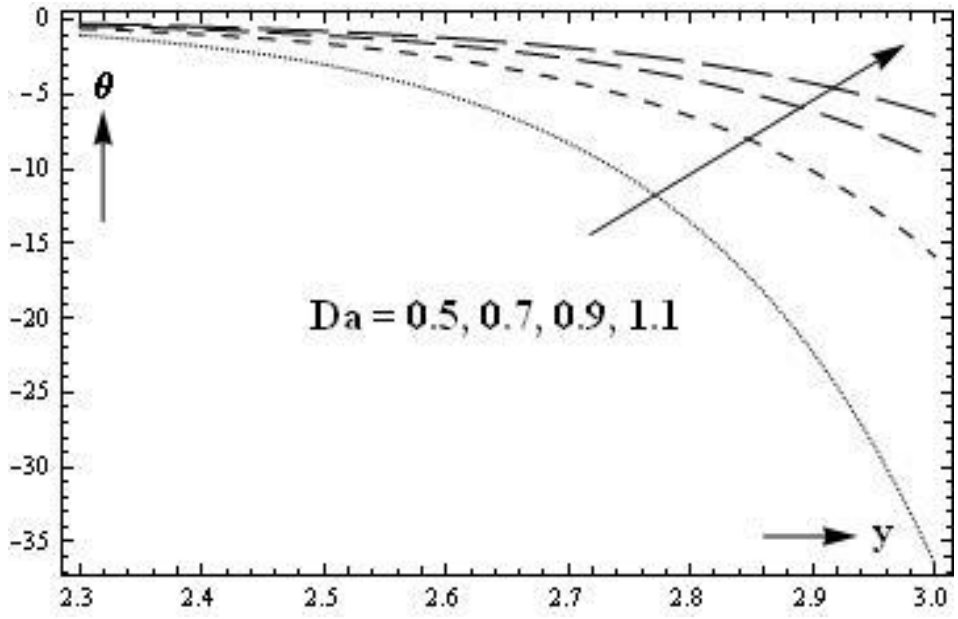

Figure 7.4: Consequences of Da on temperature distribution θ.

($\epsilon = 0.2;\ H_0 = 1, Br = 3; E_1 = 0.1; E_2 = 0.2; E_3 = 0.4; \beta = 0.1; \lambda_1 = 1$)

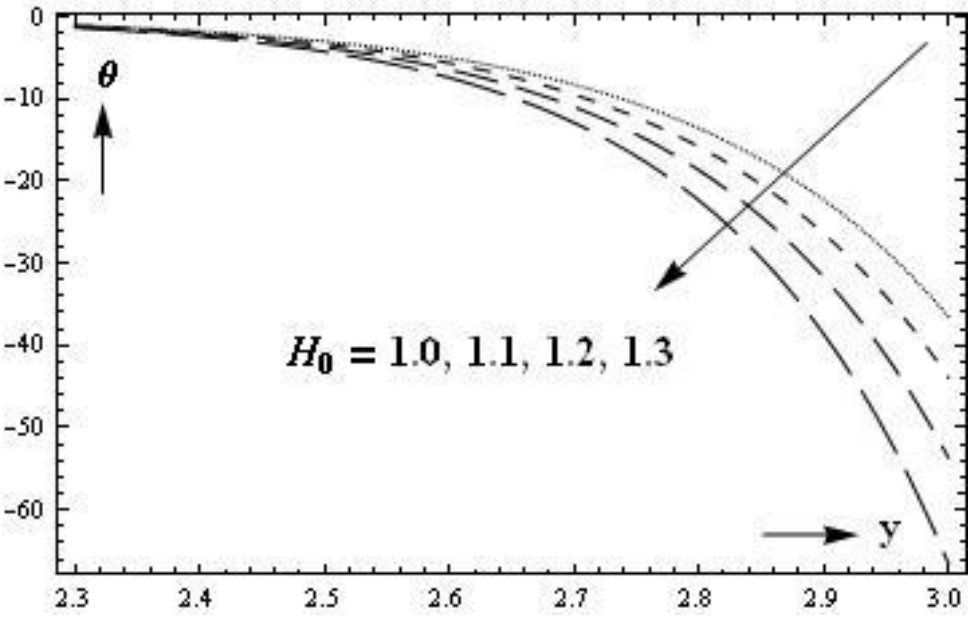

Figure 7.5: Consequences of H_0 on temperature distribution θ.

($\epsilon = 0.2;\ Br = 3; E_1 = 0.1; E_2 = 0.2; E_3 = 0.4; Da = 0.5; \beta = 0.1; \lambda_1 = 1$)

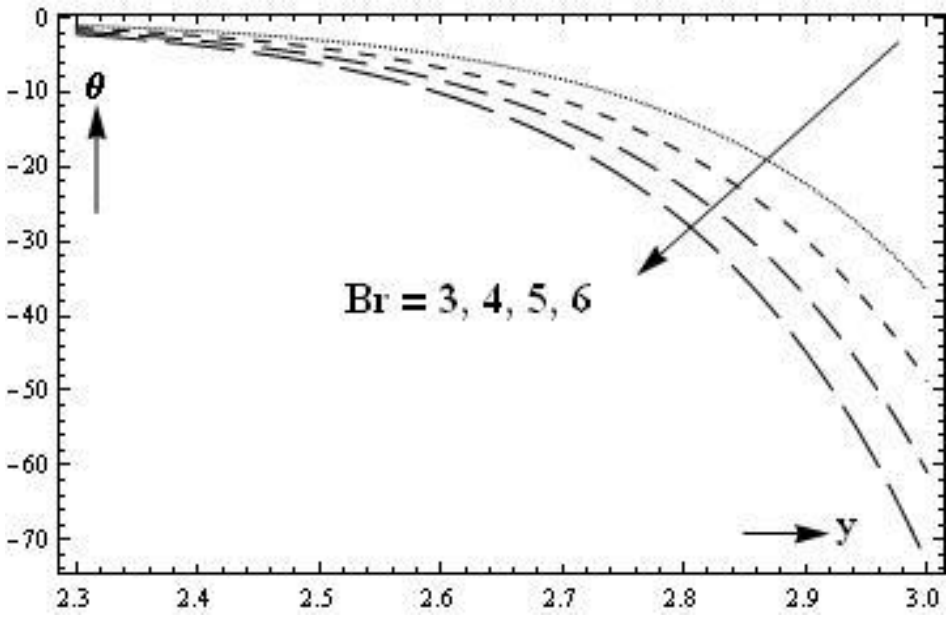

Figure 7.6: Consequences of Br on temperature distribution θ.

($\epsilon = 0.2;\ H_0 = 1; E_1 = 0.1; E_2 = 0.2; E_3 = 0.4; Da = 0.5; \beta = 0.1; \lambda_1 = 1$)

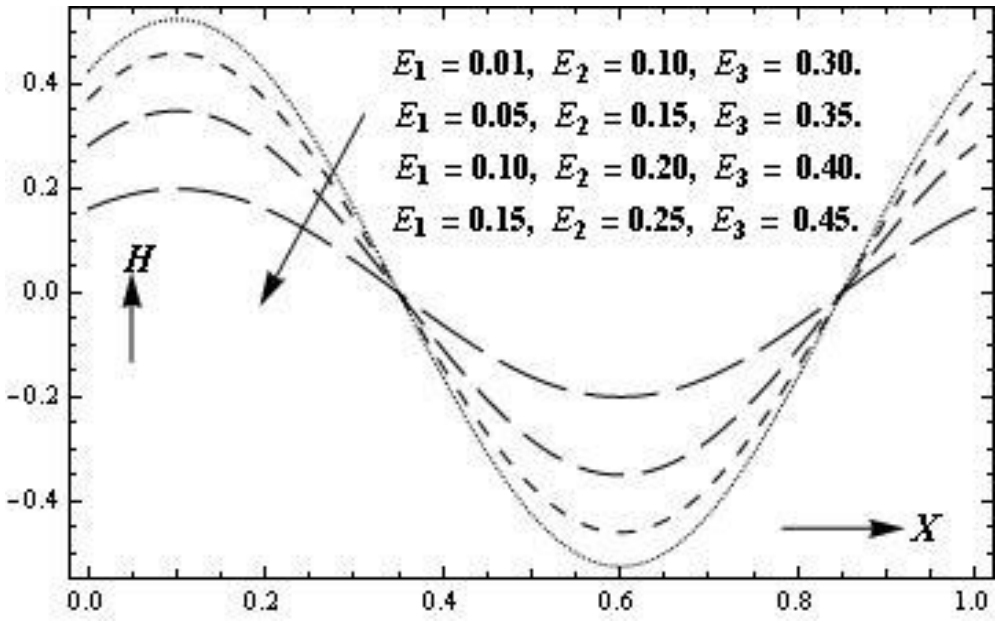

Figure 7.7: Consequences of E_1, E_2, E_3 on Heat transfer coefficient H.

($\epsilon = 0.2;\ H_0 = 1, Br = 3; Da = 0.5; \beta = 0.1; \lambda_1 = 1$)

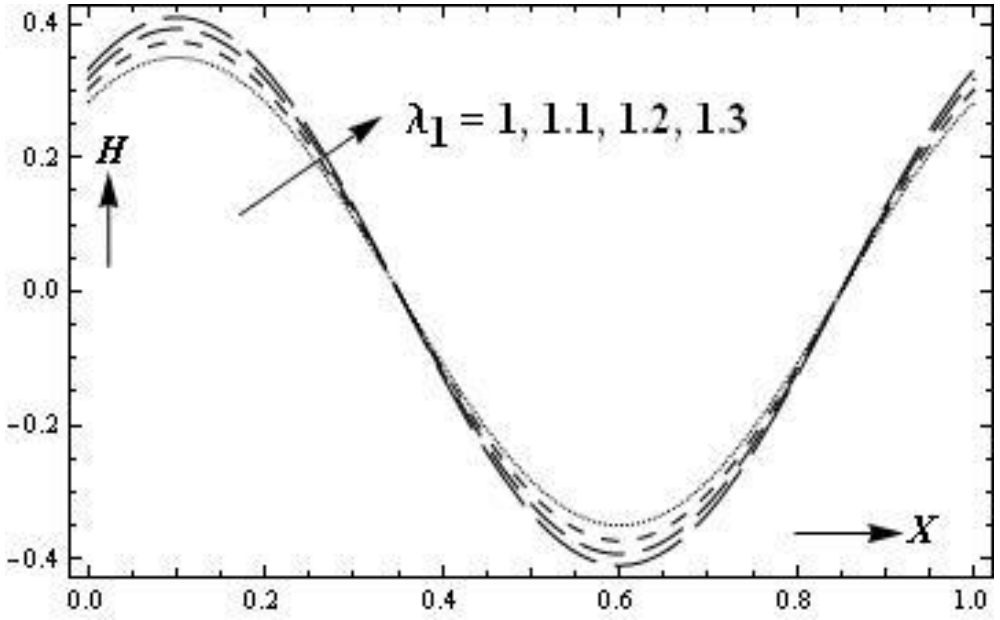

Figure 7.8: Consequences of λ_1 on Heat transfer coefficient H.

($\epsilon = 0.2;\ H_0 = 1, Br = 3; E_1 = 0.1; E_2 = 0.2; E_3 = 0.4; Da = 0.5; \beta = 0.1$)

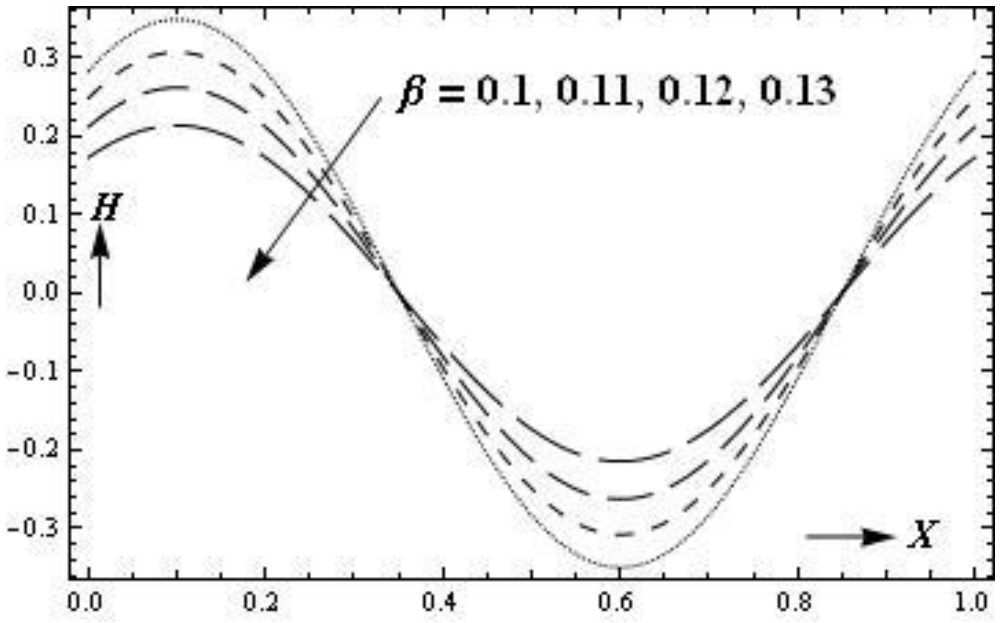

Figure 7.9: Consequences of β on Heat transfer coefficient H

($\epsilon = 0.2;\ H_0 = 1; Br = 3; E_1 = 0.1; E_2 = 0.2; E_3 = 0.4; Da = 0.5; \lambda_1 = 1$)

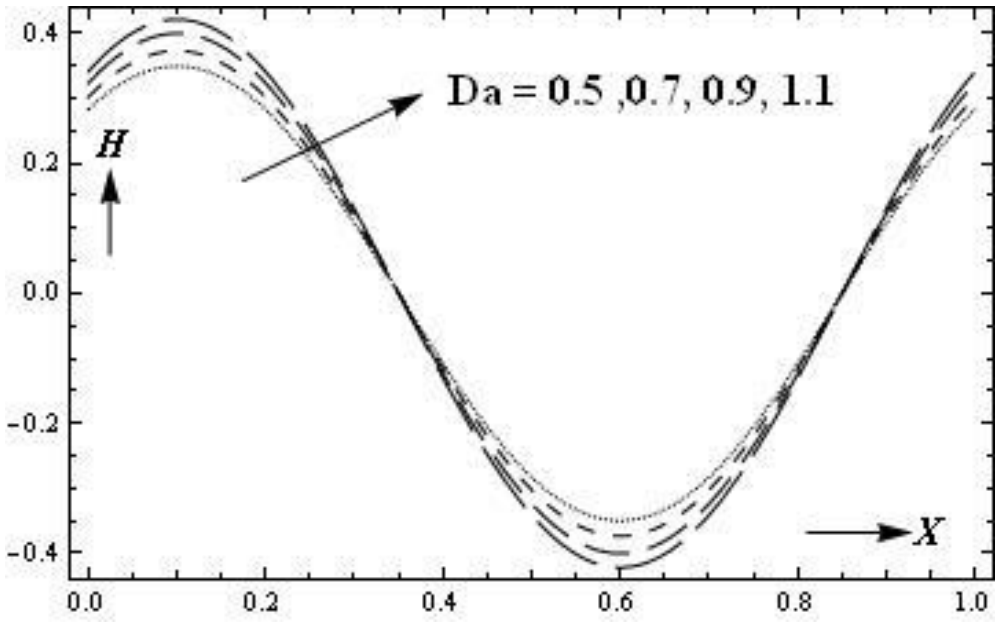

Figure 7.10: Consequences of Da on Heat transfer coefficient H.

($\epsilon = 0.2;\ H_0 = 1; Br = 3; E_1 = 0.1; E_2 = 0.2; E_3 = 0.4; \beta = 0.1; \lambda_1 = 1$)

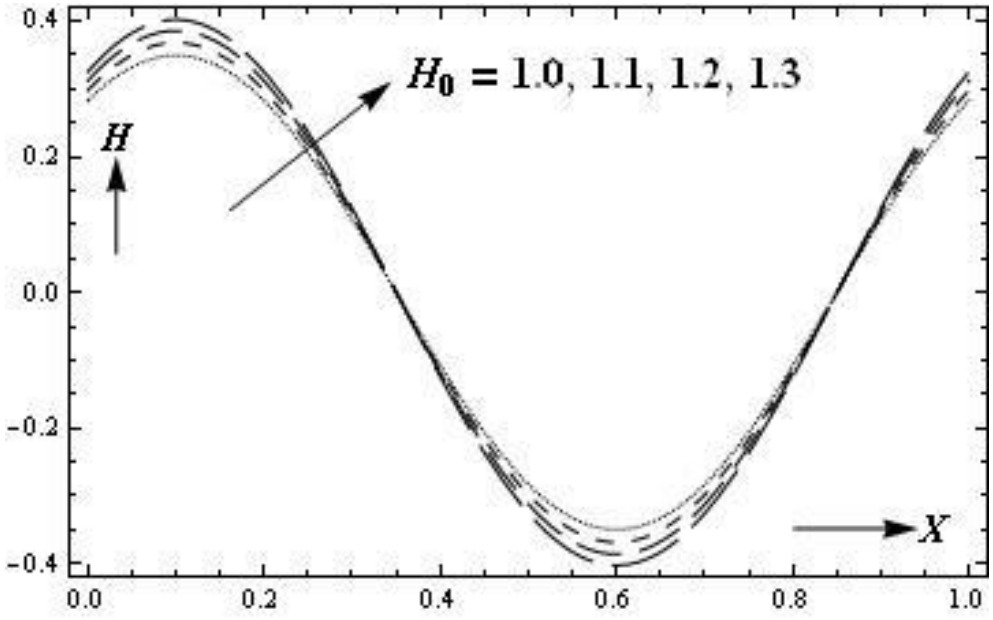

Figure 7.11: Consequences of H_0 on Heat transfer coefficient H.

($\epsilon = 0.2;\ Br = 3; E_1 = 0.1; E_2 = 0.2; E_3 = 0.4; Da = 0.5; \beta = 0.1; \lambda_1 = 1$)

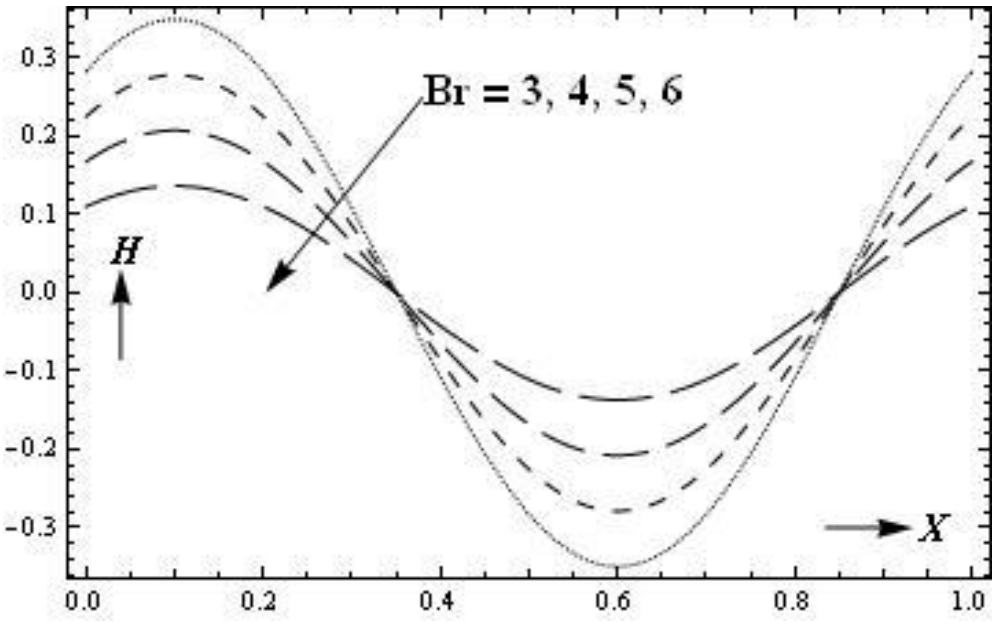

Figure 7.12: Consequences of Br on Heat transfer coefficient H.

($\epsilon = 0.2;\ H_0 = 1; E_1 = 0.1; E_2 = 0.2; E_3 = 0.4; Da = 0.5; \beta = 0.1; \lambda_1 = 1$)

Chapter 8

Conclusions and Scope for the Future Work

8.1 Conclusions

Since the research carried out by Latham [5] and Shapiro [9], peristaltic flow and its parameters have been studied by a number of authors for quite some time. Recently, the peristaltic flow with couple stress and Jeffrey fluid has gained more interest because of its applications in science and engineering. The study of MHD analysis shows ways for the therapeutic use of the influence of external magnetic field in the clinical treatment of hypertension and other hemodynamic diseases. Heat transfer analysis may be significant due to its relevance in industry and biomechanics. For practical applications, trapping phenomenon may be useful to understand the influence of wall properties on the flow characteristics of ureters in transporting diseased urine and chyme transport in intestine. However, the peristaltic flow of the non-Newtonian, couple stress and Jeffrey fluids through porous medium under wall effects and slip conditions has received less concentration.

- This work presents symmetric peristaltic transport through uniform porous channel under slip and wall effects in various conditions.
- The theoretical analysis begins with the most general form of the Navier-Stokes equation of fluid motion and with the assumptions that gravitational forces are of no significance, the density and viscosity are constant over space and time.
- For inertia free flow, the Reynolds number is considered to be small. The analysis of peristaltic flow reveals that long wavelength approximation and low Reynolds number make way for asymptotic methods for solving the problem. A closed solution of zeroth-order in the wave number is obtained.
- Analytical results in this research are used for an investigation of the effect of time average velocity, temperature distribution, heat transfer coefficient and trapping phenomenon on peristaltic motion to provide a possible use in physiology and industry.
- Graphs are traced for various parameters of interest such as slip parameter, Darcy number, Hartmann number, couple stress parameter/Jeffery parameter and elastic parameters. Comparison of earlier studies regarding peristaltic flow has been made. Graphs show a parabolic path traced by velocity with maximum value at the centre of the conduit and minimum near the walls.

Couple stress fluid:

1. Since the resistive kind of force is generated by wall damping, the velocity drops as the viscous damping force E_3 increases, physically this signifies that dampness has an adverse effect on the velocity.
2. By increasing the value of the porosity parameter Da the permeability of the medium increases which accelerates the fluid and thus temperature enhances.
3. As expected heat transfer coefficient shows an oscillatory behavior which is because of the propagation of sinusoidal waves along the channel walls. It can be noticed that there is a decrease in the absolute value of heat transfer coefficient for increase in the values of $E_1,\ E_2,\ E_3$. This result may be applicable for flow of blood in the human arteries and veins since they possess the properties of elasticity, damping and stiffness.
4. Mean velocity decreases with increase in the couple stress parameter. It is observed that the fluid becomes more viscous with an increase in the couple stress parameter, hence as the fluid viscosity increases, the fluid flow velocity decreases.
5. It can be also seen that the velocity increases by decreasing β under MHD fluid flows for couple stress fluid. According to the Navier conditions, the existence of slip at the surface is linearly proportional to the shear stress at the surface. Therefore, this result can be beneficial for the study of fluid flow in microcirculatory systems under the slip condition.
6. It is noticed that the magnitudinal value of time average velocity reduces with rise in the Hartmann number under the presence of elastic parameters. The transverse magnetic field applied to the flow behaves as a retarding force for the fluid flow and thus reduces the velocity of the flow. This may serve as an application for control of bleeding during surgery.

Jeffrey fluid:

1. The slip parameter β measures the amount of slip at the surface. It is observed that, the mean velocity distribution decreases with increase in the values of slip parameter. Consequently, with the increase of slip parameter the thickness of boundary layer increases.

2. For increasing Brinkman number Br thermal diffusivity decreases so temperature profile decays.
3. In the study of peristaltic flow of Jeffrey fluid in a compliant wall in uniform duct, it is found that the velocity profile is a decreasing function of all the parameters considered except Jeffrey parameter.
4. In the study of the effect of magnetic field the average velocity increases with Jeffrey parameter and Hartmann number but decreases with other parameters.
5. With the formation of the bolus it can be concluded that fluid flows more rapidly at the central part of the channel. Also the size of the bolus changes randomly with the variation of all the physical parameters. The stream lines decreases with Jeffrey parameter, slip parameter and Hartmann number.

These modeling's may set insight in validating and reducing the complexity of modeling some non-Newtonian fluids as in, blood flow in the blood vessels under certain physiological conditions and flow of urine in the ureter.

8.2 Scope for the future work

The scope of this thesis is to model peristaltic flow in which parameters of peristalsis are considered with the intention of gaining insight in the bio-fluid dynamics. This may provide the technically oriented reader, some elementary knowledge of the anatomy and physiology of the ureter.

In this work, investigation is performed for many different conditions. A wide value of amplitude ratios and wave numbers would be recommended for the next development.

This analysis may be undertaken using homotopy analysis. Further the study can be promoted under suction and injection analysis.

References

[1] Jaffrin, M. Y. and Shapiro, A. H., Peristaltic pumping, Ann. Rev. Fluid Mech., Vol. 3, 1971, pp: 13-36.

[2] Beaver, G. S. and Joseph, D. D., Boundary conditions at a naturally permeable wall, J. Fluid Mech., Vol. 30, 1967, pp: 197-207.

[3] Saffman, P. G., On the boundary condition at the surface of a porous medium, Studies in Appl. Math., Wiley online library, 1971.

[4] Kill, F., The function of the urethra and the renal pelvis, Saunders, Philadelphia, 1957.

[5] Latham, T. W., Fluid motion in a peristaltic pump, M.S. Thesis, MIT, Cambridge, MA. 1966.

[6] Shapiro, A. H., Pumping and retrograde diffusion in peristaltic waves, Proc. Workshop in Ureteral revolume flow rate in children, Nat. Acad. Sci., Washington, D. C, Vol. 1, 1967, pp: 109-126.

[7] Burns, J. C. and Parkes, J., Peristaltic motion, J. Fluid Mech., Vol. 29(4), 1967, pp: 731-743.

[8] Fung, Y. C. and Yih, C. S., Peristaltic transport, J. Appl. Mech., Trans. ASME, Vol. 35, 1968, pp: 669-675.

[9] Shapiro, A. H., Jaffrin, M. Y. and Weinberg, S. L., Peristaltic pumping with long wavelength at low Reynolds number, J. Fluid Mech., Vol. 37(4), 1969, pp: 799-825.

[10] Zien, T. F. and Ostrach, S. A., A long wave length approximation to peristaltic motion, J. Biomech., Vol. 3, 1970, pp: 63-75.

[11] Yin, F. C. P. and Fung, Y. C., Comparison of theory and experiment in peristaltic transport, J. Fluid Mech., Vol. 47(1), 1971, pp: 93–112.

[12] Bohme, G. and Friedrich, R., Peristaltic flow of visco-elastic liquids, J. Fluid Mech., Vol. 128, 1983, pp: 109-122.

[13] Pozrikidis, C., A study of peristaltic flow, J. Fluid Mech., Vol. 180, 1987, pp: 515-527.

[14] Provost, A. M. and Schwarz, W. H., A theoretical study of viscous effects in peristaltic pumping, J. Fluid Mech., Vol. 279, 1994, pp: 177-195.

[15] Toklu, E., A new mathematical model of peristaltic flow on esophageal bolus transport, Vol. 6(31), 2011, pp: 6584-6593.

[16] Gupta, B. B. and Seshadri, V., Peristaltic pumping in non-uniform tubes, J. Biomech., Vol. 9, 1976, pp: 105-109.

[17] Misery, A. M. E. L., Shehawey, E. F. El. and Hakeem, A., Peristaltic motion of an incompressible generalized Newtonian fluid in a planar channel, J. Phy. Soc. Japan, Vol. 85 (1), 1996, pp: 3524-3529.

[18] Abd El Naby, A. E. H. and Misiery, A. E. M. El., Effects of an endoscope and generalized Newtonian fluid on peristaltic motion, J. Appl. Math. and Comp., Vol. 128, 2002, pp: 19-35.

[19] Mishra, M. and Rao, A. R., Peristaltic transport of a Newtonian fluid in an asymmetric channel, Z. Angew, Math. Phys., Vol. 54, 2003, pp: 532-550.

[20] Mekheimer, Kh. S., Peristaltic transport of Newtonian fluid through uniform and non-uniform annulus, Arab. J. Sci. Eng., Vol. 30, 2005, pp: 69-83.

[21] Hayat, T. and Ali, N., Effects of variable viscosity on the peristaltic transport of a Newtonian fluid in an asymmetric channel, Appl. Math. Modeling, Vol. 32, 2008, pp: 761-774.

[22] Lew, H. S., Fung, Y. C. and Lewenstein, C. B., Peristaltic carrying and mixing of chyme in the small intestine, J. Biomech., Vol. 4, 1971, pp: 297-315.

[23] Raju, K. K. and Devanathan, R., Peristaltic motion of a non-Newtonian fluid, Rheol. Acta, Vol. 11, 1972, pp: 170-178.

[24] Goldsmith, H. L. and Skalak, R., Hemodynamics, Ann. Rev. Fluid Mech., Vol. 7, 1975, pp: 213-247.

[25] Srivastava, L. M. and Srivastava, V. P., Peristaltic transport of blood: Casson model-II, J. Biomech, Vol. 17(11), 1984, pp: 821-829.

[26] Rath, H. J. and Reese, G. W., Peristaltic flow on non-Newtonian fluids containing small spherical particals, Arch. Mech., Vol. 36(2), 1984, pp: 263-277.

[27] Srivastava, L. M. and Srivastava, V. P., Peristaltic transport of a non-Newtonian fluid: Applications to the vas deferens and small intestine, Annals of Biomed. Eng., Vol. 13, 1985, pp: 137-153.

[28] Maiti, J. C. and Misra, J. C., Non-Newtonian characteristics of peristaltic flow of blood in micro-vessels, Comm. Nonlinear Sci. and Num. Simulation, Vol. 18(8), 2013, pp: 1970-1988.

[29] Mittra, T. K. and Prasad, S. N., On the influence of wall properties and Poiseuille flow in peristalsis, J. Biomech., Vol. 6, 1973, pp: 681-693.

[30] Muthu, P., Ratish Kumar, B. V. and Chandra, P., On the influence of wall properties in the peristaltic motion of micropolar fluid, ANZIAM, Journal, Vol. 45, 2003, pp: 245- 260.

[31] Srinivasacharya, D., Radhakrishnamacharya, G. and Srinivasulu, Ch., The effects of wall properties on peristaltic transport of a dusty fluid, Turkish J. Eng. Env. Sci., Vol. 32, 2008, pp: 357- 365.

[32] Mokhtar, A. Abd Elnaby. and Haroun, M.H., A new model for study the effect of wall properties on peristaltic transport of a viscous fluid, Comm.. Nonlinear Sci. and Num. Simul., Vol. 13, 2008, pp: 752-762.

[33] Sankad, G. C. and Radhakrishnamacharya, G., Influence of wall properties on the peristaltic motion of Herschel-Bulkley fluid in a channel, ARPN J. Eng. and Appl. Sci., Vol. 4(10), 2009, pp: 27-35.

[34] Ali, N., Hayat T. and Asghar, S., Peristaltic flow of a Maxwell fluid in a channel with compliant walls, Chaos, solitons and Fractals, Vol. 39, 2009, pp: 407-416.

[35] Sankad, G. C. and Radhakrishnamacharya, G., Effect of wall properties on peristaltic transport of micropolar fluid in a non-uniform channel, Int. J. Appl. Math. and Mech., Vol. 6(1), 2010, pp: 94-107.

[36] Scheidegger, A. E., The physics of flow through porous media, University of Toronto Press, 1974.

[37] Elshehawey, E. F., Sobh, A. M. and Elbarbary, E. M., Peristaltic motion of a generalized Newtonian fluid through a porous medium, J. Phys. Soc. Jap., Vol. 69, 2000, pp: 401-407.

[38] Maiti, S. and Misra, J. C., Peristaltic flow of a fluid in a porous channel: a study having relevance to flow of bile, Int. J. Eng. Sci., Vol. 49, 2011, pp: 950-966.

[39] Tripathi, D., Anwar Beg, O., Pandey, V. S. and Singh, A. K., A study of creeping sinusoidal flow of bio-rheological fluids through a two-dimensional high permeability medium channel, J. Adv. Biotech. and Bioeng., Vol. 1, 2013, pp: 52-61.

[40] Kwang, W. and Fang, J., Peristaltic transport in a slip flow, The European Physical Journal B- Condensed matter and complex systems, Vol. 16(3), 2000, pp: 543-547.

[41] Tretheway, D. C., Liu, X. and Meinhart, C. D., Analysis of slip flow in micro channels, Phys. Fluids, Vol. 14, L9, 2002.

[42] Hron, J., Roux, C.L., Malik, J. and Rajagopal, K.R., Flows of incompressible fluids subject to Navier's slip on the boundary, Comput. Math. Appl., Vol. 6, 2008, pp: 2128-2143.

[43] Ellahi, R., Effects of the slip boundary condition on non-Newtonian flows in a channel, Comm. Nonlinear Sci. Num. Simul., Vol. 14, 2009, pp: 1377-1384.

[44] Mustafa, M., Hina, S., Hayat, T. and Alsaedi, A., Slip effects on the peristaltic motion of nono fluid in a channel with wall properties, ASME J. Heat Transfer, Vol. 135(4), 2012, pp: 041701-041708.

[45] Sreenadh, S., Srinivas, A.N.S. and Selvi, C.K., Analytical solution for peristaltic flow of conducting nano fluids in an asymmetric channel with slip effects of velocity, temperature and concentration, Alexandria Engineering Journal, Vol. 55(2), 2016, pp: 1085-1098.

[46] Srivastava, L.M. and Agrawal, R.P., Oscillating flow of a conducting fluid with a suspension of spherical particles, J. Appl. Mech., Vol. 47, 1980, pp: 196-199.

[47] Agrawal, H.L. and Anwaruddin, B., Peristaltic flow of blood in a branch, J. Ranchi. Uni. Math., Vol. 15, 1984, pp: 111-120.

[48] Ali, N., Hussen, Q., Haytat, T. and Asghar, S., Slip effects on the peristaltic transport of a MHD fluid with variable viscosity, Phys Letters A, Vol. 372, 2008, pp: 1477-1489.

[49] Hayat, T., Javed, M. and Asghar, S., MHD peristaltic motion of Johnson-Segalman fluid in a channel with compliant walls, Phys. Letters A, Vol. 372, 2008, pp: 5026-5036.

[50] Sankad, G. C. and Radhakrishnamacharya, G., Effect of magnetic field on peristaltic motion of micropolar fluid with wall effects, J. Appl. Math. and Fluid Mech., Vol. 1, 2009, pp: 37-50.

[51] Jain, M., Sharma, G. C. and Singh, A., Mathematical analysis of MHD flow of blood in very narrow capillaries, Int. J. Eng. Trans. B: Appl., Vol. 22(3), 2009, pp: 307-315.

[52] Afifi, N. A. S., Mahmoud, S. R. and Al-Isede, H. M., Effect of magnetic field and wall properties on peristaltic motion of micropolar fluid, Int. Math. Forum, Vol. 6 (27), 2011, pp: 1345 -1356.

[53] Gupta, A. K., Performance model and analysis of blood flow in small vessels with magnetic effects, Int. J. Eng., IJE Transaction A: Basics, Vol. 25(2), 2012, pp: 190-196.

[54] Parthsarathy, S., Arunachalam, G. and Vidya, M., Analysis of the effects of wall properties on MHD peristaltic flow of a dusty fluid through a porous medium, Int, J. Pure and App. Math., Vol. 102 (2), 2015, pp: 247-263.

[55] Radhakrishnamacharya, G. and Radhakrishna Murthy, V., Heat transfer to peristaltic transport in a non uniform channel, Defence Science Journal, Vol. 3(3), 1993, pp: 275- 280.

[56] Vajravelu, K., Radhakrishnamacharya, G. and Radhakrishna Murty, V., Peristaltic flow and heat transfer in a vertical porous annulus, Int. J. Nonlinear Mech., Vol. 42(5), 2007, pp: 754–759.

[57] Radhakrishnamacharya, G. and Srinivasulu, C., Influence of wall properties on peristaltic transport with heat transfer, C. R. Mec. 335, 2007, pp: 369-373.

[58] Srinivas, S. and Kothandapani, M., The influence of heat and mass transfer on MHD peristaltic flow through a porous space with compliant walls, Appl. Math. Comp., Vol. 213, 2009, pp: 197–208.

[59] Ramana Kumari, A. V. and Radhakrishnamacharya, G., Effect of slip on heat transfer to peristaltic transport in the presence of magnetic field with wall effects, ARPN J. Eng. and Appl. Sci., Vol. 6(7), 2011, pp: 118-131.

[60] Sreenadh, S., Uma shankar, C. and Raga Pallavi, A., Effects of wall properties and heat transfer on the peristaltic transport of food bolus through oesophagus, A Mathematical Model, Int. J. Appl. Math and Mech., Vol. 8(7), 2012, pp: 93-108.

[61] Hayat, T., Javed, M., Asghar, S. and Hendi, A. A., Wall properties and heat transfer analysis of the peristaltic motion in a power-law fluid, Int. J. Num. Methods in Fluids, Vol. 71(1), 2013, pp: 65-79.

[62] Eldabe, N. T., Kamel, K. A., Galila M. and Abd-Allah, S. F. R., Peristaltic motion with heat and mass transfer of a dusty fluid through a horizontal porous channel under the effect of wall properties, IJRRS, Vol. 15(3), 2013, pp: 300-311

[63] Eldabe, N. T., Agoor ,B. M. and Alame, H., Peristaltic motion of non-Newtonian fluid with heat and mass transfer through a porous medium in channel under uniform magnetic field, J. Fluids, 2014, Article ID: 525769.

[64] Hina, S., MHD peristaltic transport of Eyring-Powell fluid with heat/mass transfer, wall properties and slip conditions, J. Magnetism and Magnetic. Materials, Vol. 404, 2015, pp: 148-158.

[65] Ramesh, K. and Devakar, M., Peristaltic transport of MHD Williamson fluid in an inclined asymmetric channel through porous medium with heat transfer, J. Cent. South Univ., Vol. 22, 2015, pp: 3189-3201.

[66] Vafai, K., Khan, A., Sajjad, S. and Ellahi, R., The study of peristaltic motion of Third grade fluid under the effects of hall current and heat transfer, Journal of Zeitschrift Fur Naturforschung A, Vol. 70 (4a), 2015, pp: 281-293.

[67] Sinha, A., Misra, J. C. and Shit, G. C., Effect of heat transfer on unsteady MHD flow of a blood in a permeable vessel in the presence of non uniform heat source, Alexandria Engineering Journal, Vol. 55(3), 2016, pp: 2023-2033.

[68] Stoke, V. K., Couple stress in fluid, The Physics of Fluids, Vol. 91, 1966, pp: 1709-1715.

[69] Srivastava, L. M., Peristaltic transport of couple stress fluid, Rheol. Acta, Vol. 25, 1986, pp: 638- 641.

[70] El Shehawey, E. F. and Mekheimer, K. S., Couple stresses in peristaltic transport of fluids, J. Phy. D, Vol. 27(6), 1994, pp: 1163–1170.

[71] Kothandapani, M. and Srinivas, S., On the influence of wall properties in the MHD peristaltic transport with heat transfer and porous medium, Phys. Lett. A, Vol. 372, 2008, pp: 4586-4591.

[72] Ravikumar, S. and Siva Prasad, R., Interaction of pulsatile flow on the peristaltic motion of couple stress fluid through porous medium in a flexible channel, European J. Pure and Appl. Math., Vol. 3, 2010, pp: 213-226.

[73] Pandey, S. K. and Chaube, M. K., Study of wall properties on peristaltic transport of a couple stress fluid, Meccanica, Vol. 46(6), 2011, pp: 1319-1330.

[74] Maiti, S. and Misra, J., Peristaltic transport of a couple stress fluid: some applications to hemodynamics, Journal of Mechanics in Medicine and Biology, Vol. 12(03), 2012, 1250048.(21)

[75] Raghunath Rao, T. and Prasad Rao, D. R. V., Peristaltic flow of a couple stress fluid through a porous medium in a channel at low Reynolds Number, Int. J. of Appl. Math & Mech., Vol. 8(3), 2012, pp: 97-116.

[76] Ravi Kumar, S., Effect of couple stress flow on magnetohydrodynamic peristaltic blood flow with porous medium through inclined channel in the presence of slip effect- Blood flow model, Int. J. Bio-Technology, Vol. 7(5), 2015, pp: 65-84.

[77] Kothandapani, M. and Srinivas, S., Peristaltic transport of a Jaffrey fluid under the effect of magnetic field in an asymmetric channel, Int. J. non-linear Mech.,, Vol. 34, 2008, pp: 915-924.

[78] Hayat, T., Ahamed, N. and Ali, N. Effects of an endoscope and magnetic field on the peristalsis involving Jeffrey fluid, Communications in Nonlinear Science and Numerical Simulation, Vol. 13, 2008, pp: 1581-1591.

[79] Pandey, S. K., Tripathi, D., Unsteady model of transportation of Jeffrey fluid by peristalsis, Int. J. Biomech., Vol.3(4), 2010, pp: 473-491.

[80] Suryanarayana Reddy, M., Sankar Shekar Raju, G., Subba Reddy, M. V. and Jayalakshmi, K., Peristaltic transport of a Jeffrey fluid through a porous medium in an inclined tube under the effect of a magnetic field, Int. J. Appl. Math. and Physics, Vol. 3(1), 2011, pp: 89-101.

[81] Vajravelu, K., Sreenadh, S. and Lakshminarayana, P., The influence of heat transfer on peristaltic transport of a Jeffrey fluid in a vertical porous stratum, Commun. Non linear Sci. Numer. Simul., Vol. 16, 2011, pp: 3107–3125.

[82] Rajanikanth, K., Sreenadh, S., Yadav, Y. R. and Ebaid, A., MHD Peristaltic flow of a Jeffrey fluid in an asymmetric channel with partial slip, Pelagia Research Library Advances in Applied Science Research, Vol. 3(6), 2012, pp: 3755-3765.

[83] Nadeem, S., Riaz, A. and Ellahi, R., Peristaltic flow of a Jeffrey fluid in a rectangular duct having compliant walls, Chemical Industry and Chemical Engineering Quarterly, Vol. 19(3), 2013, pp: 399-409.

[84] Abd-Alla, A. M., Abo-Dahab, S. M. and Albalawi, M. M., Magnetic field and gravity effects on peristaltic transport of a Jeffrey fluid in an asymmetric channel, Abstract and Applied Analysis, Vol. 2014, Article ID 896121, 2014.

[85] Ellahi, R. and Hussain F., Simultaneous effects of MHD and partial slip on peristaltic flow of Jeffrey fluid in a rectangular duct, J. Magnetism and Magnetic. Materials, Vol. 393, 2015, pp: 284-292.

[86] Sreenadh, S., Komala, K. and Srinivas, A. N. S. Peristaltic pumping of a power law fluid in contact with a Jeffrey fluid in an inclined channel with permeable walls, AIN Shams Eng. J. Vol.8(4), 2017, pp: 605-611.

[87] Yin, F. and Fung, Y. C., Peristaltic waves in circular cylindrical tubes, Trans. ASME J. Appl. Mech., Vol. 36, 1969, pp: 579-587.

[88] Weinberg, S. L., Eckistein, E. C., and Shapiro, A. H., An experimental study of peristaltic pumping, J. Fluid Mech., Vol. 49, 1971, pp: 461-497.

[89] Mishra, J. C. and Pandey, S. K., Peristaltic transport of blood in small vessels: Study of a mathematical model, Computers and mathematics with applications, Vol. 43(8-9), 2002, pp: 1183-1193.

[90] Kwang-Hua Chu, W. and Fang, J., Peristaltic transport in a slip flow, Euro. Physical J. B Vol. 16, 2000, pp: 543-547.

[91] Sobh, A.M., Interaction of couple stresses and slip flow on peristaltic transport in uniform and non uniform channels, Turkish J. Eng. and sci., Vol. 32, 2008, pp: 117-123.

[92] Alsaedi, A., Ali, N., Tripathi, D. and Hayat, T., Peristaltic flow of couple stress fluid through uniform porous medium, Appl. Math. Mech., Engl. Ed., Vol. 35(4), 2014, pp: 469-480.

[93] Hina, S., Mustafa, M. and Hayat, T., On the exact solution for peristaltic flow of couple stress fluid with wall properties, Bulgarian Chemical Communications, Vol. 47, 2015, pp: 30-37.

[94] Sankad G.C., Peristaltic transport of non-Newtonian fluids: Effects of wall properties, NIT, Warangal, Thesis, 2010.

[95] Sud, V. K., Sekhon, G. S. and Mishra, R. K., Pumping action of blood by a magnetic field, Bull. Math. Biol., Vol. 39 (3), 1977, pp: 385-390.

[96] Srinivasacharya, D. and Radhakrishnamacharya, G., Influence of wall properties on peristalsis in the presence of magnetic field, Int. J. Fluid Mech. Research, Vol. 34(4), 2007, pp: 374-386.

[97] Mekheimer, Kh. S., Effect of induced magnetic field on peristaltic flow of a couple stress fluid, Phys. Lett. A., Vol. 371, 2008, pp: 4271-4278.

[98] Sankad, G. C. and Radhakrishnamacharya, G., Effect of magnetic field on the peristaltic transport of couple stress fluid in a channel with wall properties, Int. J. Biomath., Vol. 4(3), 2011, pp:365-378.

[99] Shit, G. C. and Roy, M., Hydromagnetic effect on inclined peristaltic flow of a couple stress fluid, Alexandria Engineering Journal, Vol. 53(4), 2014, pp: 949- 958.

[100] Hummady, L. and Abdulhadi, A, Influence of MHD on peristaltic flow of a couple stress fluid through a porous medium with slip effects, Advances in Physics and Theories Applications, Vol. 30, 2014, pp: 34-44.

[101] Dheia, G. Sahil Al-Khafajy, S. and Abdulhadi, A.M,, Influence of MHD and wall properties on the peristaltic transport of a Williamson fluid through porous medium, Int. J. Adv. Research in Sci., Eng. and Tech., Vol. 2(11) ,2015, pp: 970-981.

[102] Tajoddin, A. and Khan, A., Slip effect on MHD peristaltic flow of non-Newtonian fluid through compliant walls, Journal of Ultra Scientist of Physical Sciences, Vol. 29(6), 2017, pp: 122-131.

[103] Hummady, L. Z. and Abdulhadi, A. M., Effect of heat transfer on the peristaltic transport of MHD with couple stress fluid through a porous medium with slip effects, Mathematical Theory and Modeling, Vol.4(7),2014, pp:1-18.

[104] Srinivas. S., Gayathri, R. and Kothandapani, M., The influence of slip conditions, wall properties and heat transfer on MHD peristaltic transport, Computer Physics Commun., Vol. 180, 2009, pp: 2115–2122.

[105] Hayat, T. and Maryiam, J., Wall properties and slip effects on the

magnetohydrodynamic peristaltic motion of a viscous fluid with heat transfer and porous space, Asia-Pacific Journal of Chemical Engineering, Vol. 6(4), 2011, pp:649-658.

[106] Das, K., Simultaneous effects of slip conditions and wall properties on MHD peristaltic flow of a Maxwell fluid with heat transfer, J. Siberian Federal University, Mathematics & Physics, Vol. 5(3), 2012, pp: 303-315.

[107] Javed, M., Hayat, T. and Alsaedi, A., Peristaltic flow of Burgers fluid with compliant walls and heat transfer, Appl. Math. Comput., Vol. 244, 2014, pp: 654-671.

[108] Eldabe, N.T.M., Hassan, M. A. and Abou-zeid, M. Y., Wall properties on the peristaltic motion of a couple stress fluid with heat and mass transfer through a porous medium, J. Eng. Mech., Vol. 142(3), 2015, 04015102.

[109] Lakshminarayana, P., Sreenadh, S. and Sucharitha, G., The influence of slip, wall properties on the peristaltic transport of a conducting Bingham fluid with heat transfer, Science Direct, Procedia Engineering, Vol. 127, 2015, pp: 1087-1094.

[110] Srinivas, S. and Muthuraj, R., Peristaltic transport of a Jeffrey fluid under the effect of slip in an inclined asymmetric channel, Int. J. Appl. Mech., Vol. 2, 2010, pp: 437.

[111] Subba Reddy, M. V. and Prasanth Reddy, D., Peristaltic pumping of a Jeffrey fluid with variable viscosity through a porous medium in a planar channel, Int. J. Mathematical Archive, Vol. 1(2), 2010, pp: 42-54.

[112] Rathod, V. P. and Mahadev, M., Peristaltic flow of Jeffrey fluid with slip effects in an inclined channel, Journal of Chemical, Biological and Physical Sciences, Vol. 2(4), 2012, pp: 1987–1997.

[113] Navaneeswara Reddy, S. and Viswanatha Reddy, G., Slip effects on the peristaltic pumping of a Jeffrey fluid through a porous medium in an inclined asymmetric channel, Int. J. Math. Archive, Vol. 4(4), 2013, pp: 183-196.

[114] Dheia, G. S. Al-Khafajy. and Abdulhadi, A. A., Effects of wall properties and heat transfer on the peristaltic transport of a Jeffrey fluid through porous

medium channel, Mathematical Theory and Modeling, Vol. 4(9), 2014, pp: 86-99.

[115] Hayat, T., Javed, M. and Ali, N., MHD peristaltic transport of a Jeffrey fluid in a channel with compliant walls and porous space, Transport in Porous Media, Vol. 74, 2008, pp: 259-274.

[116] Mahmouda, S. R., Afifi, N. A. S. and Al-Isede, H. M., Effect of porous medium and magnetic field on peristaltic transport of a Jeffrey fluid, Int. J. Mathematical Analysis, Vol. 5(21), 2011, pp: 1025 – 1034.

[117] Hayat, T., Javed, M., Asghar, S. and Mesloub, S., Compliant wall analysis of an electrically conducting Jeffrey fluid with peristalsis, Z. Naturforsch, Vol.6a, 2011, pp: 106-116.

[118] Krishna Kumari, S. V. H. N., Ramana Murthy, M. V., Ravi Kumar, Y. V. K. and Sreenadh, S., Peristaltic pumping of a Jeffrey fluid under the effect of magnetic field in an inclined channel. Applied Mathematical Sciences, Vol. 5(9), 2011, pp: 447 – 458.

[119] Jayarami Reddy, B. and Subba Reddy, M. V., Effect of magnetic field on the peristaltic pumping of a Jeffrey fluid in a channel with variable viscosity, Int. J. Appl. Math. & Eng. Sci., Vol. 5 (1), 2011.

[120] Subba Reddy, M. V., Jayarami Reddy, B., Nagendra, N. and Swaroopa, B., Slip effects on the peristaltic motion of a Jeffrey fluid through a porous medium in an asymmetric channel under the effect magnetic field, J. Appl. Math. and Fluid Mech., ISSN 0974-3170, Vol. 4(1), 2012, pp: 59-72.

[121] Bhatti, M. M. and Abbas, A. M., Simultaneous effects of slip and MHD on peristaltic MHD on peristaltic blood flow of Jeffrey fluid model through a porous medium, Alexandria Engineering Journal, Vol. 55, 2016, pp: 1017-1023.

[122] Sudhakar Reddy, M., Subba Reddy, M. V., Jayarami Reddy, B. and Ramakrishna, S., Effect of variable viscosity on the peristaltic flow of a Jeffrey fluid in a uniform tube, Pelagia Research Library, Advances in Applied Science Research, Vol. 3(2), 2012, pp: 900-908.

[123] Arun Kumar, M., Sreenadh, S. and Srinivas, A. N. S., Effects of wall properties and heat transfer on the peristaltic transport of a Jeffrey fluid in a channel, Pelagia Research Library, Advanced in Applied Science Research, Vol. 4(6), 2013, pp:159-172.

[124] Hari Prabakaran, P., Hemadri Reddy, R., Saravana,R., Kavitha, A. and Sreenadh, S., Influence of elastic on MHD peristaltic transport of a Jeffrey fluid through porous medium channel with heat and mass transfer, Advances and Applications in Fluid Mechanics, Vol. 17(1), 2015, pp: 1-16.

[125] Hussain, Q., Asghar, S., Hayat, T. and Alsaedi, A., Heat transfer analysis in peristaltic flow of a MHD Jeffrey fluid with variable thermal conductivity, Appl. Math. And Mech., Vol. 36(4), 2015, pp: 499-516.

[126] Saravana R., Sreenadh S., Venkataramana S., Hemadri reddy R., Kavita A., Influence of slip conditions, wall properties and heat transfer on MHD peristaltic transport of a Jeffery fluid in a non uniform porous channel, Int. J. of innovative technology & creative engineering, Vol 1, 2011, pp: 10 – 24.

List of papers published/communicated

List of published papers

1. Sankad, G.C., **Nagathan, P.S.**, Asha Patil and Dhange, M.Y., **Peristaltic Transport of a Herschel-Bulkley Fluid in a Non-Uniform Channel with Wall Effects,** *International Journal of Engineering Science and Innovative Technology (IJESIT)*, Vol.3(3), 2014, pp: 669-678.

2. Sankad, G.C., **Nagathan, Pratima S.**, **Influence of the Wall Properties on the Peristaltic Transport of a Couple Stress Fluid with Slip Effects in Porous Medium,** *Procedia Engineering, International Conference Computational Heat and Mass Transfer-2015*, Vol.127, 2015, pp: 862-868.
   http://doi:10.1016/j.proeng.2015.11.423

3. Sankad, G.C., **Nagathan, Pratima S.**, **Unsteady MHD Peristaltic Flow of a Couple Stress Fluid Through Porous Medium with Wall and Slip Effects,** *Alexandria Engineering Journal*, Vol.55, 2016, pp: 2099-2105.
   http://dx.doi.org/10.1016.j.acj.2016.06.029

4. Sankad, G.C., **Nagathan, P. S.**, **Transport of MHD Couple Stress Fluid through Peristalsis in a Porous Medium under the Influence of Heat Transfer and Slip Effects,** *International Journal of Applied Mechanics and Engineering*, Vol.22, 2017, pp: 403-414.
   http://doi:10.1515/ijame-2017-0024

5. Sankad, G.C., **Nagathan, P. S.**, **Influence of Wall Properties on the Peristaltic Flow of a Jeffrey Fluid in a Uniform Porous Channel under Heat Transfer,** *International Journal of Research in Industrial Engineering*, Vol.6(3), 2017, pp: 246-261.
   http://doi:10.22105/riej.2017.98628.1014

6. Sankad, G.C., **Nagathan, Pratima S., Effects of Slip on the Peristaltic Motion of a Jeffrey Fluid in Porous Medium with Wall Effects,** *Springer verlag book of Modern Mathematical Methods and High Performance Computing in Science and Technology*.

List of papers communicated

1. Sankad, G.C., **Nagathan, Pratima S., Unsteady Magnetohydrodynamic Flow of Jeffrey Fluid due to Peristaltic Motion of Uniform Channel with Slip in Porous Medium,** *Journal of Applied Mathematics and Statistics.*

2. Sankad, G.C., **Nagathan, Pratima S., Peristaltic Transport of a Couple Stress Fluid in a Inclined Non-Uniform Channel having Compliant Walls through Porous Medium,** *Caspian Journal of Applied Sciences Research, (CJASR).*